

GUIDEBOOK FOR ESTIMATING TROPICAL PEATLAND ECOSYSTEM - Carbon and Water Dynamics-

2nd Edition



BRG-JICA PROJECT

Peatland Restoration Agency – Japan International Cooperation
Agency Project for The Elaboration of Peatland Restoration



IJ-REDD+ PROJECT
Indonesia-Japan Project for Development
of REDD+ Implementation Mechanism



**GUIDEBOOK FOR ESTIMATING TROPICAL PEATLAND ECOSYSTEM
- Carbon and Water Dynamics-
2nd Edition**

Authors:

Mitsuru Osaki
Ayako Oide
Kayo Matsui
Rahmawati Ihsani Wetadewi
Haris Gunawan
Albertus Sulaiman
Awaldin
Keiji Kimura
Takashi Hirano
Hidenori Takahashi
Yohei Hamada

Published by:

JICA-BRG Project between Peatland Restoration Agency, Indonesia (BRG) and Japan International Cooperation Agency (JICA)

Published Date 20 March 2018

Information of 1st Edition "GUIDEBOOK FOR ESTIMATING CARBON EMISSION FROM TROPICAL PEATLAND IN INDONESIA". 2nd Edition is revised from this 1st Edition.

This publication was produced in its first version by the Indonesia–Japan Project for the Development of the REDD+ Implementation Mechanism (IJ-REDD+ Project) in collaboration with the Ministry of Environment and Forestry Indonesia (KLHK), Hokkaido University, the Environment Agency of Central Kalimantan Province (BLH Provinsi Kalimantan Tengah), the Agency for the Assessment and Application of Technology (BPPT), the Agency for Research and Development of Environment and Forestry (BPPLHK) Banjarbaru, the Sebangau National Park Office, the University of Palangka Raya, and Starling Resources. The first version of the publication was funded by the Japan International Cooperation Agency (JICA). The second version was produced by the Indonesia-Japan Project for Peatland Restoration (BRG-JICA Project) in collaboration with the Peatland Restoration Agency Indonesia (BRG), Hokkaido University, Kyoto University, the Research Institute of Humanity and Nature (RIHN), the National Agency for the Assessment and Application of Technology (BPPT), and the Ministry of Environment and Forestry Indonesia (KLHK). The second version of the publication was funded by the Japan International Cooperation Agency (JICA).

PREFACE

Hokkaido University and Palangka Raya University have a long history of cooperation in research on tropical peatland ecosystems dating back to 1997. The Japan International Cooperation Agency (JICA) and the Japan Science and Technology Agency (JST) have also supported this cooperation through the Science and Technology Research Partnership for Sustainable Development (SATREPS) program, a Japanese government program that promoted international joint research with the title “Wild Fire and Carbon Management in Peat-Forests in Indonesia” from 2009 to 2014. These cooperative programs have generated important research on tropical peatland ecosystems in Central Kalimantan and many outcomes of this cooperation have been included in a recently published book edited by M. Osaki & N. Tsuji (2016), “Tropical Peatland Ecosystems”, 651 p. This is the world’s first complete book on this topic and it contains 41 scholarly articles that describe various aspects of tropical peatland ecosystems.

In line with these research advances, one of the recommendations that emerged from a joint workshop between the SATREPS program and the IJ-REDD+ Project in January 2014 was to develop methodologies to mitigate climate change due to carbon emissions. To this end, translating research results into a guide that can be easily understood by all stakeholders at the provincial government level was necessary. The IJ-REDD+ Project has coordinated and facilitated with stakeholders the preparation of this guidebook on estimating carbon emissions from peatlands in Indonesia, particularly with stakeholders from Central Kalimantan.

After these projects and the first version of the guidebook, Mr. Joko Widodo, the president of Indonesia, issued a presidential regulation in early 2016 to establish the Peatland Restoration Agency (BRG) which bears the mandate of peatland ecosystem restoration for two million hectares in five years. This is the evidence of genuine concern that peatland restoration is an urgent task in Indonesia. Many stakeholders are involved in peatland management, such as oil palm and fast-wood plantation companies, local communities, and agro-industries which grow sago, nipa, coconut, coffee, cacao, and native species for food and feed production and biomass production as a source of bioenergy. In addition to coordinating the interests of multiple stakeholders, multiple elements in peatland ecosystems need to be managed including water levels, nutrient status in soil and water, vegetation, topography, and the economic system.

The Peatland Restoration Agency (BRG) must restore disturbed, degraded, and damaged peatlands over a period of five years. Hence further collaborations between Japanese and Indonesian scientists are urgently required to implement the conservation and sustainable management of peatlands in Indonesia. The BRG-JICA Project was conducted from October 2017 to March 2018 in collaboration with Hokkaido University and founded by the JICA. The BRG-JICA Project has updated its methodologies so the second version of the guidebook that is published here.

We wish to express our appreciation to all parties who have supported this cooperation.

31 March 2018

Mitsuru Osaki
Leader of the JICA-BRG Project

ACRONYMS

AVHRR	Advanced Very High Resolution Radiometer
BIG	Geospatial Information Bureau of Indonesia
C	Carbon
CH ₄	Methane
CO	Carbon Monoxide
CO ₂	Carbon dioxide
DB	Drained and Burned Land
DEM	Digital Elevation Model
DF	Drained Forest
DOC	Dissolve Organic Carbon
EC	Eddy Covariance
ECMWF	European Center for Medium-Range Weather Forecast
ER	Ecosystem Respiration
GHG	Greenhouse Gas
GIS	Geographic Information System
GOI	Government of Indonesia
GPS	Global Positioning System
GWL	Groundwater Level
GWP	Global Warming Potential
IJ-REDD+ Project	Indonesia-Japan Project for Development of REDD+ Implementation Mechanism
INDC	Intended Nationally Determined Contribution
JICA	Japanese International Cooperation Agency
LIDAR	Light detection and ranging (an optical remote sensing technology)
MODIS	Moderate Resolution Imaging Spectroradiometer
MRV	Monitoring, Reporting and Verifying
N ₂ O	Nitrous Oxide
NDVI	Normalized Difference Vegetation Index
NEE	Net Ecosystem Exchange
NEP	Net Ecosystem Production
NOAA	National Oceanic and Atmospheric Administration
OP IRGA	Open-Path CO ₂ Infra-Red Gas Analyzer
PALSAR-2	Phased Array type L-band Synthetic Aperture Radar
PAR	Photosynthetically Active Radiation
PM	Particulate Matter
RAN-GRK	<i>Rencana Aksi Nasional Penurunan Emisi Gas Rumah Kaca</i> (National Action Plan for Reducing GHG Emissions)
REDD+	Reducing Emissions from Deforestation and Degradation Plus Carbon Stock Enhancement
SAR	Synthetic Aperture Radar
SAT	Ultra-Sonic Anemometer-Thermometer
SESAME	Sensory data transmission Service Assisted by Midori Engineering

SRTM	Shuttle Radar Topography Mission
UNFCCC	United Nations Framework Convention on Climate Change
WI	Wetlands International



1.1. Background

Indonesia holds approximately 15 million hectares of peat soil, which represents 50% of the world's total tropical peatland area (DNPI, 2014). Peatlands store a huge amount of carbon in the form of organic matter accumulated in waterlogged and anaerobic conditions. In natural conditions when peatland hydrology is intact, peatlands are capable of providing multiple environmental benefits including water regulation, carbon storage, and biodiversity maintenance.

Despite such ecological functions, peatlands have been utilized for economic development for decades. Peatland development often involves the construction of drainage canals, which inevitably lower water levels and put hydrological integrity at risk. Once peat soils are exposed to the air, they start to decompose and become dry and vulnerable to fires – which are major sources of greenhouse gas (GHG) emissions. In 2010, emissions from peat decomposition and burning contributed to 44 percent of Indonesia's total GHG emissions (DNPI, 2014).

For this reason, sustainable peatland management must be a central component in Indonesia's strategy to combat climate change and its devastating impacts on its land and people. The important role of peatlands is also reflected in the recent Ministry of Environment and Forestry decree (No S.661 /MenLHK-Setjen/Rokum/2015), as well as the national action plan for GHG (RAN-GRK). The decree not only bans the issuance of new business licenses on peatlands, but also requires concession holders to halt peatland clearing and maintain the minimum groundwater level (GWL) at 40cm.

Groundwater level is the most important environmental factor in peatland management (Shigenaga et al., 2016). This guidebook aims to provide practical methods for estimating carbon emissions from peat decomposition and burning by using real-time GWL data as a key parameter. It also provides a method for predicting GWLs for several days into the future. These models can be used for various purposes in practice, including developing science-based national and regional development strategies and early fire warning systems.

1.2. What is this guidebook about?

This guidebook provides step-by-step procedures to:

- Collect spatial information from remote sensing data sources
- Collect field sampling data of GWL and other parameters
- Estimate GWL distribution based on the field samples and remote sensing data
- Establish a linear relationship (model) between carbon emissions and GWLs
- Predict GWLs several days into the future based on field sampling data.

Although the methods outlined in this guidebook were initially developed in Central Kalimantan during the JICA-JST Project from 2010 to 2014 (see Preface for the project background), this guidebook provides general procedures which are replicable for peatlands throughout Indonesia.

1.3. Guidebook Organization

This guidebook is organized into four parts: **I.** Introduction, **II.** Field surveys, **III.** Ground Water Table, **IV.** Carbon Emissions, and **V.** Future Considerations.

Part I of this guidebook provides introductory information including information on guidebook structure.

Part II of this guidebook explains how to conduct field surveys to obtain basic information on peatlands.

Part III of this guidebook explains how to predict Ground Water Level (GWL) several days in advance based on daily average GWL data observed in the field. Figure 17 illustrates the framework of the GWL Prediction Model.

Part IV of this guidebook introduces a protocol to estimate the amount of carbon emissions from peatland due to microbial decomposition and peat burning. It is divided into four sections: 1) Data collection and processing, 2) Data analysis, 3) Carbon emission modeling from peat decomposition, and 4) Carbon emission modeling from peat burning. Based on the framework presented in Figure 1, each section provides step-by-step procedures in sub-sections.

Part V of this guidebook suggests further developments for an Integrated Sensing System to understand models introduced in Parts III and IV. Part V also discusses potential applications of these models.

1.4. Who is this guidebook for?

This guidebook is intended to be used by a wide range of stakeholders in Indonesia who wish to develop and implement sustainable management practices on peatland by knowing the amount of carbon emissions from land use and land use change, and by preventing peatland fires. These stakeholders include:

- Policy makers;
- Peatland managers (such as concession holders);
- Researchers; and
- Local authorities.



Peatlands can be classified into three zones based on the distance from the coast; coastal peatland, intermediate peatland and inland peatland. Coastal zone is affected by high salinity from the sea water and the tidal effect. On the other hand, inland peat is an oligotrophic environment. We need to apply an efficient cultivation system for restoration as well as agricultural demands. From the point of soil nutrient spatial conditions, zone-specific management is necessary. Different peat zones have different properties in water quality, soil and vegetation. Aiming at a large-scale application of zoning in the future, it is necessary to monitor several associate factors that determine the peatland properties, which leads establishment of an improved model system for tropical peatlands monitoring.

2.1. What needs to be measured for field survey

Soil properties and water quality and condition determine the types of vegetation. In field survey, these environmental factors related to each other are measured. There are established methodology and description methods for each measurement, which are introduced 2.3 Analytical items.

The general information is needed to record at each plot such as:

- date of measurement and sampling
- crew members present
- location of plot (e.g. management district, etc.)
- plot identification – name and/or number of the sampled plot or stand/GPS information and precision ($\pm X$ m)
- plant community/site type: e.g. intact forest, logged forest, grassland, oil palm or other (if other, describe)
- geomorphic setting: river banks, peat dome, interior or basin, etc.
- ecological condition – evidence of any recent or past disturbances such as:
 - timber harvest
 - hydrological status (e.g. drained or undrained)
 - recent wildfire and other disturbances such as natural (e.g. disease, insects, etc.) or anthropogenic (e.g. roads, trails, nontimber harvest or use, etc.)
 - plantations/restoration sites (e.g. age of planted trees)
- topography
- soil surface description: wet, dry, litter presence, etc.

In addition to descriptive data, it is valuable to establish permanent photo points in plots.

2.2. Survey Design

Survey plan can be designed by the following steps, which must be carried out in a transparent and consistent manner. Opinions and ideas from the crew members who are experienced in each survey need to be reflected and well-justified.

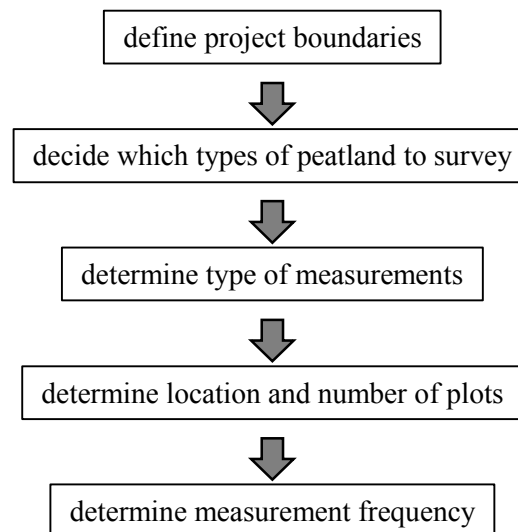


Figure1 Suggested steps in the preparation of measurement plan.

Based on the purpose of survey, site selection, types of survey (e.g. transect survey, area survey, etc.) and sampling design including analytical items (e.g. water quality, soil, vegetation, etc.) can be determined. Seasonal changes should also be considered in tropical peatlands, which has a big seasonal difference in water and soil condition.

2.3. Analytical items

Not all the analytical items are necessary or infeasible at field survey. Therefore, some of them will be selected based on the project purpose. The accuracy of measurement devices used at field also needs to be considered. The measurement values given by devices for outside use are usually less accurate than those analyzed under well-equipped condition in laboratory. If a high accuracy is required, sample collection as well as field measurement needs to be carried out for detail analysis in laboratory.

Following analytical items are useful to determine each plot.

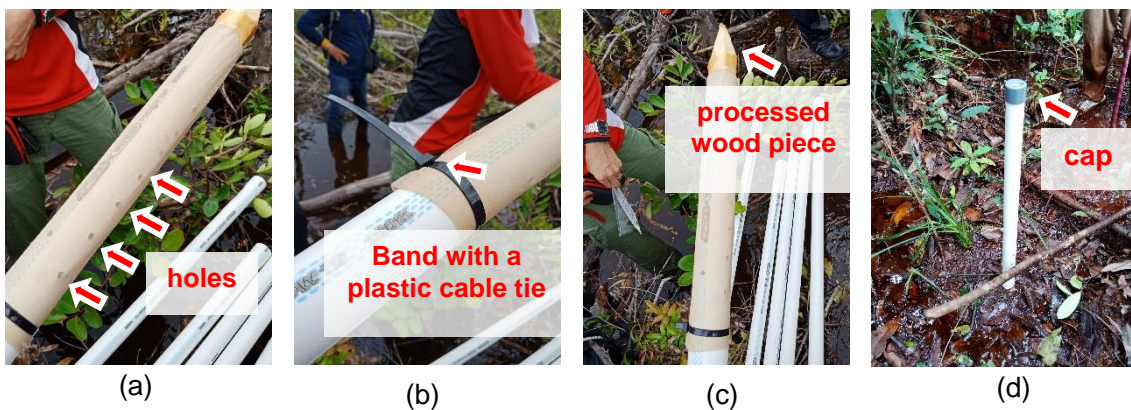
- Soil physical properties
 - Soil texture (simple diagnosis at field / lab analysis)
- Soil chemical properties such as
 - EC (field measurement / lab analysis)
 - pH (field measurement / lab analysis)
 - Concentrations of exchangeable cations (K^+ , Na^+ , Ca^{2+} , Mg^{2+}) (lab analysis)
 - CEC (lab analysis)
- Ground water
 - Water level (field measurement)
 - Water qualities such as:
 - pH (field measurement / lab analysis)
 - EC (field measurement / lab analysis)
 - Concentrations of cations and anions (K^+ , Na^+ , Ca^{2+} , Mg^{2+} , PO_4^{3-} , NH_4^+) (field measurement / lab analysis)
 - BOD, COD, DO (field measurement / lab analysis)

2.4. Specific measurements

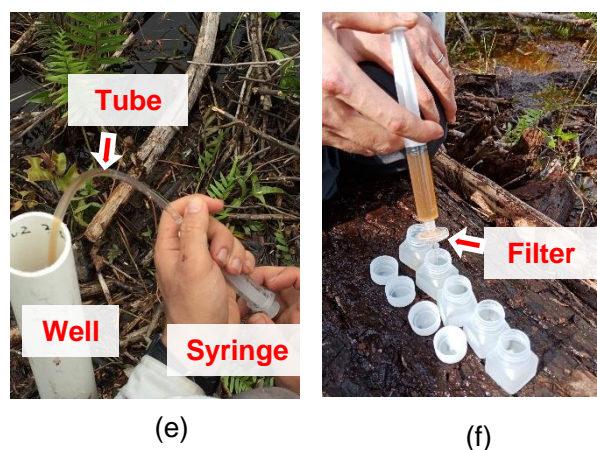
2.2.1 WATER

Several measurements such as pH and EC etc. will be conducted at field by using portable devices for each analytical item. To obtain water samples to apply for measurement, firstly a well will be established in each sampling site.

A long plastic pole, an electric drill, tights and plastic cable ties are the main materials for establishment of a well. The pole should be cut according to the depth of water table at each site, which needs to be checked in advance. One end of the pole will be drilled to make some holes on the side. Two layers of tights will cover the end of the pole with holes (a). It must cover all holes and be tied with a rubber band so that ground water be filtrated through them into inside of the pole (a). The covered tights will be band with a plastic cable tie (b). Wood piece is processed to put into the end of the pole, which is useful to penetrate peat (c). The pole is penetrated straight to peat and ground water can be taken from inside of the pole. It is better to put a cap on the pole end to avoid contamination of ground water inside the pole (d).



Using a tube and a syringe, ground water will be withdrawn into the syringe (e). Then, a filter is put on the syringe to collect water samples and apply to the measurement devices such as pH, EC and DO meters (f). Note that calibration must be done before measurement for each device following the devices' manuals. When analyze a new sample, wash a residue adhering to the inner surface of a devise with a liquid to be analyzed next, then discard the liquid and dispense a new liquid to be analyzed. At least triplicate is necessary to obtain a data value.



2.2.2 SOIL

Soil samples will be collected by an auger at the points of determined intervals along a transect line. However, when a rapid change is expected on a transect, appropriate subdivisions should be set between the intervals. At field survey, observation of site and soil collected will be recorded.

Peat monitoring sheet is shown in appendix, which will be useful for recoding all the necessary information of sampling plot and survey area (see appendix. Peat Monitoring sheet).

For collecting soil samples, the depth of soil sampling will be decided based on the purposes of survey (i.e. 0-15 cm, 15-30 cm, 30-50 cm, 50-100 cm, 100-200 cm, 200-300 cm, 300-500 cm and > 500 cm). A soil sample is packed into a plastic bag. Air must be removed from the plastic bag before sealing as shown below. Also, peat soil water will be collected into plastic bottles by filtration at the depth of water level of each soil sampling points as explained in 2.4.3. WATER chapter.



Air is removed from a soil sampling bag.

2.2.3 VEGETATION

A tree survey contains all kinds of detailed information about the trees. The survey will reveal information such as species of the tree based on scientific name, physical measurements of the tree such as height and diameter, age of the tree etc.

Firstly, survey plot will be set by area measurement (a). The plots for tree survey should be representative, so the places that are specifically disturbed are not recommend to be set a survey plot. Three or four people are recommended to conduct tree survey in one square plot. At least one of them must be the experienced in identifying tree species. Each crew member is responsible for measurement, tree identification or recording.

(a) A survey plot is set by area measurement.



For the purposes of survey, the minimum size (cm) in stem diameter of mature trees to be measured will be decided. (i.e. trees with over 10-cm stem diameter). The main stem (trunk) diameter must be measured at 1.3 m above the soil surface (Kauffman et al., 2016). Within the individual plots, trees of each species are counted. All trees need to be tagged with special tags and numbers (b). These results are then expressed as percentages of the total for that area (i.e. *Lithocarpus dasystachys* makes up 15% of all the trees).

(b) A tree stem is measured and tagged with special tags and numbers



If possible, trees that are measured should be identified to the species or genus level. For the tallest tree of each species in an area, its height was measured using a clinometer. However, it is usually difficult in forests with a high tree density. The example of result table is shown in Table below.


Table 1 Results of tree survey

Species	Number of trees	Basal area (cm ²)	Basal area (%)
<i>Lithocarpus dasystachys</i>	62	16157	15.32
<i>Tetractomia tetrandra</i>	36	8750	8.30
<i>Combretocarpus rotundatus</i>	4	6557	6.22
<i>Xylopia fusca</i>	8	5345	5.07
<i>Cratoxylon glaucum</i>	10	5083	4.82
<i>Syzygium sp.</i>	23	4849	4.60
<i>Shorea teysmanniana</i>	20	4446	4.22
<i>Horsfieldia crassifolia</i>	7	4195	3.98
<i>Lithocarpus gracilis</i>	1	4137	3.92
<i>Mezzettia parvifolia</i>	7	4130	3.92
<i>Elaeocarpus mastersii</i>	10	3529	3.35
<i>Dactylocladus stenostachys</i>	3	3513	3.33
<i>Stemonurus secundiflorus</i>	5	3426	3.25
<i>Ilex hypoglauca</i>	10	2767	2.62
<i>Mezzettia umbelliflora</i>	4	2757	2.61
<i>Santiria griffithianum</i>	11	2718	2.58
<i>Neoscortechinia kingi</i>	5	2652	2.51
<i>Diospyros pseudomalabarica</i>	8	2301	2.18
<i>Gymnacranthera farquhariana</i>	12	2209	2.09
<i>Shorea balangeran</i>	1	1304	1.24
<i>Grewia sp.</i>	10	1265	1.20
<i>Garcinia sp.</i>	3	1077	1.02
Others (35 sopecies)	67	12297	12
Total	327	105466	100.00

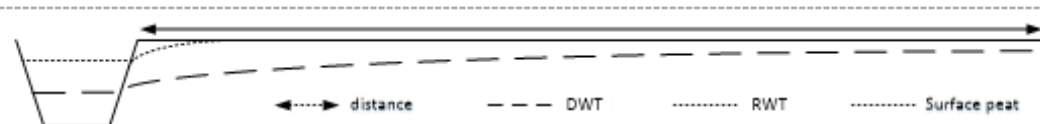
Reference

Kauffman et al. (2016) Protocols for the measurement, monitoring, and reporting of structure, biomass, carbon stocks and greenhouse gas emissions in tropical peat swamp forests. Working Paper 221.Center for International Forestry Research. DOI: 10.17528/cifor/006429

Appendix

		Peat profile	
1	Name of surveyor		
2	Date, Time		
3	Code / Number of sampling		
4	Administrative location		
5	GPS coordinate		
6	Peat maturity		Sapric/Hemic/fibric/Mineral/Charcoal(S/H/F/M/C) write in 'Peat profile'
7	Peat thickness (cm)		
8	Depth of substratum (cm)		
9	Depth of charcoal (cm)		
10	Substratum soil type		Clay/sand
11	Drainage pattern / type		natural/artificial (describe) . . .
12	Distance for nearest canal (m)		primary/secondary/etc.
13	Canal water table (WT) (cm) (Interview and/or observation)		Present ___ (cm); wet season ___ (cm); dry season ___ (cm)
14	GWT of sampling point (cm) pH / EC ($\mu S/cm$)/DOC $\times 2$		
15	Landuse		
16	Year of canal construction		
17	Previous landuse		
18	Year of converting landuse		
19	Soil classification		
20	Number of samples	(total)	
21	From auger		
22	From core (undisturbed)		

Sketch:



Peat profile: Necessary information from soil observation, which are recorded in the tables will be drawn in the right space.

Sketch: in a transect survey, record general information in a visually understandable way such as site names, water level in dry season (DWT) and in rainy season (RWT), peat depth etc.

Reference of peat monitoring sheet

1.	Name of surveyor	Write the name who records
1.	Date, Time	Write the date and time you conduct sampling in this point.
2.	Code / Number of sampling	Write the code of sampling point.
3.	Administrative location	Write administrative location. (Ex: name of village, district etc.)
4.	GPS coordinate	Record GPS (X; Y) data at this point.
5.	Peat maturity	Rapid assessment of peat maturity by squeezing amount of sample at field. For further explanation, see BBLSDP 2014 (page 4, pdf page 9).
6.	Peat thickness (cm)	The depth of mineral soil layer from the surface by auger measurement
7.	Depth of substratum (cm)	Measure the depth where the mineral soil appeared
8.	Depth of charcoal (cm)	Record the depths where charcoal is observed during collecting samples. Usually an artificial place has more charcoal layers than natural forests. Charcoal tends to appear in the upper layers in Natural forest due to the frequent fires in current decades.
9.	Substratum soil type	Define mineral soil type. (Mineral Soil Classification: Clayey, Sandy, Loamy, etc.)
10.	Drainage pattern / type	Describe drainage pattern / type (natural, artificially built, etc.)
11.	Distance for nearest canal/stream (m or km)	Measure the sampling point to the nearest canal around, and recognize the canal (primary/secondary/branch etc.)
12.	Canal water table (WT) (cm)	Measure the water table level from ground surface at the nearest canal. By interview (if possible). Difference between rainy season and dry season.
13.	GWT of sampling point (cm)	Measure water table level at the sampling point using after you dig peat soil or make a well. Measure pH, EC and DOC as a site representative water quality.
14.	Landuse	Describe present vegetation cover (forest, bare land, plantation etc.)
	Year of canal construction	Record when canal was built. (Interview)
	Previous landuse	Record the previous landuse / land cover. (Interview)
	Year of converting landuse	Record the year of converting land use to the present condition. (Interview)
15.	Soil classification	Classify soil type of the samples using common soil taxonomy system or local taxonomy system (WRB, IISDA, FAO, etc.)
16.	Number of samples	Total number of samples taken from auger and cores
	From auger	The number of samples taken from auger.
	From core (undisturbed)	The number of core samples.

Peat profile: Necessary information from soil observation, which are recorded in the tables will be drawn in the right space.

Sketch: in a transect survey, record general information in a visually understandable way such as site names, water level in dry season (DWT) and in rainy season (RWT), peat depth etc.

2.5. Peat Thickness Estimation with a Phenology Classification Method

Hypothesis

According to studies of Central Kalimantan peatlands (Shimada et al. 2017), peat thickness is predictable by forest phenology type above the peat layer. Peat swamp forest (PSF) phenology type in Central Kalimantan was classified into eight major types (PHIL, W1, W2, W2D-A, W2D-Z, W1D, PHOB-Z, PHOB-V) using multi-temporal (1992–1993) monthly National Oceanic and Atmospheric Administration (NOAA) Advanced Very High Radiometer (AVHRR) data. Specifically, fluctuation patterns of the vegetation index among three seasonal periods (i.e., the former half of the five-month rainy season, the latter half of the five-month rainy season, and the two-month dry season) were classified.

Tropical peatlands are characterized by high groundwater levels and their seasonal fluctuations. High groundwater level usually leads to a decrease in vegetation activity owing to anoxic stress to plant roots. Considering the hydrological buffer function of the peat layer, we focused on phenological difference due to the hydro-periodical difference of PSF and its relation to peat thickness. Riverine PSF and PSF fringing on shallow peat layers have greater water flow and seasonal groundwater level fluctuations in comparison to inner forests on deeper peat layers which tend to have permanently high groundwater levels that moderately fluctuate. Since the hydroperiod is a seasonal characteristic of peatlands in Southeast Asia, PSF phenology was hypothesized to be a predictor of underlying peat thickness. The result of the association of ombrophobous PSF phenology types (PHOB-Z and PHOB-V [Remark 1]) with significantly shallower peat layers (Table X. 1) indicates the influence of flooding stress due to a waterlogging in the rainy season. This supports a part of the hypothesis (Figure 2-1).

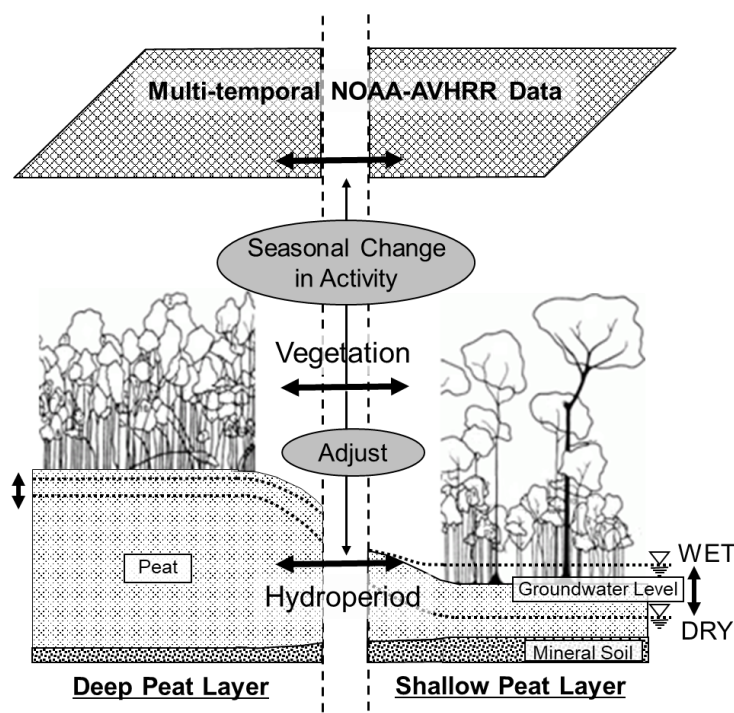


Figure 2-1: Phenological pattern, mean peat thickness, and percentage of areal extent among eight peat swamp forest types in Central Kalimantan (cited from Shimada et al. 2017)

PSF phenology types that have maximum vegetative activity during the latter rainy season (i.e., W2 and W2D-A) occur on relatively deeper peat layers (Table X. 1). The root mean square error (RMSE) for the peat thickness estimation map was derived by assigning each associated mean peat thickness value (Table X. 1 and Figure X. 6) to PSF types in Central Kalimantan and was found to be 2.49 m. Individually, the phenology types on deeper peat layers (i.e., W2, W2D-A, and W2D-Z) tend to have greater errors (RMSE = 2.33 m, RMSE = 3.17 m, and RMSE = 2.77 m, respectively) in peat thickness estimation.

Table 2-1: Phenological pattern, mean peat thickness, and percentage of areal extent among eight peat swamp forest types in Central Kalimantan (cited from Shimada et al. 2017).

Phenology type	Phenological pattern*						Mean peat thickness (m)	Percentage of areal extent (%)
	WET1	→	WET2	→	DRY			
PHIL	1	(+)	(-)	1	(-)	0	0.75	0.5
W1	1	(-)	0	(+)	(-)	0	–	0.8
W1D	1	(-)	0	(+)	1		1.56 ^{bc}	9.1
W2	0	(+)	1	()	0		4.70 ^{ab}	6.4
W2D-A	0	(+)	1	(-)	1		4.59 ^a	13.6
W2D-Z	0	(+)	1	(+)	1		2.64 ^b	47.2
PHOB-Z	0	(+)	0	(+)	1		1.35 ^c	13.3
PHOB-V	0	(-)	0	(+)	1		0.84 ^c	9.1

*WET1: former half of the rainy season (September 1992 to January 1993)

WET2: latter half of the rainy season (February to June 1993)

DRY: dry season (July to August 1993)

0: Normalized Difference Vegetation Index (NDVI) during a seasonal period < annual mean NDVI

1: NDVI during seasonal period > annual mean NDVI

(+): positive gradient between seasonal periods

(-): negative gradient between seasonal periods

a > b > c: values followed by the same letter are not significantly different at a significance level of $P < 0.05$ (Sheffé's test)

2.2.2. Peat Thickness Estimation Method

Here, we explain the steps involved in the derivation of the phenological classification map (i.e., the prediction map for peat thickness).

Step 1. Preparation of time-series satellite imagery data

- Acquisition of time-series vegetation index data product or raw reflectance imagery data which are to be calculated into a vegetation index. High temporal resolution image data such as Terra/Aqua-Moderate Resolution Imagery Spectroradiometer (MODIS) and NOAA-AVHRR are preferable since the elimination of contamination from noise or clouds can be more easily achieved.
- Vegetation index time-series imagery products can be freely acquired through various web archive data center portals, e.g., United States Geological Survey (USGS) Global Visualization Viewer (GloVis: <https://glovis.usgs.gov/>), USGS EarthExplorer

(<https://earthexplorer.usgs.gov/>), National Aeronautics and Space Administration (NASA) Earthdata Search (<https://search.earthdata.nasa.gov/search>), and Global Land Cover Facility (GLCF: <http://www.landcover.org/>).

- A dataset of more than one year is required for analysis.
- The vegetation index can be the NDVI (eq (1)), the Enhanced Vegetation Index (EVI: eq (2)), or the Temperature Adjusted Vegetation Index (TAVI: eq (3) and eq (4)). TAVI, which includes not only vegetation chlorophyll activity but also vegetation transpiration activity, can be a more sensitive indicator than NDVI in the tropics (Foody et al. 1996).

$$\text{NDVI} = \frac{\text{NIR}-\text{Red}}{\text{NIR}+\text{Red}} \quad \text{eq (1)}$$

$$\text{EVI} = G \times \frac{\text{NIR}-\text{Red}}{\text{NIR}+C_1 \cdot \text{Red}-C_2 \cdot \text{Blue}+L} \quad \text{eq (2)}$$

$$\text{TAVI} = \frac{\text{NDVI}}{T_s} \times 100 \quad \text{eq (3)}$$

Where,

NIR: reflectance in the wavelength of near-infrared,

RED: reflectance in visible red,

Blue: reflectance in visible blue,

L: canopy background adjustment,

G: gain factor,

*C*₁, *C*₂: the coefficients of the aerosol resistance term,

*T*_s: surface radiation temperature calculated by the split window algorithm using two thermal bands (Price 1990) [eq (4)].

$$T_s = \frac{[T_x+3.3(T_x-T_y)](5.5-\varepsilon_x)}{4.5-0.75T_x(\varepsilon_x-\varepsilon_y)} \quad \text{eq (4)}$$

Where,

*T*_x, *T*_y: brightness temperature (K) at thermal bands *x* and *y*,

*ε*_x, *ε*_y: emissivity at the wavelength bands *x* and *y*.

In the estimation case of Shimada (2001), datasets of 10-day composite NOAA-AVHRR data products on NDVI and channel-4 and channel-5 radiation temperature (*T*_x and *T*_y, respectively) over the Sumatra-Kalimantan area were collected from the Earth Resources Observations Systems (EROS) Data Center (Shimada et al. 2001). *T*_s was calculated using eq (4) by assuming the surface emissivity (*ε*_x, *ε*_y) to be 0.96 (Nemani et al. 1993). The image data period was set as April 1992 to September 1993 to avoid the effects of the large-scale forest fire in 1994

Step 2. Preprocessing of time-series satellite imagery data

- Monthly composite imagery data (e.g., NDVI, EVI, *T*_s, and other indices) should be prepared from shorter time period composites such as eight-day, 10-day, or 16-day

composite data by maximum filter so as to reduce the effects of cloud contamination.

- Monthly composite data should be smoothed by the three-month moving median filter to eliminate remaining contamination due to clouds and noise (Fig. X. 2).
- TAVI, if adopted for the phenological classification, should be calculated using median-smoothed monthly images.
- The monthly vegetation index imagery dataset which was trimmed into a one-year period should be aggregated into three seasonal index images with a one-year mean image. The concept of the discrimination method of the seasonal period within a year is shown in the next step (Step 3).

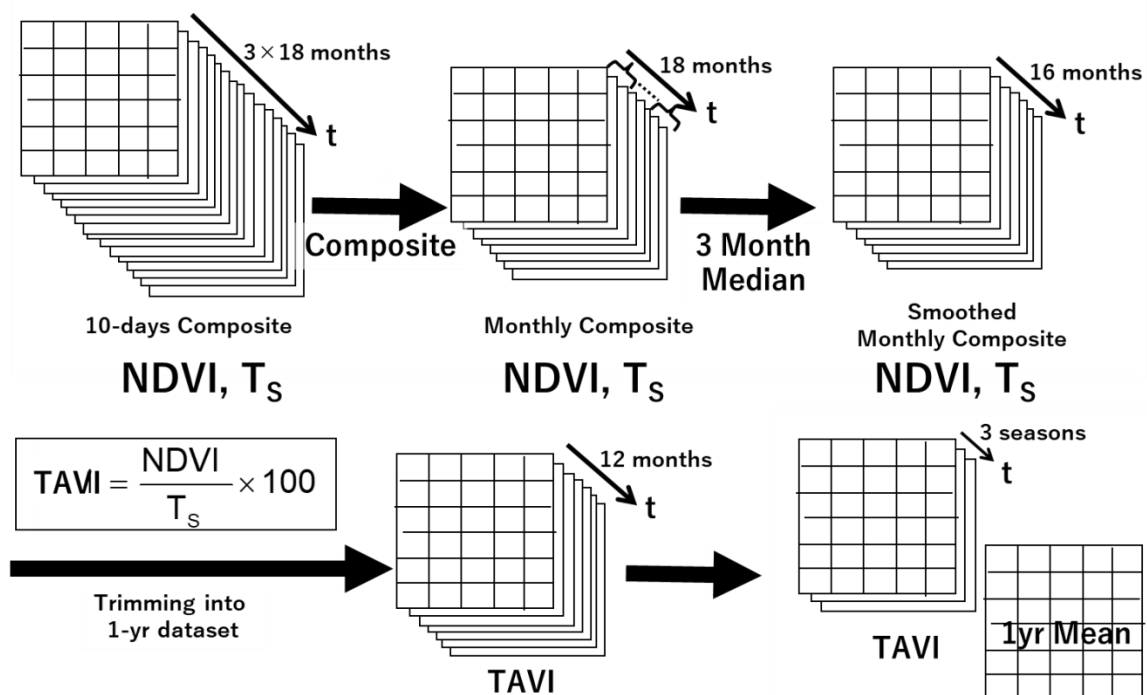


Figure 2-2: Image preprocessing scheme example of deriving one-year mean and seasonal Temperature Adjusted Vegetation Index (TAVI) data from the 10-day composite National Oceanic and Atmospheric Administration (NOAA) Advanced Very High Radiometer (AVHRR) and T_s time-series data.

Step 3. Seasonal period discrimination

- A year of the tropical region can be divided into two seasonal periods, i.e., the wet (rainy) season and the dry season. Each region has its own unique seasonal distribution, e.g., the wet season typically occurs in Central Kalimantan from June to October, with the remaining months constituting the dry season (~ two months) and intermediate months. To reflect vegetative responses resulting from regional and real-time micrometeorology, data corresponding to the region and time of imagery acquisition should be used. Since extraction of vegetation seasonal characteristics is important and the wet season is longer than the dry season, the wet season is divided into two seasonal periods, i.e., the former and latter wet periods (WET1 and WET2, respectively).

Including the dry seasonal period (DRY), three seasonal periods are discriminated (Fig. X. 3).

- Monthly precipitation data and evapotranspiration rate data at the target area and time period are needed to set the ranges of the seasonal periods.
- Identify the month of the year when monthly evapotranspiration exceeds monthly precipitation. Classify these consecutive months as the dry period and the remaining months as the wet period. The wet period should be split in half and the first half of the period classified as WET1 and the second half classified as WET2.

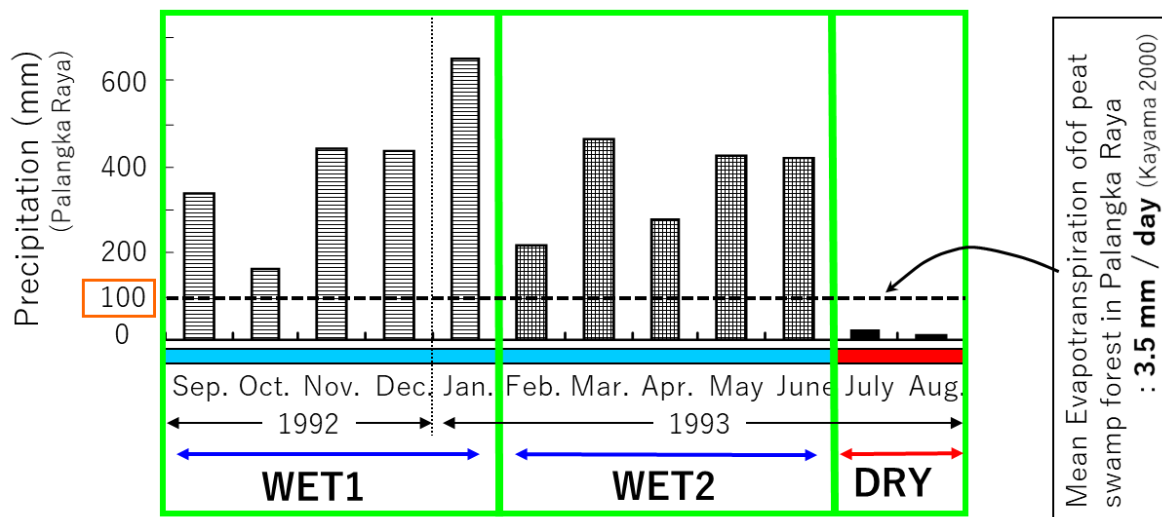


Figure 2-3: Discrimination of three seasonal periods in a target year (September 1992 to August 1993) in a peat swamp forest near Palangka Raya, Central Kalimantan

Step 4. Phenological type classification

- The pixel value of each seasonal vegetation index (e.g., \overline{TAVI}_{WET1} , \overline{TAVI}_{WET2} , and \overline{TAVI}_{DRY}) is to be compared to the corresponding one-year mean vegetation index value (e.g., \overline{TAVI}_{1yr}) to assess vegetative activity during different seasonal periods (Fig. X. 4).
- If a value of the seasonal vegetation index exceeds the annual mean value, the vegetation at the corresponding pixel for the seasonal period is considered active, while pixel values below the annual mean value are considered inactive (Table X. 1). All combinations of active and inactive vegetation among the three seasonal periods create six patterns (i.e., in the following order, WET1:WET2:DRY = +:+:-, +:-:-, +:-:+, -:+:+, -:-:+, -:+::-).
- The gradient of vegetation index values between consecutive seasonal periods (i.e., between WET1–WET2 and WET2–DRY) can be analyzed. The total number of possible phenology patterns is 10.
- Each vegetation phenology type can be named, e.g., the ombrophilous type as PHIL and the ombrobobous type as PHOB (Fig. 4, Table X. 1).

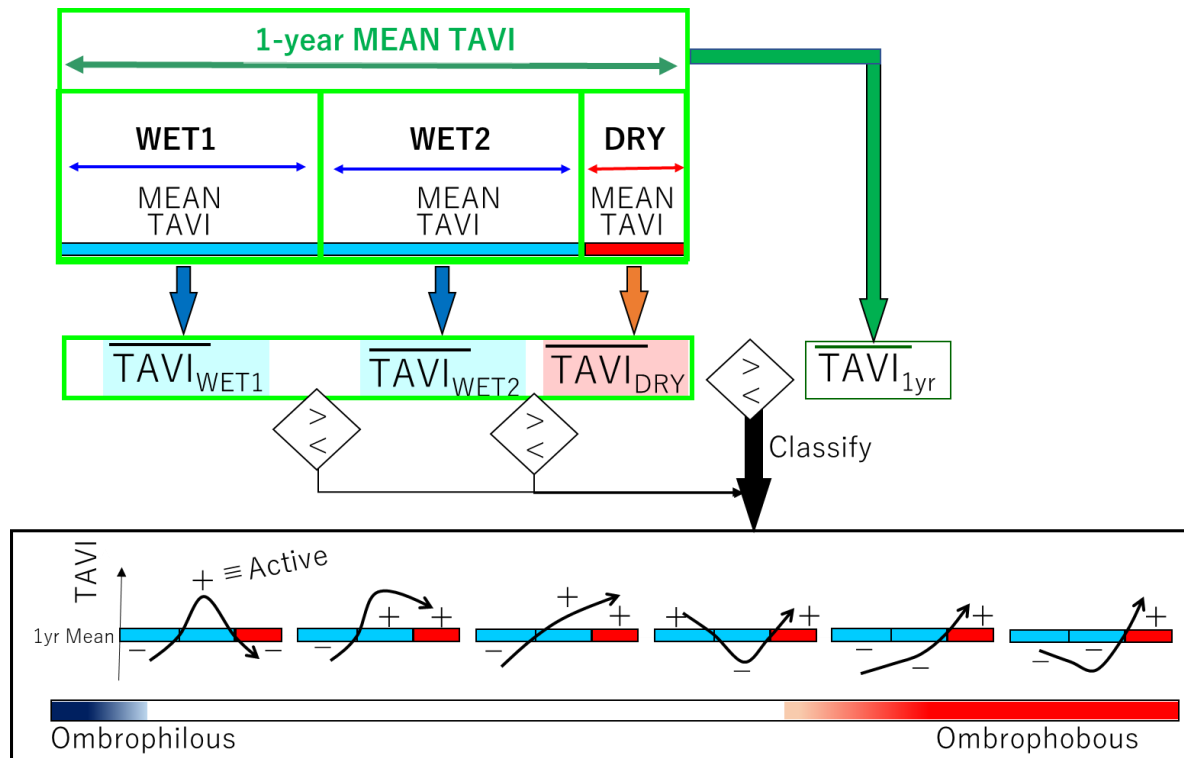


Figure 2-4: Schematic figure on phenology type classification using the Temperature Adjusted Vegetation Index (TAVI) among three seasonal periods in a target year (September 1992 to August 1993) in a peat swamp forest near Palangka Raya, Central Kalimantan.

Figure 2-5: Output map of the phenological schematic figure on discriminating three seasonal periods in a target year (September 1992 to August 1993) in a peat swamp forest near Palangka Raya, Central Kalimantan.

Step 5. Assigning phenological type to peat thickness

As vegetation phenology relates to peat thickness (Fig. X. 1, Table X. 1), the mean thickness value for each phenology type (Table X. 1) can be used to derive an estimated peat thickness map (Fig. X. 6).

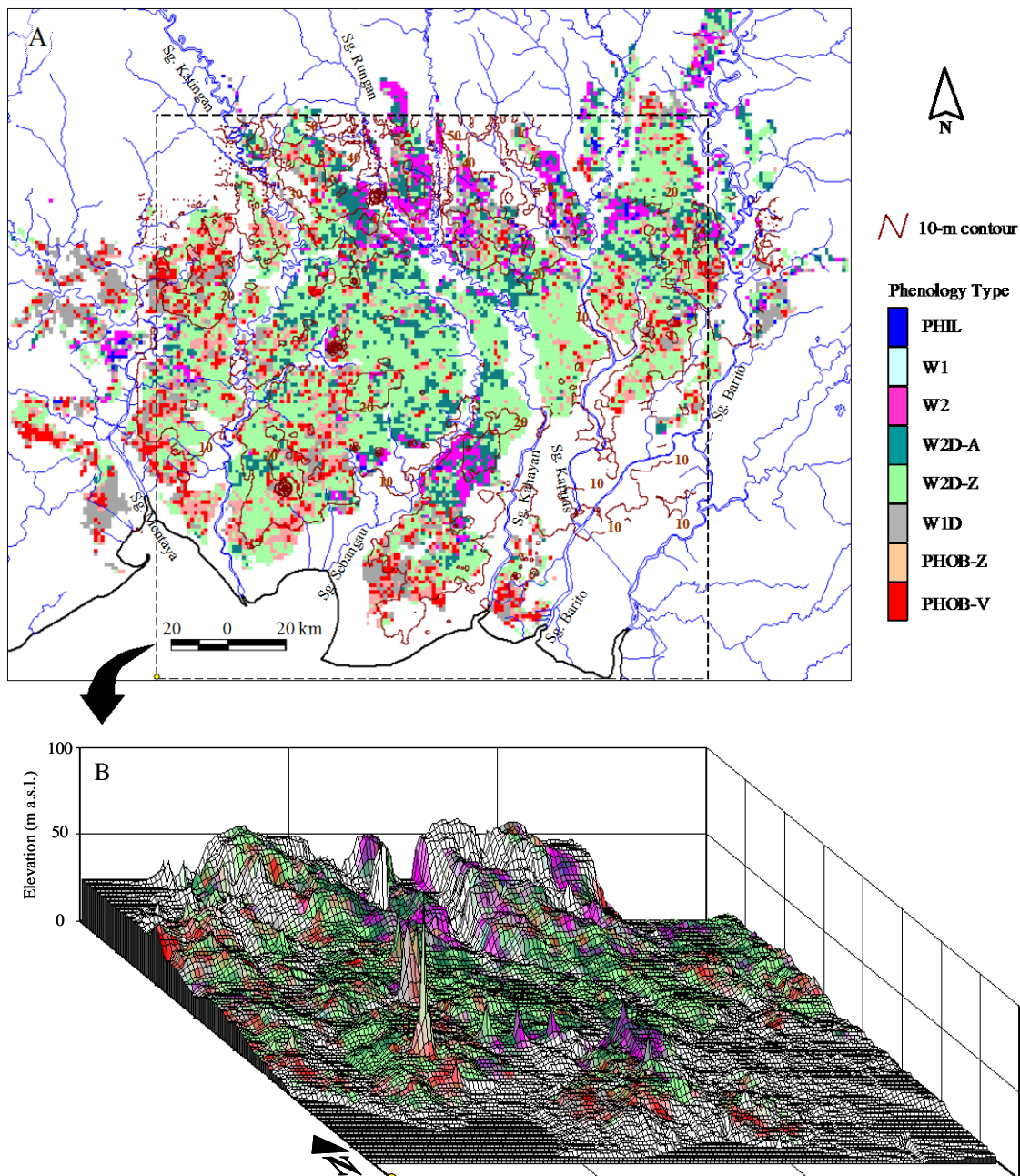


Figure 2-6: Phenology classified map of a peat swamp forest in Central Kalimantan derived using the Temperature Adjusted Vegetation Index derived from National Oceanic and Atmospheric Administration (NOAA) Advanced Very High Radiometer (AVHRR) (September 1992 to August 1993) data. Each phenology type corresponds to a phenological pattern and a specific peat thickness (Table X. 1; cited from Shimada 2001).

REFERENCES

- Shimada S. (2001). Distribution of Carbon in Peat Layer and Estimation of Carbon Mass using Satellite Data in a Tropical Peatland, Central Kalimantan, Indonesia, Hokkaido University Ph.D. thesis.
- Shimada S., Takada, M., Takahasi, H. (2017) Peat Mapping, In: Tropical Peatland Ecosystems (Osaki & Tsuji Eds.) Chapter 31, Springer Japan.



3.1. Ground Water Table (GWL) Monitoring

Groundwater level measurements

GWL is a key parameter for estimating carbon emissions from peat decomposition and burning. Therefore, it is important that GWL is measured in every type of peatland identified based on distinctive land use and land cover characteristics in the study area (see Sub-section 2.2.1). GWL data are collected through the steps described below.

Step 1. Prepare equipment for field measurements

A minimum list of equipment needed for the field measurement of GWL is provided below, and should be adjusted based on the field condition. This guidebook suggests that GWL be monitored and recorded by using the SESAME system¹, which comes with water level, temperature and precipitation sensors (see Figure 3).

- SESAME system
- SIM card for mobile network
- Laptop computer with a modem
- Iron pipe
- PVC pipe
- Eijkelkamp² peat auger
- Cleaver
- GPS receiver
- Compass
- Measuring tape

Activate the SIM card. Top up the card (if it is prepaid) before it expires for seamless data transmission.

Obtain a server access license (user ID and



¹ SESAME system SESAME 01-II: http://www.midori-eng.com/english/image/sesame-01-2_pamph.pdf

² The Eijkelkamp auger is a peat sampler used for soil profile description and classification. The details about the Eijkelkamp auger are available at <https://en.eijkelkamp.com/products/augering-soil-sampling-equipment/peat-sampler.html>.

password) for data acquisition³.

Set up the modem on a laptop computer for data transmission.

Figure 3-1. SESAME system

Test the Internet connection.

Step 2. Select locations for field measurements

Select field measurement locations based on the following conditions:

The locations must be physically accessible and legally permissible for the installation of the SESAME system and its maintenance.

GSM/GPRS/Q-CDMA network coverage is available (because the SESAME system transmits data through the mobile network).

If the network coverage is not available at the ground surface level, an antenna may be mounted above the vegetation canopy to catch the signal.

The locations are representative of distinctive peatland types identified by the remote sensing imagery (see Sub-section 2.2.1 on Peatland Type).

The SESAME system should be installed at every distinctive type of peatland, as the Carbon Emission Model will be developed per peatland type.

The SESAME system should be installed at the CO₂ flux observation sites as well (see Sub-subsection 2.1.2.2).

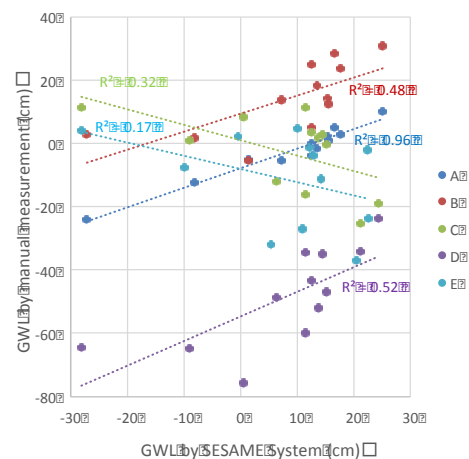
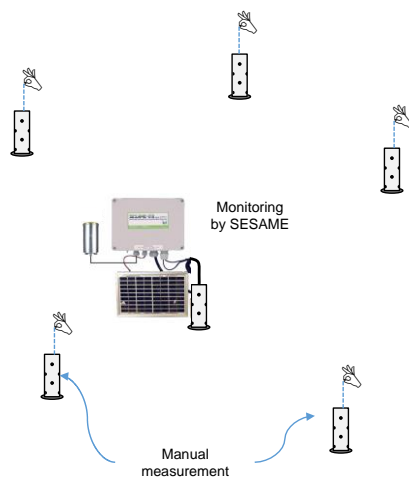
The location is safe from potential thefts of instruments.

³ The server is currently maintained by Midori Engineering Laboratory in Japan. Contact Mr. Yukihsa Shigenaga (email: shigenaga@midori-eng.co.jp; Telephone: +81-11-555-5000; URL: <http://www.midori-eng.co.jp>) for details.

Box 2. How many units of the SESAME system should be installed in the area of interest?

Because GWL is affected by a number of factors including precipitation, vegetation types, land cover, slope of the land, peat depths and water channels (i.e., rivers and canals), there is no single answer to which how many units of the SESAME system are needed in order to represent GWLs over a certain area of peatland. The following method can be adopted to determine the number of SESAME system units to be installed in the study area.

- Install one SESAME system at a sampling location representative of a peatland type based on distinctive land use and land cover characteristics (e.g., drained forest or DF) found in the study area, and measure and record GWL at the location.
- Additionally, set up PVC pipes for manual GWL monitoring randomly in several locations within the same peatland type (DF) in the area. Measure and record GWLs manually at these locations once a month at least for one year. 12 GWL data from each monitoring pipe will be obtained. Then plot GWL data from the SESAME system on the X axis and manual GWL data on the Y axis to obtain their relationships.



- Examine the correlation of each regression line. If the correlation is strong, the data obtained by the SESAME system can be used to represent GWLs at the manual monitoring location. Consider to install another SESAME system at the manual monitoring location which showed a weak correlation.
- Caution needs to be taken for areas in which GWLs tend to change considerably within a short distance and/or short time interval (e.g., areas close to a drainage canal).

Step 3. Install a SESAME system in the selected location

Measure peat depths at the selected location to install the SESAME system.

Install an iron pipe all the way into the mineral soil through the peat layer so that the pipe stays stable (①).

Build a metal platform to hold a rain gauge sensor and the SESAME instrument cabinet. The metal platform must be placed high enough to be free from potential flood damage (②).

Make 0.5 cm diameter holes in a PVC pipe to serve as a water gauge (③).

Install the SESAME instrument cabinet on the iron pipe (④). There is a solar panel on the box. Therefore, the installation must be directed into the sunlight.

Install the rain gauge sensor on the metal platform (⑤).

Install the water logger sensor into the PVC pipe (⑥).

Install an iron pipe all the way into the mineral soil through the peat layer. It must be placed several meters away from the SESAME system (⑦).

Install a ground surface elevation laser sensor into the PVC casing. The laser sensor must be placed high enough to be free from potential flood damages (⑧).

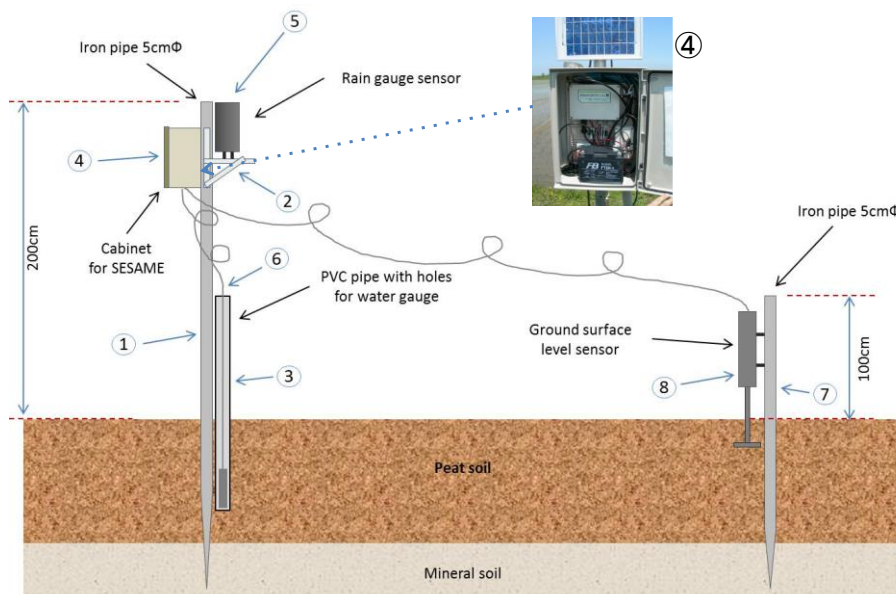


Figure 3-2. Illustration of SESAME system installation

Step 4. Activate the SESAME system and start recording GWL and other microclimate parameters

Check that all components (GWL sensor, rain gauge, temperature sensor and ground surface elevation sensor) are working properly.

Activate the SESAME system and start recording GWL at the interval of 10 minutes and other microclimate parameters (i.e., precipitation and air temperature).

Check that the data from the SESAME system are transmitted to the server without any errors. If there are errors, you must check whether the SESAME system is properly installed in the field.

3.2. Soil Moisture Mapping with a Remote-Sensing Dataset

Step 1. Download an existing peatland map

A peatland map of the study area is needed to delineate peatland from non-peat areas. Indonesia has several peatland maps developed by various institutions and organizations, including the Ministry of Agriculture (MoA) and Wetlands International (WI) (see Figure 2). These are the most frequently cited maps in Indonesia. Peatland maps (in ESRI shape file) from these sources may be obtained by sending a formal letter of request.

Ministry of Agriculture
<http://www.pertanian.go.id>

Wetlands International
<http://indonesia.wetlands.org/Infolahanbasah/PetaSebaranGambut/tabid/2834/language/id-ID/Default.aspx>

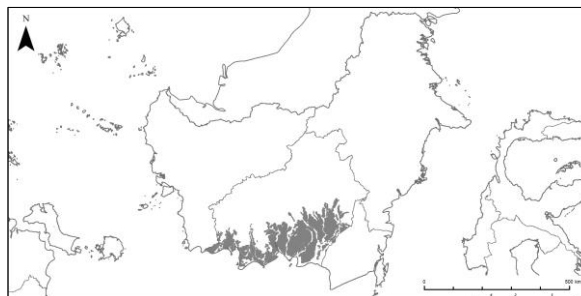


Figure 2. Peatland map of Central Kalimantan by Wahyunto, et al. (2004)

Box 1. An alternative approach: Create a new peatland map

A new peatland map can be developed by using a spatial model. There are various methodologies to create a new peatland map, and the following is an example.

- Obtain and pre-process satellite imagery of the study area. In order to reduce data gaps and improve interpretation, it is recommended to use a combination of medium- to high-resolution optical satellite images as well as Synthetic Aperture Radar (SAR) data.
- Obtain BIG (Badan Informasi Geospasial) topography maps at the 1:50,000 scale and SRTM digital elevation model data. These data are used to determine geomorphological features such as peat dome structures and hydrological networks of the study area.
- Obtain NOAA Advanced Very High Resolution Radiometer (AVHRR) data of selected years from the USGS Global Land 1-km AVHRR Project, and evaluate vegetation activities by normalized difference vegetation index (NDVI). In order to estimate accurate peatland distribution in the study area, it is recommended that the NDVI analysis be based on the land cover of the past (e.g., 1990), when peatland was relatively undisturbed and its original condition and distribution could be assessed.
- Conduct ground-truthing to verify peat and non-peat areas in the study area.
- Manually delineate peat boundaries on a GIS platform based on the NDVI values, slope raster data, and morphological and hydrological network information obtained through remote sensing analyses. Peatlands generally occur on gentle slope areas with slope angles of less than or equal to 0.2° , and manual delineation should be conducted in reference to such areas.
- Conduct a geo-statistical analysis to estimate peat thickness distribution within the study area.
- Based on the distribution of peat thickness, filter out areas with peat thickness less than 50 cm (according to the definition of peatland), and develop the final peatland map of the study area.

Step 2. Download soil moisture data

Download soil moisture data from an available source to be used to estimate the spatial distribution of GWLs in the study area.

One source of global soil moisture data available for free of charge is the volumetric soil water layer product of the European Center for Medium-Range Weather Forecast (ECMWF). It is available at <http://apps.ecmwf.int/datasets/data/interim-full-daily/>.

Before downloading the data, you must select the applicable time-series (i.e., daily), coordinate system (e.g., WGS 84), coordinates, and grid size (e.g., 0.5 degrees). They must match those applied in Step 2 of Sub-section 2.2.1 (Peatland Type).

Step 3. Download NCAR/NCEP soil moisture data

Another source of global soil moisture data that is freely available and can be used to estimate the spatial distribution of GWL in the study area is the volumetric soil water layer product of NCEP (<https://rda.ucar.edu/datasets/ds083.2/>). After registration, a Grigs2 six-hourly file of soil moisture data can be obtained. These data have a resolution of $\sim 0.25^\circ \times 0.25^\circ$ and can be downscaled to $1 \text{ km} \times 1 \text{ km}$ by using NOAA land surface models that have been installed in the Weather Research and Forecasting (WRF) software.

Step 4. Download forest cover change data

Download a forest cover change data product from an available source to be used to identify forest and non-forest areas in the study area.

One source of forest cover change data is the Global Forest Change product developed by NASA, available at <https://earthenginepartners.appspot.com>.

Step 5. Download surface reflectance data

Download a surface reflectance data product from an available source to be used to identify undrained and drained areas in the study area.

One source of surface reflectance data is the MODIS surface reflectance product (MOD09A1), available at <http://modis.gsfc.nasa.gov/data/dataproduct/mod09.php>.

This MODIS surface reflectance product allows you to identify these areas based on plant physiological responses to different degrees of dryness on vegetated land surfaces.

Step 6. Download burned area data

Download a burned area data product from an available source to be used to estimate the spatial distribution of burned areas in the study area.

One of the burned area products available globally is MODIS burned area product (MCD45A1). It is available at <http://modis.gsfc.nasa.gov/data/dataproduct/mod45.php>.

Original imagery data obtained by aerial photography may be used in combination with the MODIS burned area product to improve the accuracy.

Advanced techniques such as LiDAR (Light Detection and Ranging) and PALSAR-2 (Phased Array type L-band Synthetic Aperture Radar) may be used if they are available and applicable. They are high resolution and can determine ground surface levels with an accuracy of several centimeters. However, even if these high-resolution remote sensing techniques are adopted, field measurements must still be conducted for ground-truthing purposes (see Sub-subsection 2.1.2.3 on Burn Scar Measurements).

3.3. Groundwater level (GWL) analysis

The SESAME system records real-time GWL data at a 10-minute interval (see Sub-subsection 2.1.2.1). The data must be downloaded from the server and analyzed to obtain the lowest monthly average GWL(s) in the study year(s). This value will be used as a key parameter for the Carbon Emission Models explained in Sections 2.3 and 2.4. Obtain at least several lowest monthly average GWL values in the study years (i.e., several continuous years of GWL observation) in order to improve the accuracy of the models.

Step 1. Download raw data from the SESAME server

Access the SESAME server and download raw GWL data for the selected time and location via the procedures described in Annex 2.

You must install the SESAME software on your computer first to be able to access the server. To obtain this software, contact Midori Engineering Laboratory.

Step 2. Organize the raw data into observation data

Make a .csv file (e.g., Excel), and add field names to the spreadsheet.

Organize the downloaded raw data as observation data for each variable (i.e., GWL, precipitation, and ground surface level) via the procedures described in Annex 3.

Repeat this for all downloaded raw data collected at each type of peatland.

Check to see if data are complete.

If there are missing data for a short time period, make an interpolation and fill the data gaps.

If data gaps are caused by mobile network failure, the missing data can also be obtained directly from the SESAME system (data logger). The SESAME system stores data in a memory card for three months.

Step 3. Convert the observation data into daily average values for each parameter

Take the daily average of each observation data recorded at a 10-minute interval.

Add the daily average values for each variable in a new column on the spreadsheet (see Figure 12).

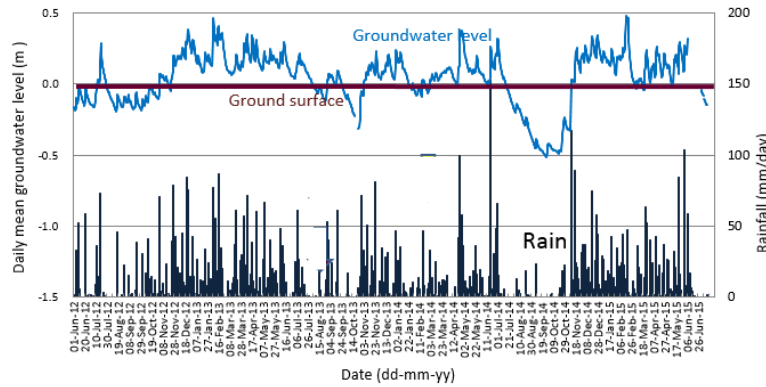


Figure 12. Example for time-series daily average GWLs with other parameters

Step 4. Obtain a linear relationship between daily soil moisture and daily average GWL for each type of peatland

Draw a scatter graph by plotting the observed (measured) daily average GWLs on the Y-axis and the remote-sensing based daily soil moisture data of all grid cells on the X-axis.

Soil moisture data can be obtained in the procedure explained in Step 2 of Sub-section 2.1.1, and daily average GWL values obtained in Step 3 above.

Obtain a linear regression equation between the daily soil moisture and the daily average GWL.

Repeat this for all peatland types (see Figure 13). The equations obtained for the regression lines will be used to simulate daily average GWLs at each peatland type in all other grids throughout the study area.

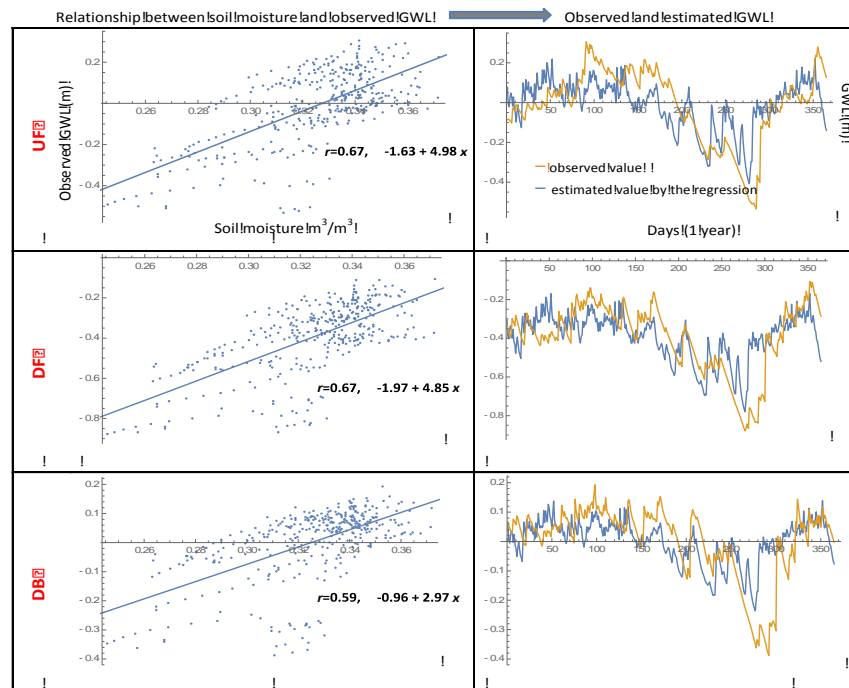


Figure 13. Example of GWL estimations for each peatland type based on the relationship between soil moisture and observed GWL data

Step 5. Estimate daily average GWL values in all other grid cells

Estimate daily average GWL at each peatland type in all other grid cells, using the equations obtained in Step 4 above and daily soil moisture data in each grid.

Step 6. Obtain the estimated monthly average GWL values in all other grid cells

Calculate monthly average GWL at each peatland type in all other grid cells based on the estimated daily average GWL values obtained in Step 5 above.

Step 7. Find the lowest value of the estimated monthly average GWLs for each peatland type in every grid cell

Find the lowest value from the estimated monthly average GWLs of the selected year obtained in Step 6 above.

Repeat this for each peatland type in every grid cell. These values are the **lowest monthly average GWLs in the study year** used as a key parameter for estimating annual average carbon emissions as described in Sections 2.3 (Carbon Emission Model from Peat Decomposition) and 2.4 (Carbon Emission Model from Peat Burning).

3.4. Ground Water Level Mapping

The GWL instrument (such as SESAME) results suggest a strong relationship between GWL and soil moisture in peatlands. This fact can be used to create a GWL map based on the soil moisture map. Required steps are described as follow:

1. Select the area of interest and download soil moisture data from <https://rda.ucar.edu/datasets/ds083.2/>. The data contain 52 layers of atmospheric moisture and four layers of soil moisture collected every six hours. The data can be downloaded from other sources such as ECMWS but in the Gribs file format. The data typically have a resolution of $0.25^{\circ} \times 0.25^{\circ}$.
2. Downscale the grid resolution into a $1 \text{ km} \times 1 \text{ km}$ mesh with a land surface model. The most powerful model is called the Weather Research and Forecasting (WRF) model. The WRF model is a numerical weather prediction and atmospheric simulation system designed for both research and operational applications. WRF is run in the Linux environment so Linux Ubuntu, HDF5, NetCDF, WRF v. 9, and NCL software should be installed. First, initial data from NCEP are processed by the preprocessing procedure using the WPS module. Make the grid by using the geogrid, ungrib, and met grid. Then process the initial data by running WFR. For three days of simulation, the system requires six hours of processing. WRF have four numerical domain D01 (largest area), D01, D02, and D04 (the smallest area). The WRF result of soil moisture map with the D0 domain is depicted in Figure 14.

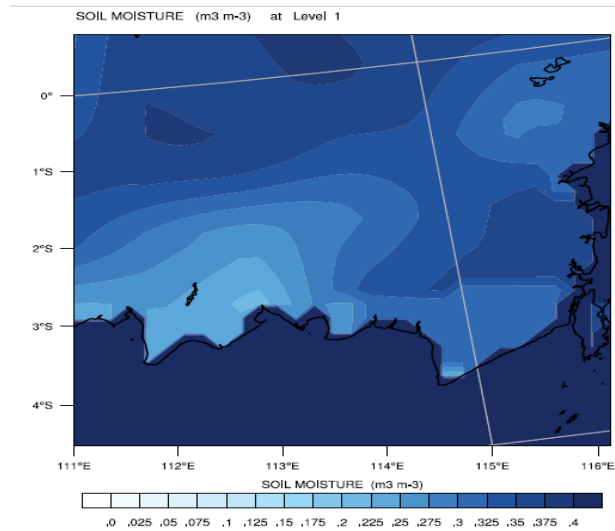


Figure 14: Soil moisture map from WRF output in the D01 domain.

3. Overlay the map with the peatland map to obtain the soil moisture map of the peatland area

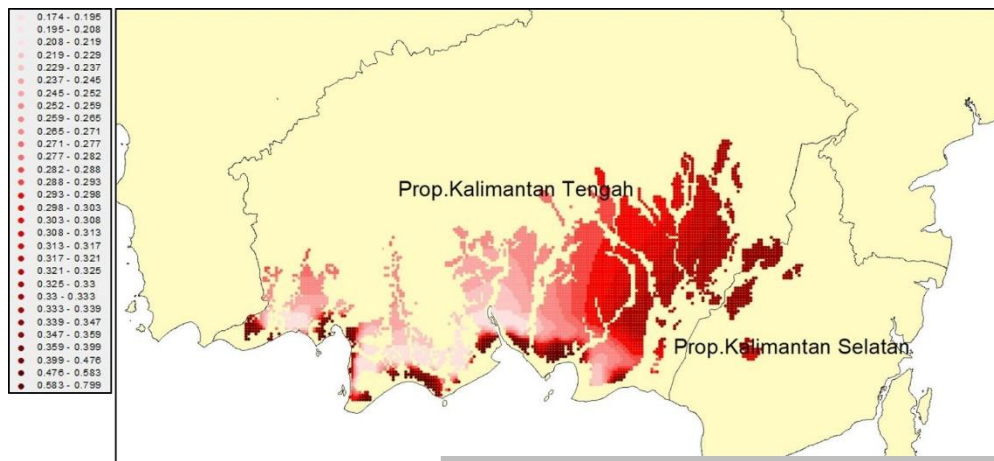


Figure 15: Soil moisture map of peatlands in Central Kalimantan.

4. Apply the empirical formula between soil moisture and GWL (Fig. 13) with three categories (i.e., UF, DF, and DB) to obtain the GWL map as follows (Fig. 16);l

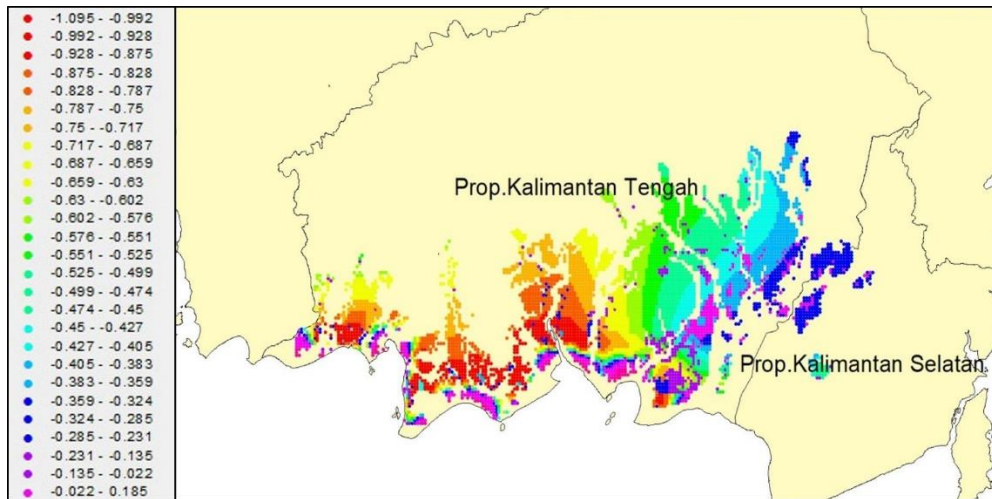


Figure 16: Ground Water Level map of peatlands in Central Kalimantan

4.1.3. Carbon Emission Model from Peat Decomposition

4.1.3.1. Carbon Emission Mapping

Box 1: What is a Carbon Emission Model from Peat Decomposition?

The Carbon Emission Model from Peat Decomposition is based on the assumption that there is a linear relationship between NEE and GWL. Based on this relationship, the model allows the estimation of the annual NEE of the study area using the lowest monthly mean GWL in the study year(s) as a key parameter.

NEE is the difference between the amount of CO₂ that is emitted by ecosystem respiration (RE) and absorbed by photosynthesis (gross primary production). Therefore, the relationship between net ecosystem production (NEP) and NEE is given by:

$$NEE = -NEP$$

$$NEP = GPP - RE$$

RE is found to increase with soil temperature and decrease as GWL (or soil moisture) rises. In forest ecosystems, CO₂ exchange between biomass and atmosphere usually occupies most of the carbon flow. If other carbon sources are negligible, the carbon balance of the forest ecosystem can be determined by NEE as follows:

- NEE > 0: carbon source (emission)
- NEE = 0: carbon neutral
- NEE < 0: carbon sink

Step 1. Obtain a linear relationship between the observed lowest monthly mean GWL in the study year(s) and annual NEE

Use the lowest monthly average GWL value for each peatland type selected from the observed monthly average GWL in the study years as described in Step 7 of sub-section 2.2.2. Use the annual NEE values for each peatland type obtained in sub-section 2.2.3.

Draw a linear regression line between the observed lowest monthly mean GWL in the study year(s) on the *x*-axis and observed annual NEE on the *y*-axis and obtain a relationship for each peatland type (Fig. 14) in the study area. Each regression equation obtained in this step will be used to estimate annual NEE values throughout the study area. The equation can be used to estimate NEE or CO₂ emissions for different years or other locations in the study area based on the estimated spatial distribution of GWL.

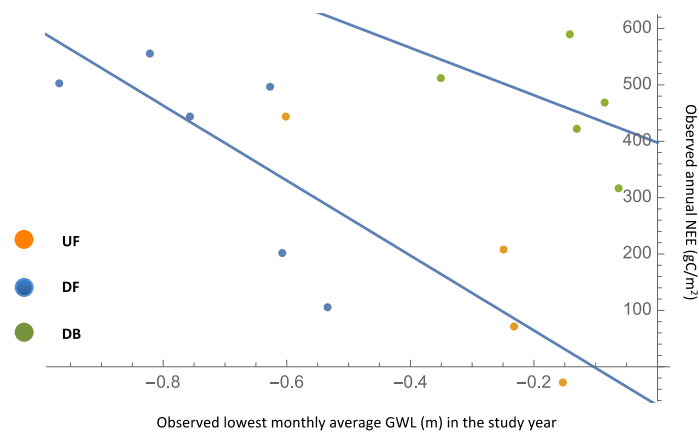


Figure 14: Example of relationships between the lowest monthly mean GWL (m) in the study years and annual NEE ($\text{g C m}^{-2} \text{ year}^{-1}$) observed in Central Kalimantan (Hirano et al., 2012)

Step 2. Estimate annual NEE using the estimated lowest monthly mean GWL in the study year(s) in all other grid cells

Estimate annual NEE for each peatland type in all other grid cells (i.e., areas beyond the observation points) using the equations obtained in Step 1. Use the estimated lowest monthly mean GWL value in the study year obtained in Step 7 of sub-section 2.2.2. Calculate the total NEE from the study area by summing up NEE values from each grid cell using the following equation:

$$T = \sum_{i=1}^N A_i [a_i X_i + b_i Y_i + g_i Z_i + \dots] \quad \text{eq (13)}$$

Where,

T : total NEE,

A_i : peatland area in grid cell i ,

α_i : the ratio of peatland type X area in grid cell i ,

β_i : the ratio of peatland type Y area in grid cell i ,

γ_i : the ratio of peatland type Z area in grid cell i ,

X_i : NEE value of peatland type X area in grid cell i ,

Y_i : NEE value of peatland type Y area in grid cell i ,

Z_i : NEE value of peatland type Z area in grid cell i ,

N : the number of grid cells.

Step 3. Generate a map of estimated annual CO_2 emissions

Generate a map of estimated annual CO_2 emissions (positive NEE values) based on the grid file created in Step 2 of sub-section 2.2.1. and the NEE values obtained in Step 2. Fig. 15 shows an example of annual NEE maps for 2012 in Central Kalimantan created on a 0.5° grid file.

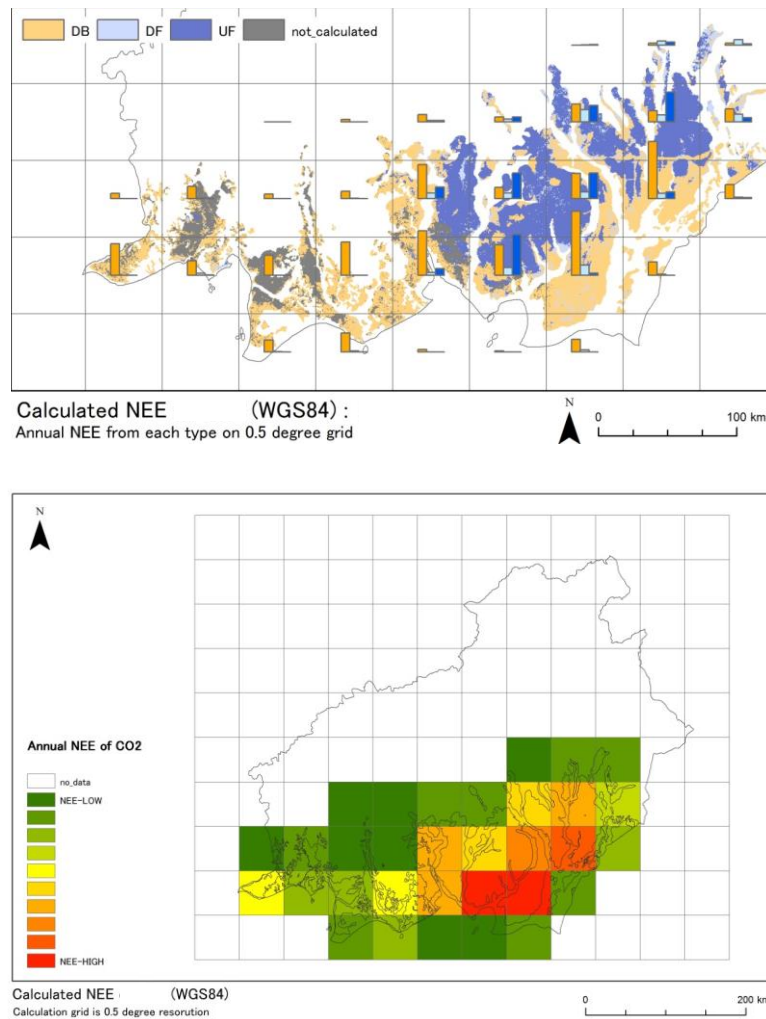


Figure 15: Map of estimated annual NEE values for each peatland type (top) and for total NEE (bottom) in 2012 on grid files for Central Kalimantan

4.1.3.2. Carbon Emission from Time Series Data

Time-series data of GWL can be used to estimate a time series of carbon emission of peat decomposition by applying the Hirano model. We describe the procedure as follows.

Step 1: Obtain time-series data with a daily time interval from the SESAME instrument

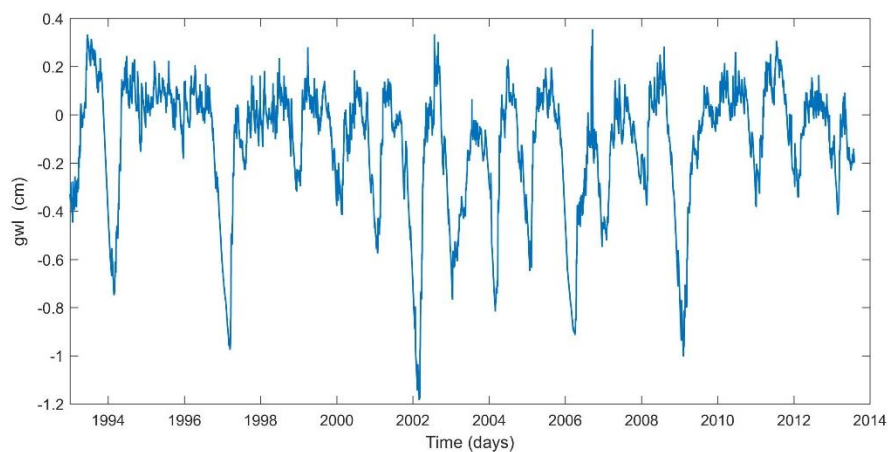


Figure 16: Time series of Ground Water Level in Central Kalimantan

Step 2: Apply the Fast Fourier Transform to obtain the GWL spectrum

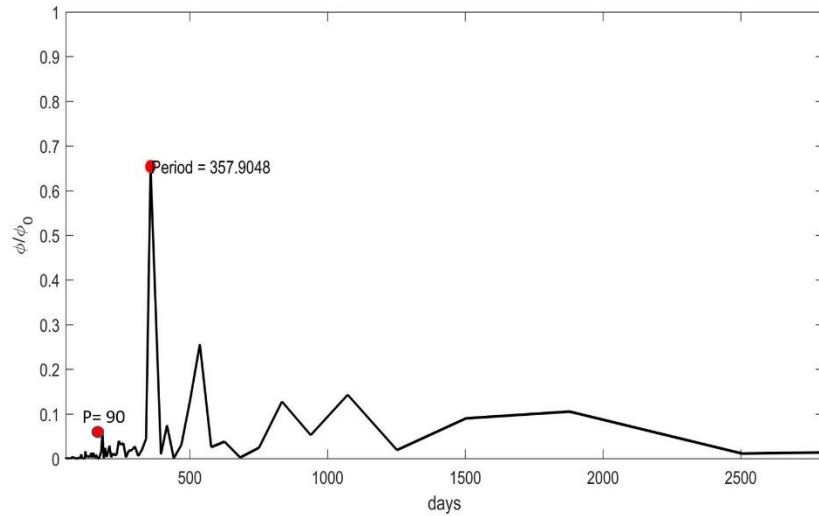


Figure 17: Normalized Ground Water Level power spectrum

Step 3: Due to the significance of the power spectrum over more than 90 days, this should be used as a cut-off frequency in a lowpass filter (Fig. 18)

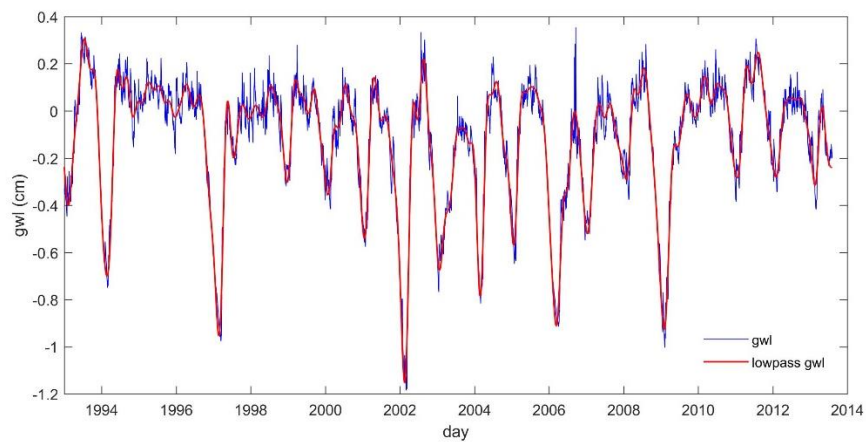


Figure 18: Ground Water Level time series with the lowpass filter with a cutoff period of 90 days

Step 4: Apply the Hirano model to obtain a time series of carbon emission (Fig. 19)

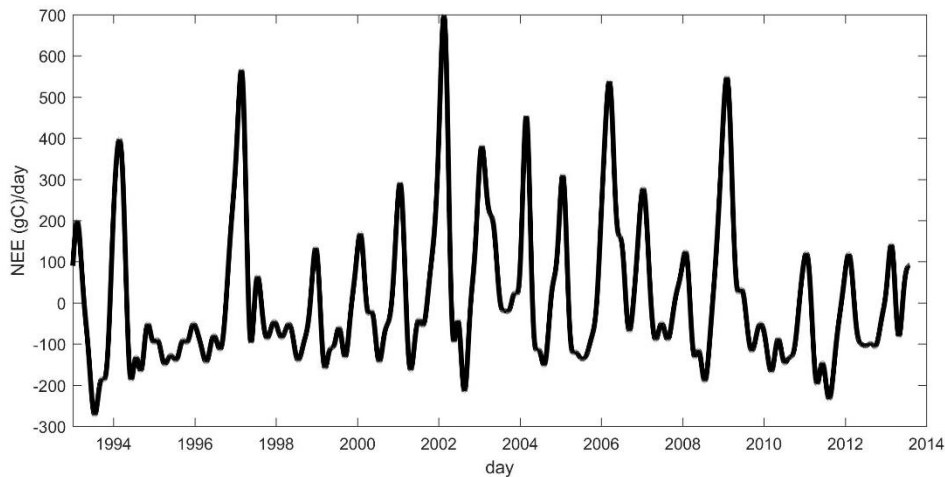


Figure 19: Time series of carbon emission of peat decomposition
A positive value indicates carbon emission and a negative value indicates a carbon sink.

3.5. Ground Water Level Prediction

L

❖ What will you learn in Part III? ❖

- How to predict daily groundwater level (GWL) for several days ahead
 - ✓ Key points to understand:
 - The GWL Prediction Model uses the Kalman Filter technique introduced by Rudolf E. Kalman.
 - The Kalman filter is an algorithm or mathematical calculation which uses time-series values observed over time and returns estimates of uncertain variables in a linear system. It separates time-series noise, and can be used to estimate the past, present and future state of the variables (i.e., GWL).
 - The GWL Prediction Model takes a linear model based on the observed GWL values. This means that the future state of the variables (i.e., predicted GWL) has a proportional value to the current average value and statistical noise.
 - The model reduces the noise from the observed GWL values. In this model, the slope is assumed constant.
 - It is useful to apply the GWL Prediction Model in practice. **40 cm below the ground surface** is the threshold of GWL not only for preventing peatland fires but also for keeping peat carbon stored belowground.

Groundwater level can be used as an ecological indicator for peatland management. Lowering GWL causes various ecological disturbances such as carbon emissions, damages to faunal and floral species, loss of ecosystem services, and devastating peatland fires. Early information about the condition of GWLs will help local authorities, land managers and local communities prevent the occurrence of such disturbances and act upon them in a timely manner. The GWL Prediction Model forecasts GWLs for several days ahead.

Surface peat fires tend to start when the GWL drops to about 20 cm below the ground surface, and expand to the surrounding area when it becomes lower than 40 to 50 cm (Putra et al., 2008). Similarly, it is necessary to maintain the GWL higher than 40 cm below the ground surface in order to make replanting successful and minimize fire risks (Wösten et al., 2006).

Figure 17 shows the framework of the GWL Prediction Model. It only uses observed daily average GWLs obtained in Step 3 of Sub-section 2.2.2 (GWL analysis). Therefore, the data collection and analysis procedures can be seen in the relevant sections above (see 2.1.2.1 on GWL measurements and 2.2.2 on GWL analysis), and will not be repeated in this section.

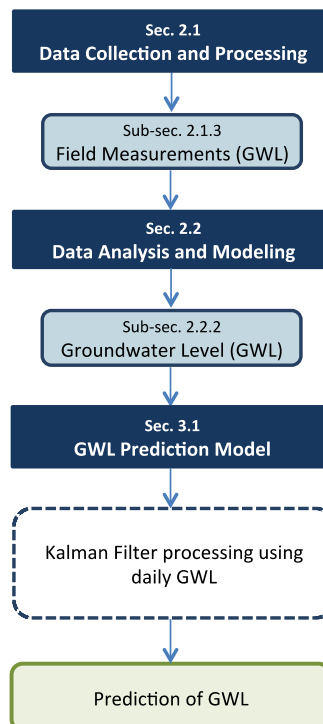


Figure 17. Framework for the GWL prediction

3.5.1. Takahashi Model on Groundwater Level Prediction

Step 1. General understanding of water balance in peatland ecosystem

Term definition and dimension in this section

Groundwater level, GWL, [m]: the height of groundwater table on the basis of ground surface level

Daily mean GWL: Average of hourly GWL from 0 o'clock to 24 o'clock.

Daily change of GWL, dGWL: Difference of GWL between at 0 o'clock and 24 o'clock.

Daily total rainfall, [mm day⁻¹]: Total amount of rainfall from 0 o'clock to 24 o'clock.

For GWL prediction, a general and correct understanding of water balance in peatland ecosystem is necessary. The peatland ecosystem is generally consisted from three basic layers, vegetation, peat and mineral soil layers (Fig. 3.5.2-1). The permeability of the mineral soil layer is generally low, so then the surface groundwater is held in peat layer. The peat layer is divided into the saturated and the unsaturated layers, below and above the groundwater table.

The main water resource to the peatland is rainfall in tropical area. Some part of rainfall is intercepted by vegetation and evaporated to the atmosphere directly. The most of rainfall reaches to the peat layer and increases the volume of unsaturated layer and the moisture of unsaturated layer.

The water in the peat layer uses for evapotranspiration, evaporation from ground surface and transpiration through vegetation, and horizontal outflow of groundwater through peat layer, actually the difference of in- and outflow of groundwater from the upper section and to the lower section. The amount of water loss through the mineral soil layer is not so large because of the low permeability of the mineral soil layer.

In the case of a tropical peat swamp forest in the Sebangau River catchment, the 51% of rainfall was used for evapotranspiration and the remains was used for outflow and change of ground water level (Kayama, M. et al., 2000).

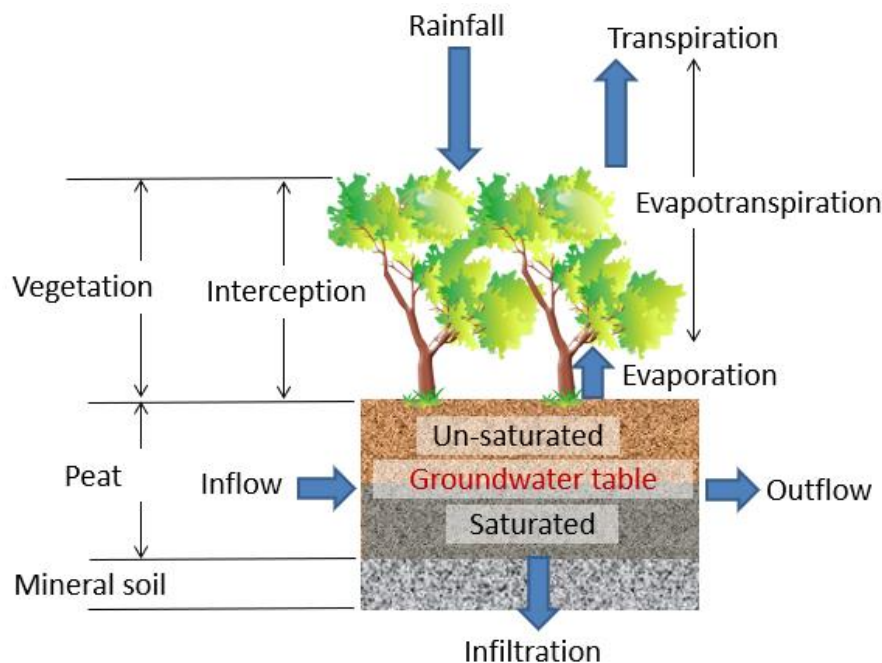


Fig. 3.5.2-1. Water balance of peatland ecosystem

Step 2. Water balance model for prediction of GWL in peatland ecosystem

Water balance in a peat layer is shown in Eq. 3.5.2-1 with several hypothesis as follows, The interception of rainfall by vegetation is zero, the change of water content in the unsaturated peat layer is zero, the infiltration through the mineral soil layer is zero, and the runoff is a difference of inflow and outflow in saturated layer of peat.

$$dW = dW_{rain} - dW_{loss} \quad \text{Eq. 3.5.2-1}$$

Where dW : Daily change of GWL,

dW_{rain} : Daily change of GWL by daily rainfall,

dW_{loss} : Daily loss of GWL by horizontal runoff and evapotranspiration

In the case of the tropical peat swamp forest, the evapotranspiration has no big difference through a year with $3\text{-}4 \text{ mm day}^{-1}$ (Takahashi, H., 1999). So then, daily changes of GWL by horizontal runoff and evapotranspiration are combined to daily change of GWL as dW_{loss} .

Daily horizontal runoff in a peatland, which was estimated from the change of GWL during night, was shown as a function of GWL (Takahashi, H. et al, 2000). The dW_{loss} is also shown as a function of GWL as follows in this section.

$$dW_{loss} = f_1(W) \quad \text{Eq. 3.5.2-2}$$

where W: Distance of GWL from the ground surface.

The daily change of GWL, dW_{rain} by daily rainfall is calculated by following equation which is drawn from Eq. 3.5.2-1.

$$dW_{rain} = dW + dW_{loss} \tag{Eq. 3.5.2-1'}$$

The value of dW_{rain} has a linear relation with the amount of the daily rainfall (Umeda, Y. and Inoue T., 1985, Takahashi H. and Yonetani Y., 1997). But the relationship between the daily amount of rainfall, R, and the daily change of GWL, dW_{rain} is shown in following equation,

$$dW_{rain} = f_2(R) \tag{Eq.3.5.2-3}$$

where R: daily amount of rainfall.

The $f_2(R)$ is decided by data of field observation in the site in this section.

Step 3. Procedure for GWL prediction

Definition of daily GWL is the height of groundwater table on the basis of ground surface level at 0 o'clock of the day, and the definition of daily rainfall is the accumulated rainfall from 0 o'clock to 24 o'clock of the day.

Determination process of Eq. 3.5.2-2 and Eq. 3.5.2-3, which are the key equations for GWL prediction, is described using the data measured in the peatland of Central Kalimantan.

Procedure-1. Determine $f_1(W)$ in Eq. 3.5.2-2

- Data-1: Daily GWL [m] at 0 o'clock ----- Column S in Fig. 3.5.2-2.
- Data-2: Daily total rainfall [mm day⁻¹] ----- Column W in Fig. 3.5.2-2.
- Data-3: Daily mean GWL [m] ----- Column Y in Fig. 3.5.2-2.
- Data-3: Daily change of GWL [m] ----- Column AA in Fig. 3.5.2-2.

	A	B	C	D	S	W	Y	AA
	y	m	d	h	Daily GWL (m)	Daily total rain (mm/day)	Daily mean GWL (m)	dGWL/day (m)
1								
2	2016	5	14	0	-0.15	7.5	-0.161	-0.014
3	2016	5	15	0	-0.164	4.8	-0.12	0.052
4	2016	5	16	0	-0.112	1	-0.096	0.012
5	2016	5	17	0	-0.1	17.5	-0.104	-0.006
6	2016	5	18	0	-0.106	0	-0.125	-0.038
7	2016	5	19	0	-0.144	0	-0.158	-0.031
8	2016	5	20	0	-0.175	0	-0.189	-0.03
9	2016	5	21	0	-0.205	0	-0.219	-0.032
10	2016	5	22	0	-0.237	0	-0.242	-0.014
11	2016	5	23	0	-0.251	29	-0.238	0.039
12	2016	5	24	0	-0.212	4.5	-0.225	-0.025
13	2016	5	25	0	-0.237	3.5	-0.238	0
14	2016	5	26	0	-0.237	0	-0.248	-0.025
15	2016	5	27	0	-0.262	0	-0.27	-0.025
16	2016	5	28	0	-0.287	0	-0.292	-0.016
17	2016	5	29	0	-0.303	54.5	-0.281	0.134
18	2016	5	30	0	-0.169	0	-0.193	-0.031
19	2016	5	31	0	-0.2	11	-0.181	0.028
20	2016	6	1	0	-0.172	0	-0.179	-0.015
21	2016	6	2	0	-0.187	0	-0.2	-0.025
22	2016	6	3	0	-0.212	106.5	-0.197	0.156

Fig. 3.5.2-2. Sheet-1: Daily total rainfall [mm day⁻¹] and Daily change of GWL [m]

	A	B	C	D	E	F	G	H	I
	y	m	d	daily total rain (mm/day)	Daily mean GWL (m)	dGWL/day (m)	-mean GWL (m)	-mean GWL (m)+0.4	-dGWL/day (m)
1									
2	2016	5	19	0	-0.158	-0.031	0.158	0.558	0.03
3	2016	5	20	0	-0.189	-0.03	0.189	0.489	0.03
4	2016	5	21	0	-0.219	-0.032	0.219	0.519	0.03
5	2016	5	22	0	-0.242	-0.014	0.242	0.542	0.01
6	2016	5	27	0	-0.27	-0.025	0.27	0.57	0.02
7	2016	5	28	0	-0.292	-0.016	0.292	0.692	0.01
8	2016	6	2	0	-0.2	-0.025	0.2	0.6	0.02
9	2016	6	6	0	-0.052	-0.038	0.052	0.452	0.03
10	2016	6	7	0	-0.098	-0.044	0.098	0.498	0.04
11	2016	6	8	0	-0.14	-0.043	0.14	0.54	0.04
12	2016	6	9	0	-0.174	-0.029	0.174	0.574	0.02
13	2016	6	21	0	-0.275	-0.02	0.275	0.675	0.03
14	2016	6	22	0	-0.292	-0.014	0.292	0.692	0.01
15	2016	6	23	0	-0.31	-0.022	0.31	0.71	0.02
16	2016	6	24	0	-0.33	-0.018	0.33	0.73	0.01
17	2016	6	30	0	-0.393	-0.018	0.393	0.793	0.01
18	2016	7	5	0	-0.442	-0.013	0.442	0.842	0.01
19	2016	7	6	0	-0.455	-0.014	0.455	0.855	0.01
20	2016	7	7	0	-0.471	-0.016	0.471	0.871	0.01
21	2016	7	11	0	-0.486	-0.019	0.486	0.886	0.01
22	2016	7	12	0	-0.502	-0.014	0.502	0.902	0.01
23	2016	7	15	0	-0.517	-0.013	0.517	0.917	0.01
24	2016	8	7	0	-0.421	-0.025	0.421	0.821	0.02
25	2016	8	8	0	-0.44	-0.013	0.44	0.84	0.01
26	2016	8	9	0	-0.454	-0.012	0.454	0.854	0.01
27	2016	8	10	0	-0.472	-0.025	0.472	0.872	0.02
28	2016	8	11	0	-0.491	-0.013	0.491	0.891	0.01

Fig. 3.5.2-3. Sheet-2: Selected Daily total rainfall [mm day⁻¹] and Daily change of GWL [m]

#1. Prepare Data-1 (Daily GWL [m] at 0 o'clock). Data-2 (Daily total rainfall [mm day⁻¹]) and in Sheet-1.

- #2. Calculate Data-3 (Daily change of GWL [m]) which is the difference of Daily GWL and it of next day in Sheet-1.
- #3. Select the day without rainfall excepting next day of rainfall in Sheet-1. The green color column are selected days.
- #4. Selected days are listed in Sheet-2.
- #5. Signs of Daily mean GWL and Daily change of GWL in columns E and F are changed from minus to plus and enter columns G and I for easy search of functional relationship together. The values of the columns G and I mean the distance of the groundwater table from the ground surface and the amount of daily loss of groundwater level.
- #6. Add an experimental factor $\alpha = 0.4$ in this case, to column G and enter column H.
- #7. Determine the suitable function for Eq. 3.5.2-4 using the approximate curve system of the Excel. The logarithmic function is the most suitable one for relationship between GWL and the daily loss of GWL in this case. But if the experimental factor α is not used in the equation, the loss of GWL will approach to the infinity as GWL approach to ground surface as shown in Fig. 3.5.1-4a. The experimental factor $\alpha = 0.2$ is used in this analysis, Fig. 3.5.2-4a.

Finally, Eq. 3.5.2-2 is decided as next equation.

$$dW_{loss} = -0.028 \ln(W - 0.2) + 0.012 \quad \text{Eq. 3.5.2-4}$$

where dW_{loss} : Daily loss of GWL by horizontal runoff and evapotranspiration
W: Distance of GWL from the ground surface.

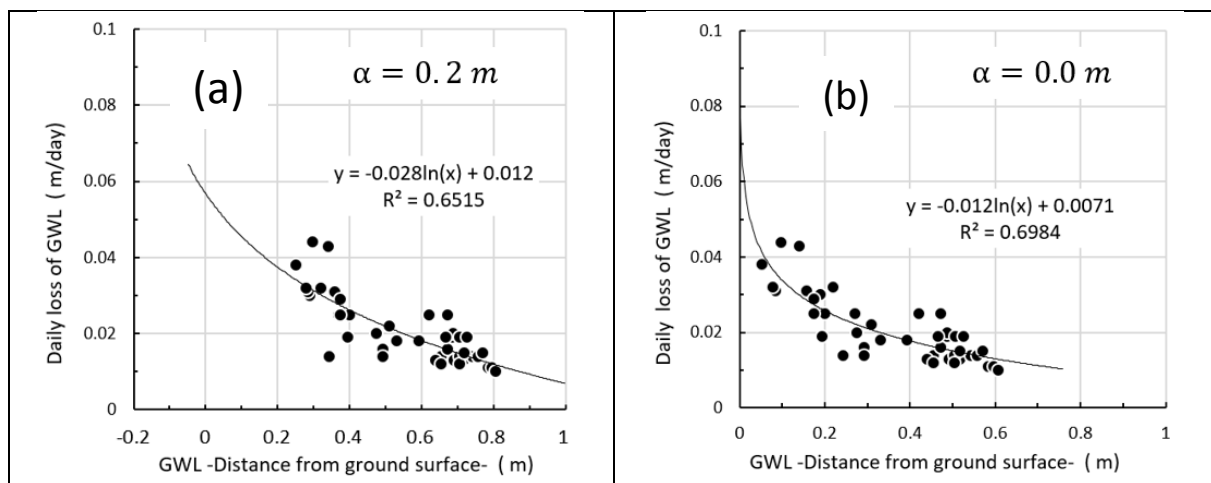


Fig. 3.5.2-4. Relationship between GWL and the daily loss of GWL with (a) and without (b) the experimental factor $\alpha = 0.2$.

Procedure-2. Determine $f_2(R)$ in Eq. 3.5.2-3

- Data-1: Daily GWL [m] at 0 o'clock ----- Column S in Fig. 3.5.2-5.
- Data-2: Daily total rainfall [mm day⁻¹] ----- Column W in Fig. 3.5.2-5.
- Data-3: Daily mean GWL [m] ----- Column Y in Fig. 3.5.2-5.
- Data-3: Daily change of GWL [m] ----- Column AA in Fig. 3.5.2-5.

- #1. Calculate the daily loss of GWL using Eq. 3.5.2-4 and enter the result in the column AB in the Sheet-1 (Fig. 3.5.2-5).
- #2. Calculate the real change of GWL by rainfall by adding the daily loss of GWL(Column AB) to the observed change of GWL(Column AA) and enter the results to Column AC).
- #3. Select the day when rain fell more than 2.0 mm day⁻¹ and list up the amount of rainfall and the real change of GWL (Column AC in Sheet-1) by rainfall on the Sheet-3 (Fig. 3.5.2-6).

#4. Determine the suitable function for Eq. 3.5.2-5 using the approximate curve system of the Excel. The quadric function is the most suitable one for relationship between the daily total rainfall and the raise of GWL by rainfall in this case with the determination index 0.828 (Fig. 3.5.2-6a). The liner function is not suitable one with the smaller determination index 0.7787 (Fig. 3.5.2-6b).

Finally, Eq. 3.5.2-3 is decided as next equation.

$$dW_{rain} = -12.335R^2 + 2.970R + 0.0062 \quad \text{Eq. 3.5.2-4}$$

where dW_{rain} : Daily change of GWL by daily rainfall
 R: Daily total amount of rainfall

	A	B	C	S	W	Y	AA	AB	AC
	y	m	d	GWL at 0 o'clock (m)	Daily total rain (mm/day)	Daily mean GWL (m)	dGWL (m/day)	loss GWL (m/day)	dGWL by rain (m/day)
1									
2	2016	5	14	-0.15	7.5	-0.161	-0.014	0.0174	0.0034
3	2016	5	15	-0.164	43	-0.12	0.052	0.0195	0.0715
4	2016	5	16	-0.112	1	-0.096	0.012	0.0208	0.0328
5	2016	5	17	-0.1	17.5	-0.104	-0.006	0.0204	0.0144
6	2016	5	18	-0.106	0	-0.125	-0.038	0.0192	-0.0188
7	2016	5	19	-0.144	0	-0.158	-0.031	0.0175	-0.0135
8	2016	5	20	-0.175	0	-0.189	-0.03	0.016	-0.014
9	2016	5	21	-0.205	0	-0.219	-0.032	0.0146	-0.0174
10	2016	5	22	-0.237	0	-0.242	-0.014	0.0136	-0.0004
11	2016	5	23	-0.251	29	-0.238	0.039	0.0138	0.0528
12	2016	5	24	-0.212	4.5	-0.225	-0.025	0.0144	-0.0106
13	2016	5	25	-0.237	3.5	-0.238	0	0.0138	0.0138
14	2016	5	26	-0.237	0	-0.248	-0.025	0.0133	-0.0117
15	2016	5	27	-0.262	0	-0.27	-0.025	0.0124	-0.0126
16	2016	5	28	-0.287	0	-0.292	-0.016	0.0115	-0.0045
17	2016	5	29	-0.303	54.5	-0.281	0.134	0.012	0.146
18	2016	5	30	-0.169	0	-0.193	-0.031	0.0158	-0.0152
19	2016	5	31	-0.2	11	-0.181	0.028	0.0164	0.0444
20	2016	6	1	-0.172	0	-0.179	-0.015	0.0165	0.0015
21	2016	6	2	-0.187	0	-0.2	-0.025	0.0155	-0.0095
22	2016	6	3	-0.212	106.5	-0.197	0.156	0.0156	0.1716
23	2016	6	4	-0.056	41	-0.008	0.069	0.0263	0.0953
24	2016	6	5	0.013	0	-0.005	-0.05	0.0265	-0.0235
25	2016	6	6	-0.037	0	-0.052	-0.038	0.0234	-0.0146
26	2016	6	7	-0.075	0	-0.098	-0.044	0.0207	-0.0233
27	2016	6	8	-0.119	0	-0.14	-0.043	0.0185	-0.0245
28	2016	6	9	-0.162	0	-0.174	-0.029	0.0167	-0.0123
29	2016	6	10	-0.191	26.5	-0.195	0.029	0.0157	0.0447

Fig. 3.5.2-5. Sheet-1: Daily GWL [m] at 0 o'clock etc.

	A	B	C	E	F	H	I
	y	m	d	total rainfall mm/day	total rainfall m/day	dGWL by rain (m/day)	
1							
2	2016	5	14	7.5	0.0075	0.0034	
3	2016	5	15	43	0.043	0.0715	
4	2016	5	17	17.5	0.0175	0.0144	
5	2016	5	23	29	0.029	0.0528	
6	2016	5	24	4.5	0.0045	-0.0106	
7	2016	5	25	3.5	0.0035	0.0138	
8	2016	5	29	54.5	0.0545	0.146	
9	2016	5	31	11	0.011	0.0444	
10	2016	6	3	106.5	0.1065	0.1716	
11	2016	6	4	41	0.041	0.0953	
12	2016	6	10	26.5	0.0265	0.0447	
13	2016	6	11	2	0.002	-0.0216	
14	2016	6	13	20.5	0.0205	0.0395	
15	2016	6	17	3.5	0.0035	0.0067	
16	2016	6	18	13.5	0.0135	0.0203	
17	2016	6	19	3.5	0.0035	0.0037	
18	2016	6	26	2.5	0.0025	0.0001	
19	2016	6	28	8.5	0.0085	0.022	
20	2016	7	1	2	0.002	1E-04	
21	2016	7	3	9	0.009	0.0274	
22	2016	7	8	2	0.002	-0.0074	
23	2016	7	9	10	0.01	0.0353	
24	2016	7	13	6	0.006	0.0182	
25	2016	7	17	10.5	0.0105	0.0161	
26	2016	7	18	27	0.027	0.0947	

Fig. 3.5.2-6. Sheet-3: Selected days for analysis of $f_2(R)$

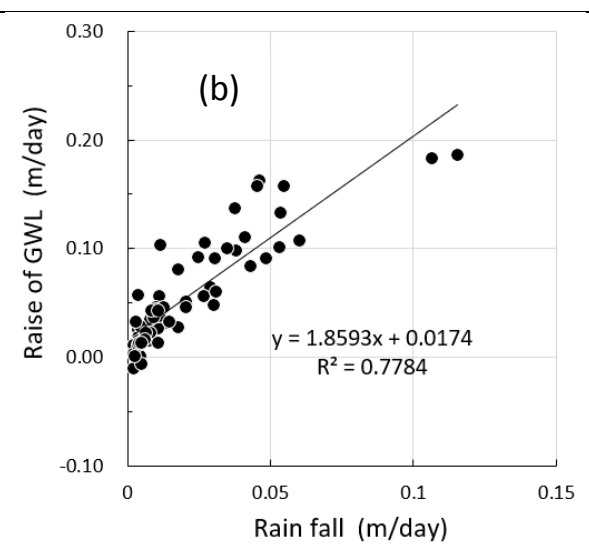
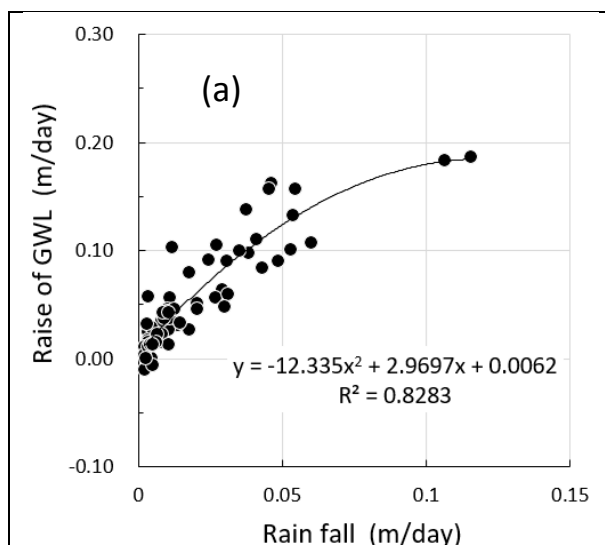


Fig. 3.5.2-7. Regression formulas for $f_2(R)$, the quadric (a) and linear (b) functions

Procedure-3. Estimate daily change of GWL by using the determined equations of dW_{loss} and dW_{rain} :

Data-2: Daily total rainfall [mm day⁻¹] ----- Column W in Fig. 3.5.2-8.

Data-3: Daily mean GWL [m] ----- Column Y in Fig. 3.5.2-8.

Data-4: Daily total rainfall [mm day⁻¹] for test with no rain from 7th Sept. to 31st Oct., 2016. ----- Column Y in Fig. 3.5.2-9.

- #1. Select the first day for GWL estimation. The 3rd Sept., 2016 is selected in this estimation.
- #2. Copy the measured daily mean GWL on 3rd Sept., 2016 in Column Y to Column AE.
- #3. Calculate GWL of next day by using the equation, which is combined $f_1(W)$ and $f_2(R)$.
- #4. Compare the estimated GWL with the measured one (Fig.3.5.2-10).
- #5. Estimate the GWL using the rainfall data in which it was no rainfall from 7th Sept. to 31st Oct., 2016 (Fig. 3.5.2-11).

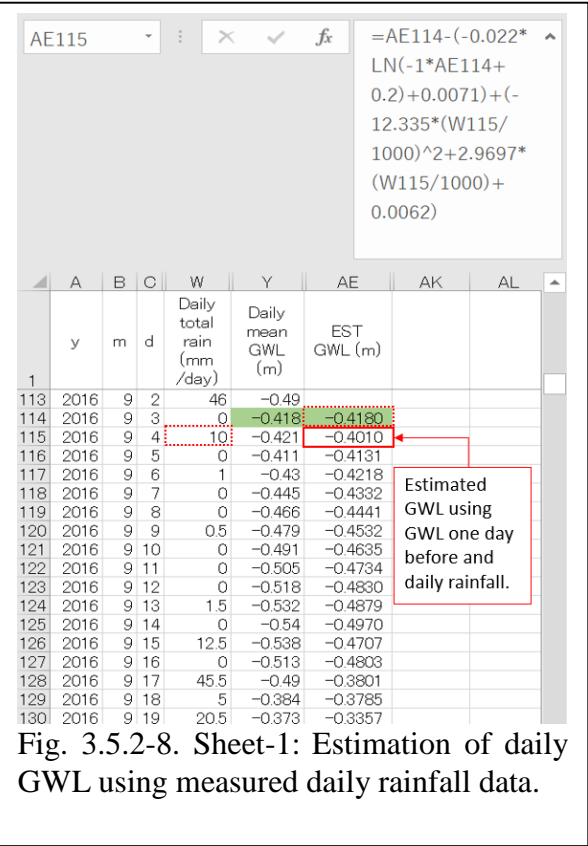


Fig. 3.5.2-8. Sheet-1: Estimation of daily GWL using measured daily rainfall data.

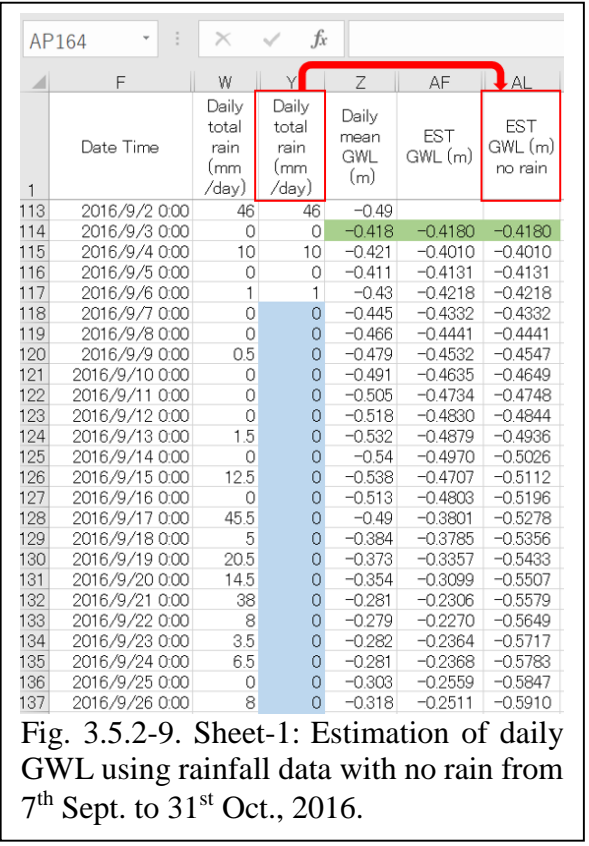
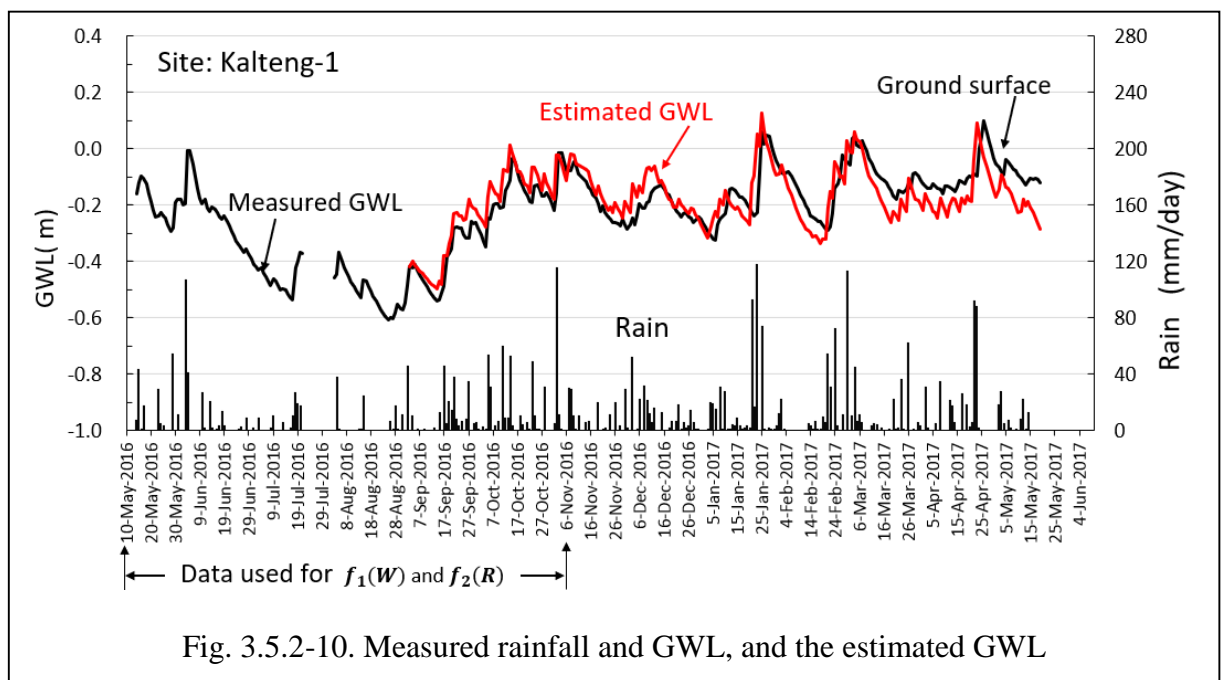
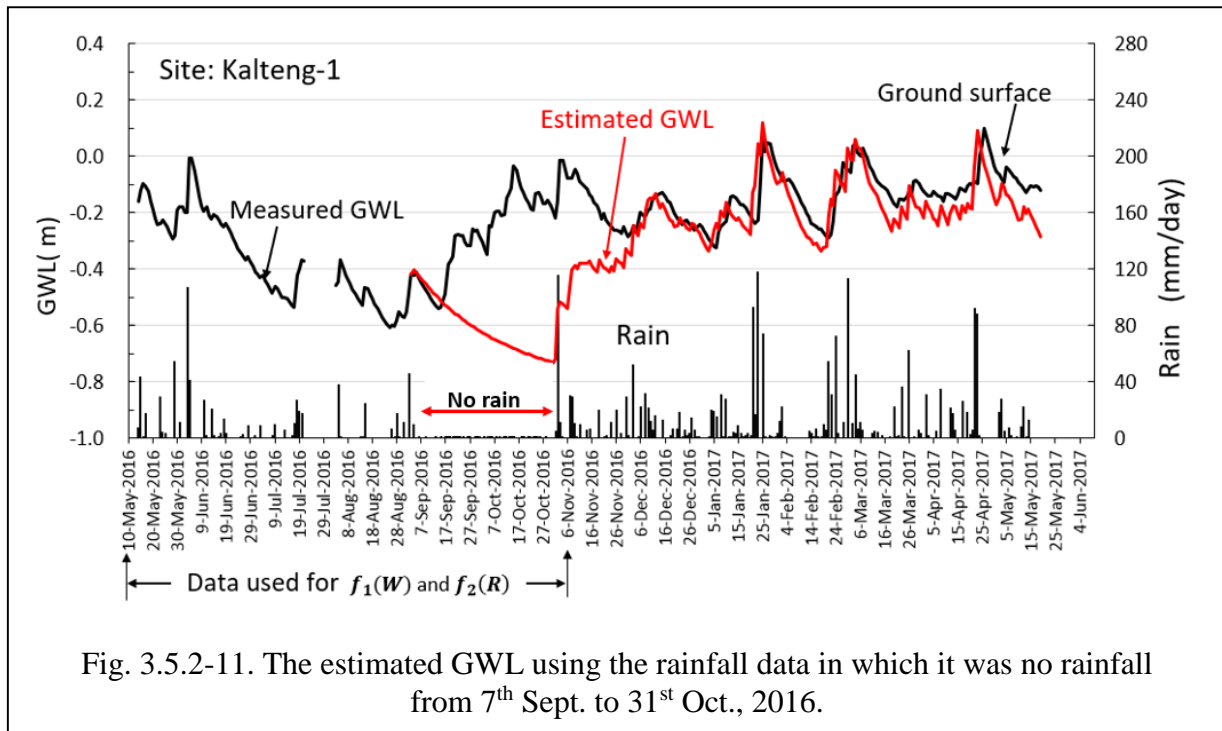


Fig. 3.5.2-9. Sheet-1: Estimation of daily GWL using rainfall data with no rain from 7th Sept. to 31st Oct., 2016.



References

- Kayama M., Takahashi H. and Limin H. S., 2000, Water Balance of a Peat Swamp Forest in the Upper Catchment of the Sebangau River, Central Kalimantan, Proceedings of the International Symposium on Tropical Peatlands, Bogor, 299-306.
- Takahashi H. and Yonetani Y., 1997, Studies on Microclimate and Hydrology of Peat Swamp Forest in Central Kalimantan, Indonesia. Rieley J.O. and Page S.E. eds, Biodiversity and Sustainability of Tropical Peatlands, Sawara Publishing Ltd., 179-187.
- Umeda Y. and Inoue T., 1985, The influence of evapotranspiration on the groundwater table in peatland. Jour. Faculty of Agriculture, Hokkaido University, 62(2), 167-181.



4.1. CO₂ flux measurements

4.1.1. Methodology of CO₂ flux measurements

CO₂ movement or CO₂ flux between the soil and the atmosphere is the primary function of soil respiration. Soil respiration returns substantial amounts of carbon to the atmosphere and is a major component of CO₂ emissions or NEE. Ecosystem disturbances, including climate change, deforestation, peatland drainage, forest and peatland fires, and land conversion, provoke changes in soil respiration and the resulting carbon balance, as the ecosystem loses important soil carbon storage due to such disturbances. Therefore, direct measurements of CO₂ fluxes should be conducted at various sites which include both intact peatland and other peatland areas characterized by varying degrees of ecosystem disturbances (see Sub-section 2.2.1 on Peatland Type). The results of these CO₂ flux measurements are used for the NEE analysis as described in Sub-section 2.2.3.

There are various methods to measure CO₂ fluxes, each with its own advantages and limitations. This guidebook recommends a micrometeorological method using a flux tower. Secondary CO₂ flux data may also be used, if such data are available for the study area.

Box 2. Alternative approaches to flux measurements

If it is not feasible to measure CO₂ fluxes with a flux tower, there are some alternative methods available, as presented below.

Incubation method: This method uses undisturbed sample soil columns stored in containers and incubated over a period of time. CO₂ fluxes are measured using a chamber which is attachable to the top of the container. Undisturbed peat samples from each peatland type should be used to avoid measurement errors. CO₂ fluxes should be measured repeatedly with different GWLs, which can be changed by supplying or draining the groundwater inside the containers. The groundwater used for this method should be drawn from the soil sampling locations.

Closed chamber method: Small chambers are used to directly measure CO₂ fluxes over a small surface area in the closed headspace for a short period of time. Chambers should be set up at each peatland type. The advantage of using this method is that it is relatively low in cost and simple to operate. However, it is easily affected by various environmental conditions in the field, and tends to create errors and biases in gas sampling.

Step 1. Prepare equipment for field measurements

A list of key instruments necessary for measuring CO₂ fluxes using a flux tower is provided below (see Figure 5).

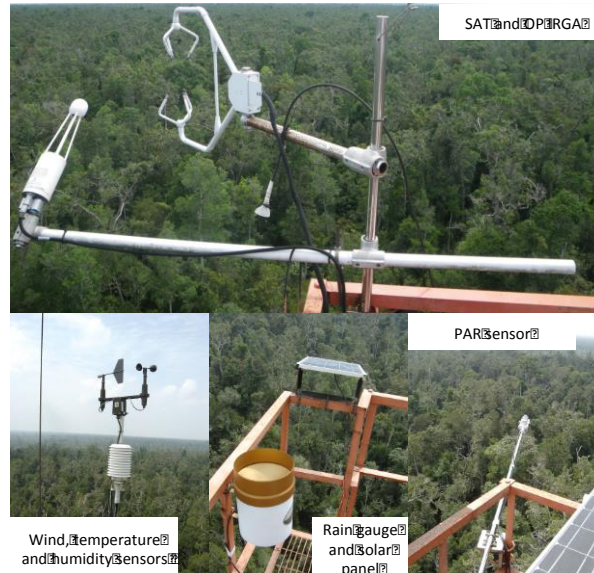


Figure 5. Flux tower instruments

Ultra-Sonic Anemometer-Thermometer (SAT):

Measures the sound speed in air in three-dimensions (especially vertical direction) in order to determine sonic virtual temperature and wind velocity in three-dimensions.

Must be settled exactly horizontally (or perpendicularly to the incline of the slope); otherwise, systematic errors will be included in the vertical wind velocity.

Open-Path CO₂ Infra-Red Gas Analyzer (OP IRGA):

Measures the attenuation of infrared radiation absorbed by CO₂ molecules intervening in the open path of the radiation in order to determine CO₂ concentration. Recommended to be settled with 10–15 degrees slant from the vertical position in order to minimize the influences of wind distortion and raindrops sticking on the lens located at the end of the open path.

The surface of the lens should be kept clean. Ideally it should be gently wiped every ten days to every month. Application of water repellent on the surface of the lens is recommended.

Most of the commercially available OP IRGAs can simultaneously measure water vapor density. CO₂ and H₂O are individually determined using the infrared radiations with different wavelengths. Based on the same eddy covariance theory, H₂O flux (i.e., evapotranspiration) from the ecosystem into the atmosphere above can be determined.

Data logger:

Stores CO₂ flux data.

The specifications required:

- Performance high enough to capture signals from several instruments at least ten times per second (>10 Hz)

- Memory capacity high enough to temporarily store the huge amount of eddy covariance data for several days

- Connections between the data logger and each sensor without noise and delay of signals

Power source:

Supplies power to run the equipment.

Recommended to use a stable commercial power supply with sufficient capacitance.

Recommended to use solar cells with rechargeable batteries.

In this system, the power generated by the solar cells is used both to drive the instruments and to charge the batteries during the daytime. In the nighttime, the power charged to the batteries is then consumed to drive the instruments.

The number of solar cells and batteries should be determined based on the power required by each instrument. It should also be taken into account that the power generation will be decreased on cloudy days and in the rainy season.

If the flux observation tower is covered by dense canopy, a solar cell panel should be placed on top of the tower. Make sure that the panel does not disturb the flow of the wind.

GPS receiver

Other microclimate measurement instruments:

Microclimate measurements are needed not only to record general weather conditions at the observation tower, but also to detect and correct invalid values in CO₂ fluxes.

Key microclimate parameters controlling rates of CO₂ fluxes should be recorded (temperatures, precipitation and GWL should be recorded with the SESAME system as described in Sub-subsection 2.1.2.1):

- Photosynthetically active radiation (PAR) as the main variable, since it strongly affects CO₂ uptake rate during photosynthesis.

- Air and soil temperatures

- Precipitation

GWL

Step 2. Select locations for field measurements

Select CO₂ flux observation locations which satisfy the following conditions:

General wind direction in the area is known.

Land surface condition in the upwind area should be generally uniform and representative of the distinctive peatland types (see Sub-section 2.2.1 on Peatland Types).

Ideally, the length of the surface area from the observation tower toward the upwind direction, also known as the fetch length, should be 100 times greater than the height of the observation tower.

Permission for building of an observation tower must be available.

There must be accessible paths for the construction of the observation tower and its maintenance.

The location is safe from potential thefts of instruments.

Step 3. Build an observation tower at the selected location

Build CO₂ flux observation towers at the locations selected in Step 2.

The tower must be taller than the surrounding vegetation.

Ideally, the height of the tower is one and a half times to twice of the height of the canopy.

For a long-term observation, the growth of vegetation should be taken into account.

The tower must be strong enough to withstand the weight of instruments and strong wind. A weak tower swaying in the wind makes the observations erroneous.

A lightning rod should be mounted on top of the tower to protect the instruments in the event of lightning strike. Working around the tower during a thunderstorm is strictly prohibited.

Step 4. Install and activate the instruments, and start recording CO₂ fluxes and other microclimate parameters

Install SAT and OP IRGA in the upwind direction from the flux tower to avoid wind distortion effects.

If the prevailing wind direction changes seasonally, the direction of SAT and OP IRGA should be also adjusted toward the upwind direction.

The distance between SAT and OP IRGA should be between 15 and 30 cm.

If <15 cm, the airflow will be disturbed.

If >30 cm, the synchronicity of both sensors will be reduced.

Activate the data logger, and start recording time-series data.

Obtain the data from the data logger every 2 – 3 months.

4.1.2. Net ecosystem exchange (NEE) analysis

The Carbon Emission Model from Peat Decomposition, described in Section 2.3, uses the eddy covariance (EC) technique to estimate NEE. Raw EC data recorded at 10 Hz (see Sub-section 2.1.2.2 CO₂ flux measurements) are used to calculate physical parameters such as three-dimensional wind velocity, air and soil temperatures and CO₂ fluxes at the interval of 30 minutes to one hour. In this calculation process, many kinds of data correction, quality control and gap filling must be conducted.

Box 3. What is Eddy Covariance?

Eddy Covariance (EC) is a method for evaluating vertical transport of energy, water vapor and gases in the near-ground atmosphere. Near the ground surface, wind blows as a turbulent flow, meaning there are many “eddies” with wide ranges in size and duration. These eddies exchange the energy and gases between the upper and the lower atmospheric layers. According to the turbulent flow theory, these vertical fluxes can be given as a function of covariance of vertical wind velocity and gas concentration. Therefore, this method is called “eddy covariance”.

Step 1. Conduct quality control on raw data

Check the raw data obtained in Sub-subsection 2.1.2.2 (CO₂ flux measurements), and make corrections if necessary.

Step 2. Calculate NEE values for the selected time interval

Organize the sequential raw data into a specific time interval (also known as averaging time). Averaging time is usually 30 minutes or 1 hour.

Calculate NEE values for each type of peatland by using the following equation.

$$NEE = \overline{w'c'} \quad (1)$$

Where:

W = vertical wind velocity (m/s)

C = CO₂ concentration (mg/m³)

' = fluctuating component

$\bar{\quad}$ = mean value

Step 3. Conduct quality control on calculated NEE values

Check the calculated NEE values, and remove all erroneous data.

Certain climatic conditions, such as heavy rain and irregular wind direction, may cause errors in NEE calculation.

If necessary, correct the erroneous NEE values with some parameters obtained in the same time interval.

Step 4. Fill data gaps in calculated NEE values

Find data gaps, and estimate missing NEE values using several techniques such as regression, lookup table, or mean daily variation.

Step 5. Calculate annual NEE values

Calculate annual NEE for each type of peatland by accumulating all values of the observation year as expressed in the following equation.

$$\text{Annual NEE} = \sum_{\text{Year}} (\text{NEE value at each time interval}) \quad (2)$$

4.1.3. Carbon Emission Model from Peat Decomposition

❖ What is a Carbon Emission Model from Peat Decomposition? ❖

The Carbon Emission Model from Peat Decomposition is based on the assumption that there is a linear relationship between NEE and GWL. Based on this relationship, this model allows you to estimate an annual NEE of the study area by using the lowest monthly average GWL(s) in the study year(s) as a key parameter.

NEE means the difference between CO₂ amount which is 1) emitted by ecosystem respiration (RE) and 2) absorbed by photosynthesis (gross primary production; GPP). Therefore, the relationship between net ecosystem production (NEP) and NEE is given by:

$$\text{NEE} = -\text{NEP}$$

$$\text{NEP} = \text{GPP} - \text{RE}$$

RE is found to increase with soil temperature, and decrease as GWL (or soil moisture) rises. In forest ecosystems, CO₂ exchange between biomass and the atmosphere usually occupies most of the carbon flow. If other carbon sources are negligible, the carbon balance of forest ecosystems can be determined by NEE as follows:

- NEE > 0: carbon source (emission)
- NEE = 0: carbon neutral
- NEE < 0: carbon sink

Step 1. Obtain a linear relationship between the observed lowest monthly average GWL(s) in the study year(s) and annual NEE

Use the lowest monthly average GWL value for each peatland type selected from the observed monthly average GWLs in the study years as described in Step 7 of Sub-section 2.2.2.

Use the annual NEE values for each peatland type obtained in Sub-section 2.2.3.

Draw a linear regression line between the observed lowest monthly average GWL(s) in the study year(s) on the *x* axis and observed annual NEE on the *y* axis, and obtain a relationship for each peatland type (see Figure 14) identified for the study area. Each regression equation obtained in this step will be used to estimate annual NEE values throughout the study area.

You can use the equation to estimate NEE (or CO₂ emissions) for different years, or other areas throughout the study area based on the estimated spatial distribution of GWL.

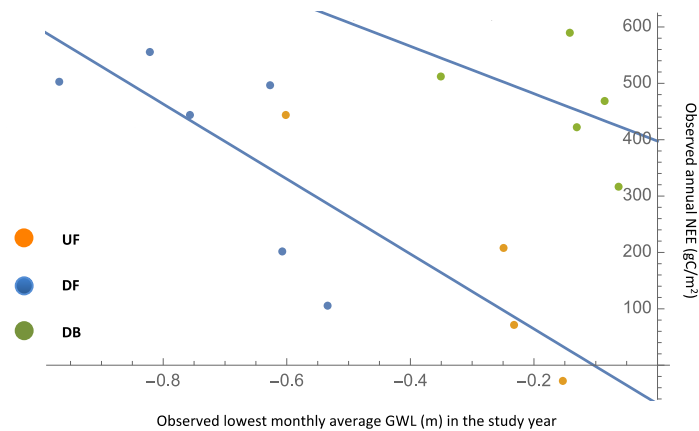


Figure 14. Example of relationships between the lowest monthly average GWLs (m) in the study years and annual NEE (gC/m²/year) observed in Central Kalimantan (Hirano et al., 2012)

Step 2. Estimate annual NEE using the estimated lowest monthly average GWL(s) in the study year(s) in all other grid cells

Estimate annual NEE for each peatland type in all other grid cells (areas beyond the observation points), using the equations obtained in Step 1 above. Use the estimated lowest monthly average GWL value in the study year obtained in Step 7 of Sub-section 2.2.2 (Groundwater level analysis).

Calculate the total NEE from the study area by summing up NEE values from each grid cell by using the following equation.

$$T = \sum_{i=1}^N A_i [a_i X_i + b_i Y_i + g_i Z_i + \dots] \quad (13)$$

Where:

T = total NEE

A_i = peatland area in grid cell i

α_i = the ratio of peatland type X area in grid cell i

β_i = the ratio of peatland type Y area in grid cell i

γ_i = the ratio of peatland type Z area in grid cell i

X_i = NEE value of peatland type X area in grid cell i

Y_i = NEE value of peatland type Y area in grid cell i

Z_i = NEE value of peatland type Z area in grid cell i

N = the number of grid cells

Step 3. Generate a map of estimated annual CO₂ emissions

Generate a map of estimated annual CO₂ emissions (positive NEE values) based on the grid file created in Step 2 of Sub-section 2.2.1 (Peatland Type) and the NEE values obtained in Step 2 above. Figure 15 shows an example of annual NEE maps of 2012 for Central Kalimantan created on a 0.5-degree grid file.

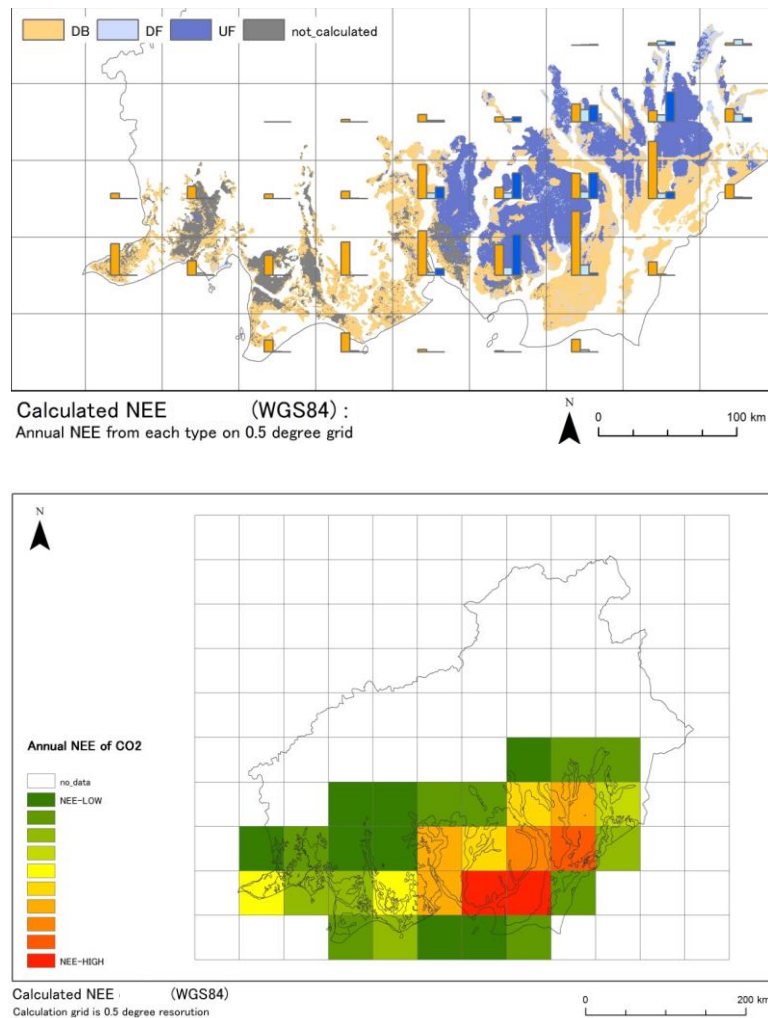


Figure 15. Map of estimated annual NEE values for each peatland type (top) and for total NEE (bottom) of 2012 on grid files for Central Kalimantan

5.1. GWL Prediction Model

Figure 18 is a graphical representation of the model described through the following steps. Detailed procedures of this model are provided in Annex 4.

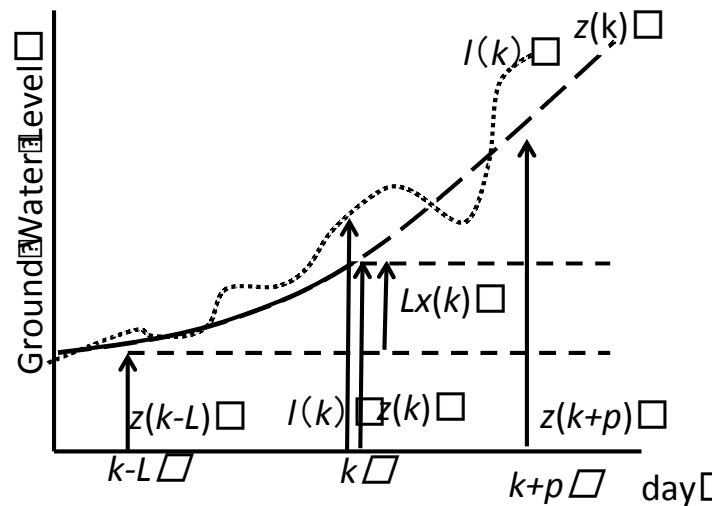


Figure 18. Illustration of the GWL prediction model based on the Kalman Filter technique

- N = the number of daily average GWL observation data
- k = current date - N
- p = the number of days ahead for the prediction of GWL
- $z(k)$ = moving average of the observed GWL data at day k
- $l(k)$ = observed GWL from the SESAME system data at day k
- $(2N+1)$ = range of moving average
- $x(k)$ = a changing rate in GWL value per day (state variable)
- L = time step width of the slope between the past and present data

Step 1. Select the daily average GWL observation data

Select the daily average GWL observation data which is to be used as an initial value for the calculation of predicted GWL values. The data may be selected arbitrarily, but must be larger than $(2N+1)$.

Determine the value of parameters as follows.

- N = the number of daily average GWL observation data
- p = the number of days ahead for the prediction of GWL

Step 2. Calculate a moving average of the daily average GWL observation data

Calculate a moving average of the GWL observation data value based on the N value determined in Step 1.

$$z(k) = \sum_{i=-N}^N l(k+i) / (2N+1) \quad (14)$$

Where:

- $z(k)$ = moving average
- $l(k)$ = observed GWL from the SESAME system

Step 3. Calculate a state variable

Calculate a state variable as defined below.

$$x(k) = [z(k) - z(k - L)] / L \quad (15)$$

Where:

$x(k)$ = the rate of change (slope) in GWL value per day (state variable)

L = time step width of the slope between the past and present data

Step 4. Apply the Kalman Filter

Apply the Kalman Filter as expressed in the following equations. The equation (16) is based on the assumption that the slope changing rate is constant.

$$x(k+1) = x(k) + w(k) \quad (16)$$

$$y(k) = Lx(k) + v(k) \quad (17)$$

Where:

$w(k), v(k)$ = white Gaussian noise

$y(k)$ = observed data at day k (observed state variable)

Calculate the observed state variable, using the following expression.

$$y(k) = l(k) - z(k - L) = Lx(k) + v(k) \quad (18)$$

Calculate $w(k)$ and $v(k)$, using the following expression.

$$w(k) = x(k) - x(k-1) \quad (k = N + L + 2, \dots, q - N) \quad (19)$$

$$v(k) = l(k) - z(k) \quad (k = N + L, \dots, q - N) \quad (20)$$

Run the Kalman Filter, using the following iteration.

$$\begin{aligned} x(k/k) &= x(k/k-1) + K(k) [y(k) - Lx(k/k-1)] \\ x(k+1/k) &= x(k/k) \\ C(k/k) &= C(k/k-1) - LK(k) C(k/k-1) \\ C(k+1/k) &= C(k/k) + W(k) \\ K(k) &= LC(k/k-1) / [L^2C(k/k-1) + V(k)] \end{aligned} \quad (21)$$

Where:

$C(k/k)$ = Variance of $x(k/k)$

$C(k+1/k)$ = Variance of $x(k+1/k)$

$W(k)$ = Variance of $w(k)$

$V(k)$ = Variance of $v(k)$

Step 5. Make a prediction of the GWL for p days ahead

Use the following model (equation) to estimate predicted values of the GWL.

$$z(k+p/k) = z(k) + px(k/k) \quad (22)$$

This equation can also be expressed as:

Forecasted GWL at day $p+k = \text{moving average} + \text{day } p \times (\text{forecasted value at day- } k)$

The predicted daily GWL values may be applied to the surrounding areas of SESAME GWL observation points, if there are no environmental factors affecting the GWL in those areas. In other words:

Peatland depth is even.

There are no drainage canals or rivers nearby the SESAME observation point.

Peatland type is uniform.

Figure 19 shows an example of GWL prediction for 3 days ahead.

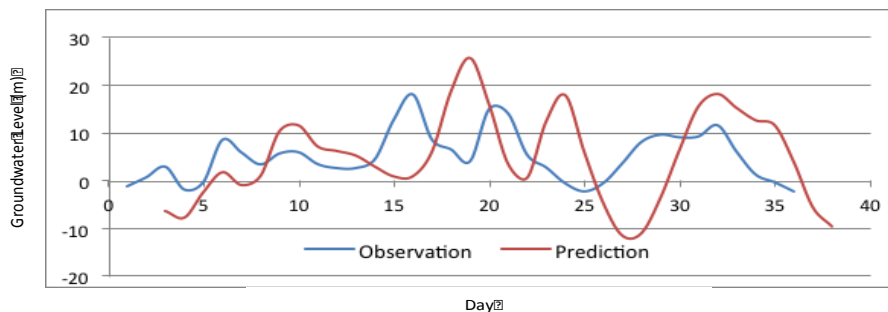


Figure 19. Illustration of GWL prediction for 3 days ahead

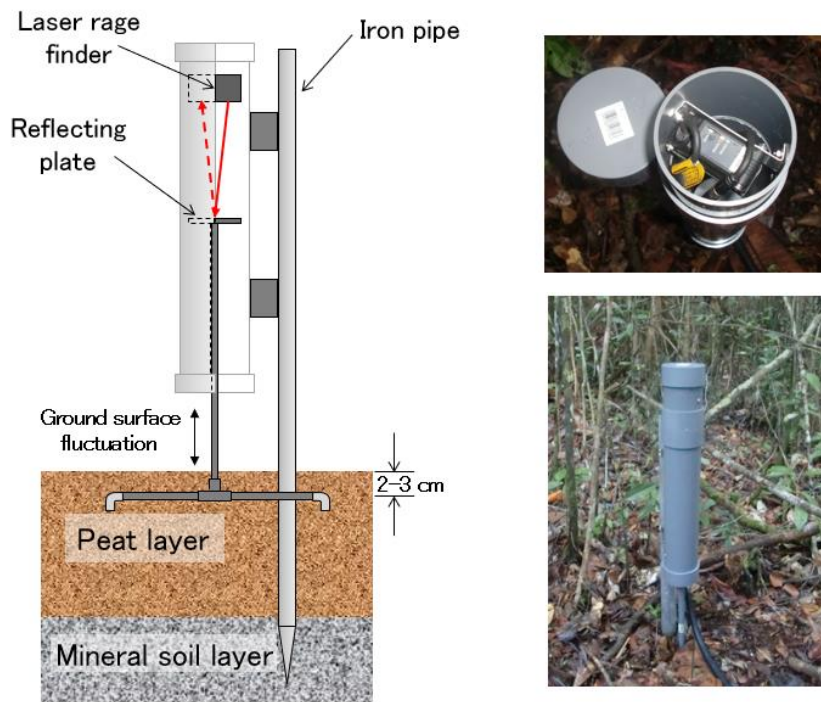
4.2. CO₂ Emission Estimation from Peat Subsidence

The subsidence of ground surface of peatland is mainly caused by biological decomposition, physical decomposition, chemical decomposition, compression by load, shrinkage, loss of matrix by water, and loss of matrix by fire (a type of chemical decomposition). Oxidation is the most important trigger of the subsidence of the peatland surface. Consequently, monitoring the ground surface level is a simple and useful way to assess decomposition and degradation of peatlands. Fluctuation of the ground surface in peatlands is affected by GWL. Monitoring of GWL should be combined with monitoring of ground surface level.

4.2.1. Instruments

Daily fluctuation of the ground surface is affected by changes in GWL. The amount of the fluctuation is usually smaller than a few millimeters. A laser distance sensor is the most suitable sensor for this purpose. The potentiometer is also suitable but the resolution is less than that of the laser distance sensor. The structure of the laser sensor and the layout of the sensor in the field are shown in Fig. 4.2.1. The laser sensor is fixed to the iron pipe which is fixed to the mineral soil layer below the peat layer. The movement of the ground surface transfers to the reflection plate through the plastic pipe which is connected to the plastic frame buried in the peat surface layer. Monitoring GWL should be done within 5 m of the ground surface level monitoring. The method of GWL monitoring is described in section 3.1. The control system of the laser distance sensor is incorporated in the same control box as GWL monitoring. Data of the ground surface level and GWL are sent simultaneously and in real time to the user through the SESAME system.

Figure 4.2.1: Schematic diagram of the laser distance meter and layout of the instrument in



the field (left), the inside of the sensor (right-top), and the full view of the sensor in the field (right-bottom)

4.2.2. Relationship between Ground Surface Level and GWL fluctuations

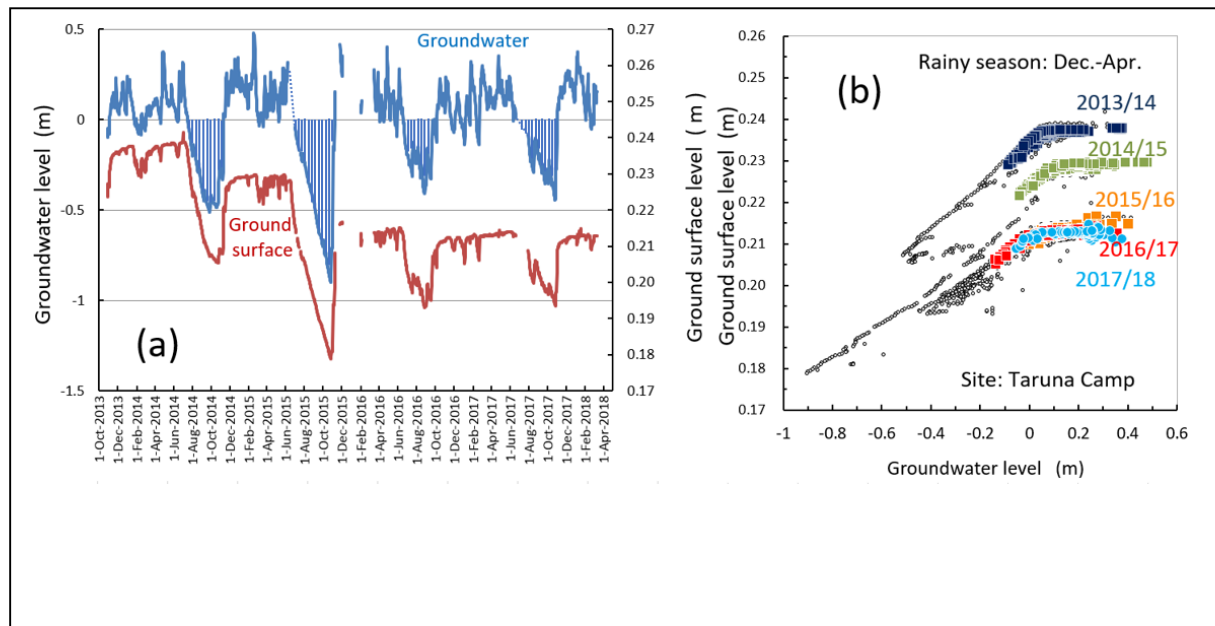
Results for ground surface level and GWL in a peatland in Central Kalimantan are shown in Fig. 4.2.2. The ground surface level changed following the change in GWL during the dry season from June to September (Fig. 4.2.2a). The change in ground water level was small despite the large change in GWL during the wet season from December to April. This means that the ground surface level during the rainy season indicates the standard level for this site.

The relationship between ground surface level and GWL is shown in Fig. 4.2.2b. There is little increase in ground surface level against the rise in GWL when $\text{GWL} > 0.1$ m. In addition, ground surface levels during the rainy season decrease year-by-year. The largest decrease was observed during the rainy season of 2015/16 and a small decrease was observed during the rainy season of 2014/2015. Conversely, decreases were small in 2016/17 and 2017/18. Differences in decreases of ground surface levels can be explained by the length and intensity of the dry season.

4.2.3. Intensity of Drought Effects on Subsidence of GWL and Carbon Loss

The intensity of drought during a dry season can be represented by accumulated low

Figure 4.2.2: Four-year records of ground surface level and GWL in a peatland in Central



Kalimantan (a) and the relationship between ground surface level and GWL (b).

GWL below the reference water level throughout the dry season.

$$GWL_{day} = \sum_{i=1}^n (|G_i - G_0|) \quad \text{eq (4.2.1)}$$

Where,

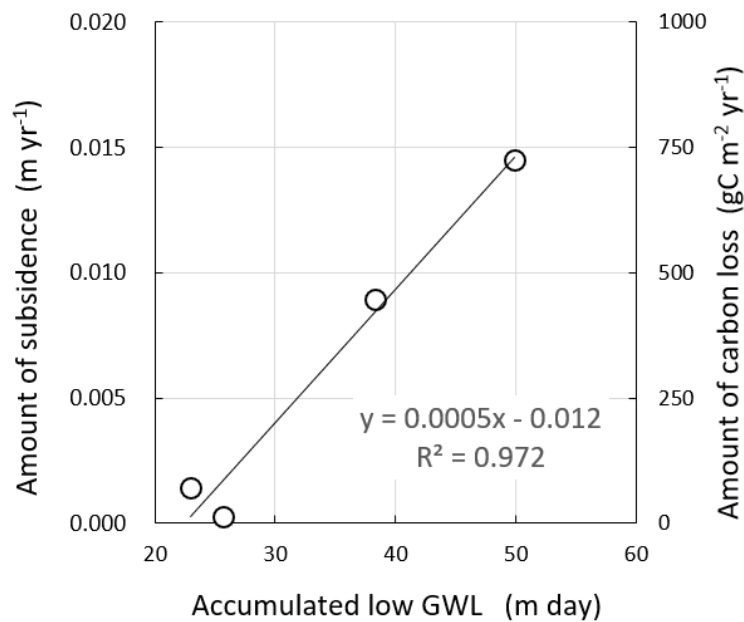
GWL_{day} : accumulated low GWL (m/day),

G_i : daily mean GWL in the dry season (m),

G_0 : reference GWL (m) with $G_i < G_0$.

GWL_{day} in Fig. 4.2.3. was calculated from June 1 to October 31 with the reference GWL ($G_i = 0$). The average ground surface level during the wet season was obtained from the ground surface level when $GWL > 0.2$ m from December to April in the following year. The amount of ground surface subsidence is the difference between the ground surface level during the wet season and of the level in the previous wet season.

The volumetric carbon density of young ombrogenous peat is $\sim 50 \text{ kg m}^{-3}$ (Shimada, 2001, 2016). The annual amount of subsidence of GSL in peatland (0.01 m) corresponds to $\sim 500 \text{ g C m}^{-2} \text{ yr}^{-1}$. This amount of carbon loss from the surface peat layer is close to the annual sum of NEE in drained and burned former forests (Hirano et al., 2012). The amount of NEE in tropical PSF shows a linear relationship with the lowest monthly GWL (Hirano et al., 2016)



Figure

4.2.3:

Relationships between accumulated low GWL (GWL_{day}), ground surface subsidence per year, and estimated carbon loss due to peat subsidence

References

- Hirano T., Segah H., Kusin K., Limin S.H., Takahashi H. and Osaki M., 2012, Effects of disturbances on the carbon balance of tropical peat swamp forests, *Global Change Biology* 18, 3410–3422.
- Hirano T., Sundari S. and Yamada H., 2016, CO₂ Balance of Tropical Peat Ecosystem, *Tropical Peatland Ecosystems* (Eds, Osaki M. & Tsuji N.), 329-337.
- Shimada S., Takahashi H., Haraguchi A. and Kaneko M., 2001, The carbon content characteristics of tropical peats in Central Kalimantan, Indonesia: Estimating their spatial variability in density, *Geochemistry*, 53: 249–267.
- Shimada S., Takahashi H. and Osaki M., 2016, Carbon Stock Estimate, *Tropical Peatland Ecosystems* (Eds, Osaki M. & Tsuji N.), 353-365.
- Takahashi H., 1999, Hydrological and Meteorological Environments of Inland Peat Swamp Forest in Central Kalimantan, Indonesia with Special Reference to the Effects of Forest Fire, *TROPICS*, 9, 17-25, Written in Japanese with English Abstract.

4.3. Methane Flux Estimation

CH₄ is the second most important greenhouse emission gas after CO₂. Tropical peatlands have a potential to be a large CH₄ source to the atmosphere because of high temperature, high GWL, and rich soil carbon which are all favorable to CH₄ production in peat. However, field studies using manual chamber systems have so far reported that soil CH₄ efflux in tropical peatlands is small (< 0.5 g C m⁻² yr⁻¹) compared to that in temperate and boreal peatlands (Melling et al., 2005; Jauhiainen et al., 2008; Hirano et al., 2009). In contrast, CH₄ efflux measured by the eddy covariance technique with an open-path CH₄ analyzer (LI7700, Licor) above a protected tropical peat swamp forest in Sarawak was considerable (Wong et al., 2018). Annual CH₄

emission from the entire peat forest ecosystem was $\sim 8 \text{ g C m}^{-2} \text{ yr}^{-1}$. The large discrepancy between soil efflux and ecosystem-scale efflux is attributable to CH_4 emissions from tree stems (Pangala et al., 2013) and termites nesting aboveground (Martius et al., 1993). Obviously, the soil chamber method cannot measure aboveground CH_4 emissions and consequently underestimates CH_4 emissions. The eddy covariance technique that can measure ecosystem-scale flux is therefore preferable.



Figure 4.4: An eddy covariance system installed above a peat swamp forest. The front white system is an open-path CH_4 analyzer (LI7700)

References

- Hirano, T., Jauhiainen, J., Inoue, T., Takahashi, H., 2009. Controls on the carbon balance of tropical peatlands. *Ecosystems*, 12, 873–887.
- Jauhiainen, J., Limin, S., Silvennoinen, H., Vasander, H., 2008. Carbon dioxide and methane fluxes in drained tropical peat before and after hydrological restoration. *Ecology*, 89, 3503–3514.
- Martius, C., Wassmann, R., Thein, U., Bandeira, A., Rennenberg, H., Junk, W., Seiler, W., 1993. Methane emission from wood-feeding termites in Amazonia. *Chemosphere*, 26, 623–632.
- Melling, L., Hatano, R., Goh, K.J., 2005. Methane fluxes from three ecosystems in tropical peatland of Sarawak, Malaysia. *Soil Biology and Biochemistry*, 37, 1445–1453.
- Pangala, S.R., Moore, S., Hornibrook, E.R., Gauci, V., 2013. Trees are major conduits for methane egress from tropical forested wetlands. *New Phytologist*, 197, 524–531.
- Wong, G.X., Hirano, R., Hirano, T., Kiew, F., Aeries, E.B., Musin, K.K., Waili, J.W., Lo, K.L., Melling, L., Micrometeorological measurement of methane flux above a tropical peat swamp forest. *Agricultural and Forest Meteorology*, accepted.

4.4. CO₂ Emission from Burn scar measurements

4.4.1. Methodology of Burn scar measurements

The area and depth of burn scar in the study area are needed when estimating carbon emissions from peat burning, as the volume of burn scar is given by the burned peat area and burned peat depth (see Section 2.4). The area of burn scar can be detected with remote sensing data (e.g., MODIS burned area product) and/or original images taken by aerial photography (see Sub-section 2.1.1 on Remote Sensing Data Set). Burned peat depths in selected sampling plots can be measured through the steps described below (see Figure 6).

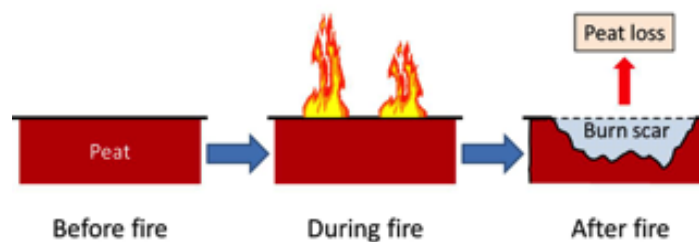


Figure 6. Illustration of burn scar measurement

Step 1. Make a burn scar map

Make a burn scar map of the study area just after a fire event, using the data prepared in the procedures described in Sub-section 2.1.1 (Remote Sensing Data Set).

Determine the burned area by a geometric analysis on the map on GIS.

Step 2. Prepare equipment for field survey

A minimum list of equipment necessary for burn scar field survey is provided below. This list should be adjusted based on the field condition.

- Eijkelpamp peat auger
- Aluminum cups and plastic bags
- Measuring tape and a rope
- Compass
- Measuring pole
- Theodolite
- GPS receiver

Step 3. Select sampling plots for field survey based on the burn scar map

Select sampling plots for field survey. The selected locations must represent the general condition of the burned area as shown in Figure 7.

The total area of plots should cover at least 15% – 20% of the total burned area.

If the number of plots is large, the locations can be randomly determined.

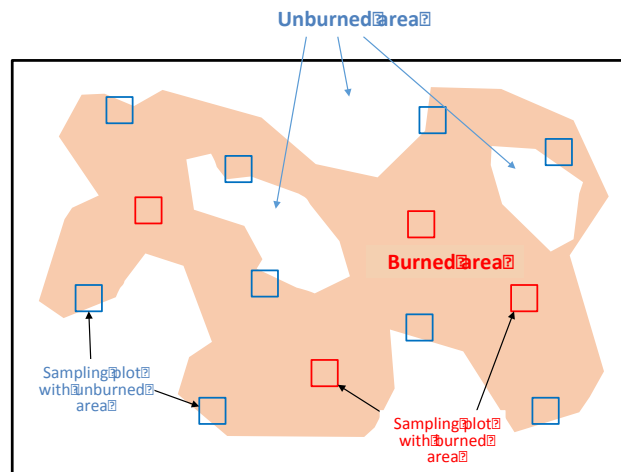


Figure 7. An example of burn scar sampling design

Step 4. Measure and record burned peat depths at the selected plots

Measure burned peat depths at several places in the sampling plots, and record them on a datasheet.

Once the rainy season begins, the burn scar gradually starts to fill in from the ingress of peat from the surrounding unburned area. Therefore, the survey should be conducted as soon as fires are out.

A measurement basis which indicates the level of ground surface before peat burning must be determined. The following objects can be used as the basis (also see Figure 8).

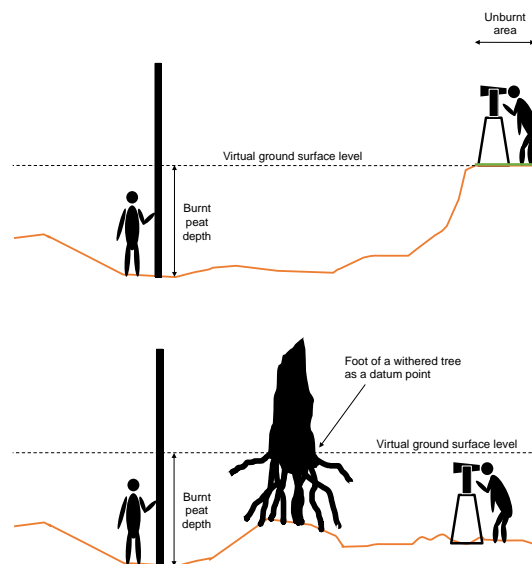


Figure 8. Illustration of burned peat depth measurements using an iron rod and a small unburned area (top) and a withered tree stand (bottom)

A small area which remains unburned: This is the most reliable basis, provided that the study area is generally flat and the ground surface level before burning can be assumed to be almost the same as the level in the surrounding area. If the plot contains an unburned area, its level can be used as the virtual ground surface level in the burned area before peat burning. If the size of each plot is large and the distribution of burned

area is patchy, it is recommended to set up sampling plots at locations where plots can contain both burned and unburned areas.

An iron rod penetrated to the mineral soil underlying the peat layer: If the plot does not contain an unburned area, an iron rod may be used as the measurement basis. However, the iron rod must be installed before peat burning occurs (i.e., the beginning of the dry season). After the installation of an iron rod, scratch a line on the rod at the ground surface level. After the peat burning, measure the distance between from the scratched line and the burn scar surface (the new ground surface). This is the depth of burned peat layer.

Withered tree stand: If the plot does not contain an unburned area, a tree trunk may be used as the measurement basis. The level of withered tree foot suggests the ground surface level before peat burning. If the area suffers from peat fires repeatedly, however, this level may suggest the ground surface level from several years ago and may not reflect the peat depth burned by the latest fire.

Step 5. Collect peat samples in an unburned area near burn scar survey plots

Determine peat-boring points at an unburned area surrounding the burned peat depth plots measured in Step 4 above. The selected unburned area should be representative of land surface conditions of the burned area. It is recommended that at least 5 boring holes be made for each plot.

Collect peat samples in 50 cm segments with an auger (see Figure 9). Take 5 cm (50 cm³) from each sample and place it into an aluminum cup before sealing it into a plastic bag. The number of samples to be collected at each boring point depends on the peat depth there.

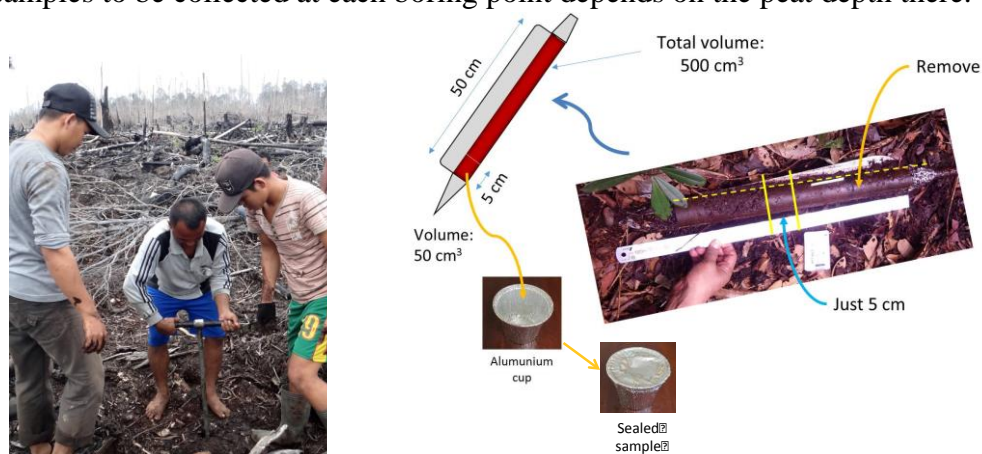


Figure 9. Procedure of peat sampling

Step 6 (Optional). Use advanced techniques for burned peat depth measurements

Select which advanced techniques to use (see Sub-section 2.1.1 on Remote Sensing Data Set).

Measure burned peat depths using the selected advanced techniques, and record data on the datasheet.

Verify the recorded data through ground-truthing.

Advanced techniques such as LiDAR and PALSAR-2 can replace the field measurement of burned peat depths. However, the analysis results should always be ground-truthed.

Data Analysis

❖ What data do you need to analyze? ❖

You will need to analyze raw data collected in field measurements in order to obtain linear relationships between GWL and remote sensing based soil moisture data (Figure 13), between GWL and NEE (Figure 14), and between GWL and carbon emissions from peat burning (Figure 16). These regression models are used to estimate carbon emissions from peat decomposition and burning, as explained at the end of the Part II of this guidebook. Therefore, the following data must be analyzed and each parameter must be calculated.

- ✓ Peatland types classified on a grid file covering the entire study area
- ✓ Lowest monthly average GWL(s) in the study year(s)
- ✓ Annual NEE in the study year
- ✓ The mass of carbon loss (or carbon emission) due to peat burning

Peatland type analysis

Peatland in the study area may consist of a variety of land use and land cover types with different degrees of ecosystem disturbances. The Carbon Emission Model from Peat Decomposition estimates the amount of CO₂ emissions from each type of peatland found in the study area. If land use and land cover characteristics were different, GWLs would be different as well; hence, the amount of CO₂ emissions from peat decomposition would vary, because the NEE is affected by the GWL. Therefore, it is important to classify the study area into different peatland types which represent distinctive characteristics of land use and land cover. Each peatland type must be clearly defined first. Detailed classification procedures are provided in Annex 1.

Step 1. Classify the study area into distinctive peatland types

Classify the study area into distinctive types of peatland by using remote sensing data set as described in Sub-section 2.1.1.

Peatland types may include:

- Undrained (intact) forest (UF)
- Drained (degraded) forest (DF)
- Drained and burned land or non-forest area (DB)
- Cropland
- Oil palm plantation
- Acacia plantation

Define forest and non-forest areas in the study area (if both areas exist).

Canopy loss areas may be classified as a drained and burned land (DB).

Define drained and undrained forest areas in the study area (if both areas exist).

Drained and undrained forest areas can be identified based on the relative dry tendency of dense forest surface. Lower dry classes can be classified as undrained forest (UF), and higher dry classes as drained forest (DF).

Step 2. Create a grid file, and extract pixel values of each peatland type into the grids

The classified study area must be prepared on a grid file, because the amount of CO₂ emissions from each peatland type will be calculated per grid cell.

Create a grid file on WGS 84 on GIS. NEE values are calculated based on a grid file on WGS 84. Therefore, it is necessary to cover the entire area of interest and to fit each grid to the pixel placement of ECMWF soil moisture data (the same grid size) described in Sub-section 2.1.1. Figure 10 shows an example of a grid file on 0.5-degree for Central Kalimantan. It shows the boundary of Central Kalimantan (blue line), new grids (black line) and ECMWF soil moisture data (gray scale).

Extract the pixel number of each peatland type from Step 1 above into every grid cell.

Calculate the area of each peatland type in each grid cell as illustrated in Figure 11. This will be used for NEE calculation in Section 2.3.

Upload the spreadsheet as an attribute table of the grid file on GIS.

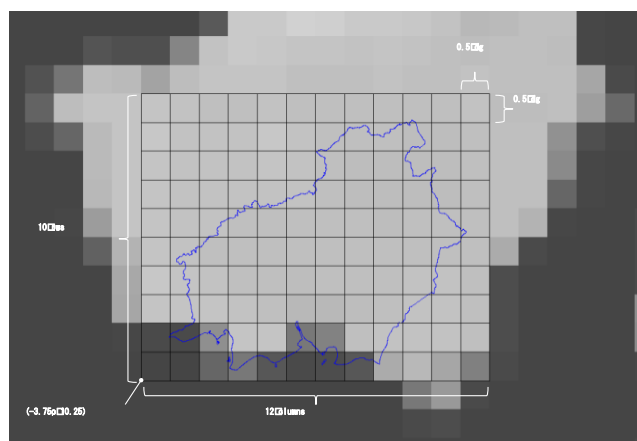


Figure 10. A grid file for Central Kalimantan

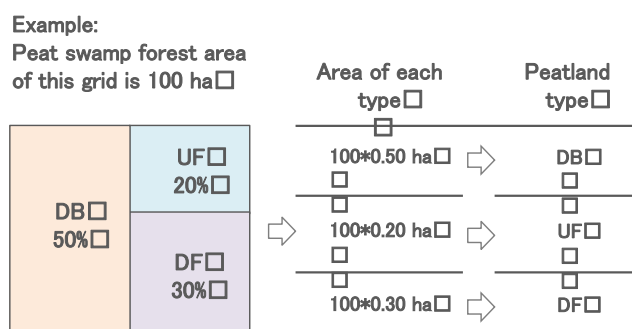


Figure 11. Example for the calculation of areas based on peatland types in a grid cell

4.4.2. Burn scar analysis

Step 1. Calculate the mean and standard deviation of burned peat depths

Calculate the mean and standard deviation of burned peat depths collected inside each plot as described in Step 5 of Sub-subsection 2.1.2.3.

Step 2. Take the average of burned peat depths among all sampling plots

Take the average of burned peat depths among all sampling plots with a standard error as given by:

$$\bar{d} = \frac{\sum_{i=1}^N d_i}{N}, \quad \Delta\bar{d} = \frac{\sqrt{\sum (\Delta d_i)^2}}{N} \quad (3)$$

Where:

N = the number of sampling plots

\bar{d} = average burned peat depth among all sampling plots

$\Delta\bar{d}$ = the standard error of average burned peat depth

d_i = average burned peat depth in Plot i

Δd_i = standard deviation of burned peat depth in Plot i

Step 3. Calculate burn scar volume

Calculate the volume of burn scar as given by:

$$\text{Burn scar volume (m}^3\text{)} = \text{Burn scar area (m}^2\text{)} \times \text{Average burn peat depth (m)} \quad (4)$$

If the burn scar area contains an error ($A \pm \Delta A$), burn scar volume V and its standard error ΔV is given as follows. If there is no error, ΔA is assumed to be zero.

$$V = A \times \bar{d}, \quad \Delta V = \sqrt{(A \times \Delta \bar{d})^2 + (\bar{d} \times \Delta A)^2} \quad (5)$$

Step 4. Calculate bulk density of peat samples

Dry peat samples collected in Step 6 of Sub-subsection 2.1.2.3 (Burn scar measurements) in an oven at 105°C for 24 hours or longer until the constant weight is achieved.

Measure the dry weight of peat (W_p) and the weight of aluminum cup (W_c).

Determine the volume of peat samples (V). It is 50 cm³, if samples are collected according to Step 6 of Sub-subsection 2.1.2.3 (Burn scar measurements).

Calculate the bulk density of peat samples as expressed in the following equation.

$$BD = \frac{(W_p + W_c) - W_c}{V} \quad (6)$$

Step 5. Calculate carbon content of peat samples

The following procedures are based on the loss on ignition (LOI) method. Carbon content can also be calculated by using an elemental analyzer.

Take a tablespoon of peat sample oven-dried as in Step 4 above, grind it, and measure the weight (M_p).

Measure the weight of a small, heat-resistant porcelain cup (M_c).

Place the peat sample into the porcelain cup, and measure the weight ($M_p + M_c$).

Burn the peat sample in a muffle furnace at a temperature >900 °C for 5 to 6 hours.

Cool the burned peat sample (ash) to room temperature in a desiccator, and measure the weight of the ash (M_a) with the porcelain cup.

Calculate the ash content (C_a) of the peat sample as:

$$C_a = \frac{(M_a + M_c) - M_c}{M_p + M_c - M_c} \times 100 \quad (7)$$

Calculate the content of organic matter in the peat sample (C_o , %) as:

$$C_o = 100 - C_a \quad (8)$$

Calculate the carbon content of peat samples (C , %), using the following equation.

$$C = C_o \times 0.58 \quad (9)$$

Step 6. Calculate total peat carbon loss (emissions) from peat burning

Calculate the total amount of peat carbon loss due to peat burning by:

$$\text{Peat carbon loss (kgC)} = \text{Burn scar volume (m}^3\text{)} \times \text{Bulk density (kg/m}^3\text{)} \times \text{Carbon content (\% of dry weight peat)} \quad (10)$$

If the bulk density and carbon content contain errors ($BD \pm \Delta BD$ and $C\% \pm \Delta C\%$, respectively), calculate carbon content ($C \pm \Delta C$, kgC/m³) first as follows. If there are no errors, ΔBD and/or $\Delta C\%$ are assumed to be zero.

$$C = BD \times C\%, \quad \Delta C = \sqrt{(BD \times C\%)^2 + (\Delta BD \times C\%)^2} \quad (11)$$

Where:

C = carbon content

BD = bulk density

After this, calculate the total peat carbon loss ($F_b \pm \Delta F_b$) given as follows. The value, F_b , will be used as the amount of carbon emissions in Section 2.4 (Carbon Emission Model from Peat Burning).

$$F_b = V \times C, \quad \Delta F_b = \sqrt{(V \times \Delta C)^2 + (C \times \Delta V)^2} \quad (12)$$

Where:

F_b = carbon loss (emission)

4.4.3. Carbon Emission Model by Burn scar analysis

❖ What is a Carbon Emission Model from Peat Burning? ❖

Similar to the Carbon Emission Model from Peat Decomposition explained in Section **Error! Reference source not found.**, this model is based on the assumption that there is a linear relationship between the mass of carbon loss from peat burning and GWL. Based on this relationship, the Carbon Emission Model from Peat Burning allows you to estimate the amount of annual carbon emissions by using the lowest monthly average GWL(s) in the study year(s) as a parameter

Step 1. Obtain a linear relationship between the amount of annual carbon emission from peat burning and observed lowest monthly average GWL(s) in the study year(s)

Draw a linear regression line between the lowest monthly average GWL(s) in the study year(s) observed at a location representative of the characteristic of the burned area on the x axis, and observed annual carbon emission from peat burning obtained in Step 6 of Sub-section 2.2.4 on the y axis (see Figure 16).

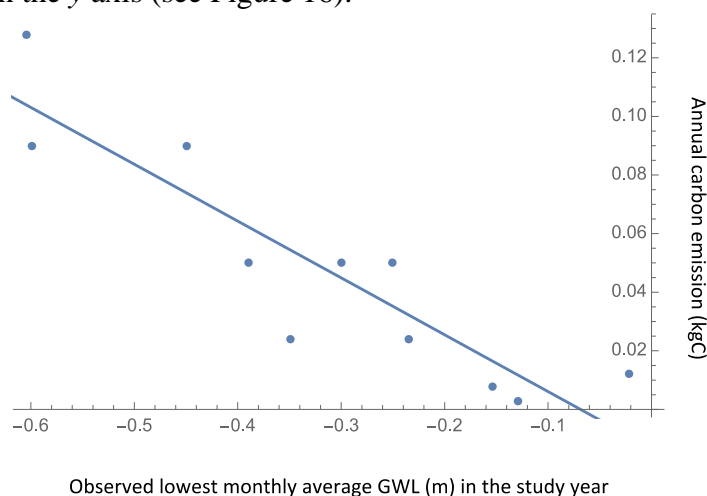


Figure 16. Example of a linear relationship between the lowest monthly average GWL(s) in the study year(s) and annual carbon emission from peat burning observed in the ex-Mega Rice area in Central Kalimantan (Putra et al., 2009)

Step 2. Estimate annual carbon emission from peat burning

Estimate annual carbon emissions from peat burning for other areas of interest. The equation obtained in Step 1 above can only be applied to other areas which indicate similar characteristics of the observed burned area.

You can use the equation to estimate the amount of carbon emissions from peat burning for different years, or in other areas beyond sampling locations as long as those areas show similar characteristics to the burned area.

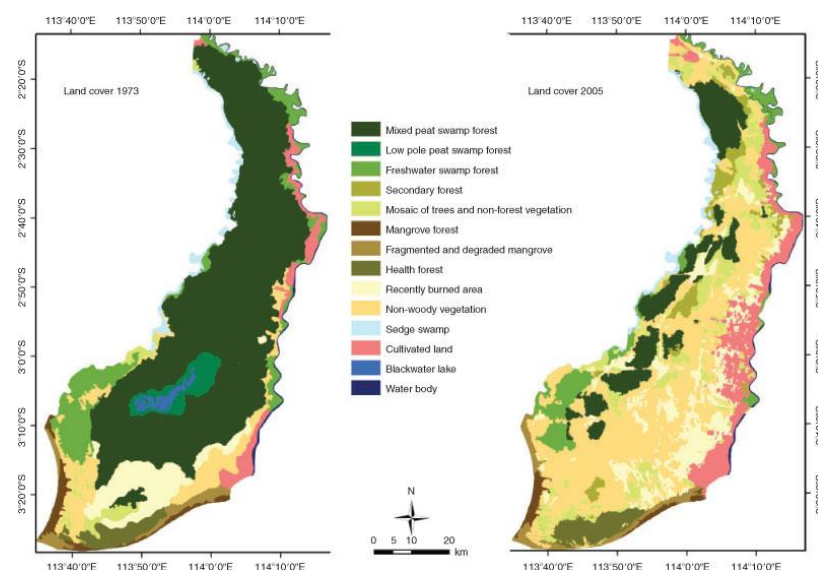
4.5. Estimation of Carbon Emission by Remote Sensing Analysis of Burn Scars

Forest fires in tropical peatlands cause deforestation and reduction of carbon density. The detection of burn scars is an important index for the carbon emission estimation. In this section, several remote sensing technologies used to detect burn scars in previous researches are reviewed.

4.5.1. Burn Scar Estimation

In Central Kalimantan, Indonesia, extensive forest fires have been occurring repeatedly in the peatlands after the rapid environmental change caused by the Mega Rice Project.

Prior studies revealed a rising trend in the rate of deforestation and identified fire as the principal factor influencing the subsequent vegetation succession. Agata et al. have analyzed a time series of satellite images of the peatlands of Central Kalimantan for the period 1973–2005. They identified a step change in fire regime, with increased burned areas and fire frequency following the peatland drainage; i.e., while peat swamp forest was the most extensive land-cover class and fires were of relatively limited extent and rarely repeated during the 23-year pre-Mega Rice Project period (1973–1996), in the 9-year post-Mega Rice Project period (1997–2005) there was a 72% fire-related loss in area of the peat swamp forest, mostly converted to non-woody vegetation rather than cultivated land and dominated by ferns or mosaics of trees. Fire is an important factor for land-cover dynamics and forest loss in the peatlands. Hence, there are high expectations on fire burn scar estimation by remote sensing technologies.



Land-cover change detected.(Agata et al.)

- Hoscilo Agata, Page Susan E., Tansey Kevin J., Rieley John O. (2011) Effect of repeated fires on land-cover change on peatland in southern Central Kalimantan, Indonesia, from 1973 to 2005. *International Journal of Wildland Fire* **20**, 578-588

4.5.2. Applicability of Synthetic Aperture Radar Analysis

Synthetic aperture radar (SAR) satellites can cover great areas and they are nearly independent of clouds. Using SAR data, the peat surface variations depending on vegetation, microtopography, and irrigation can be detected by wide-area analysis, including hydrological units.

To properly conserve and manage peat soil, it is necessary to comprehensively and precisely understand its behavior in each area. In principle, the decomposition situation of peat soil can be estimated as the amount of ground surface displacement by SAR differential interferometry (DInSAR) analysis. However, due to the characteristics of the microwaves used for this technique, intensity of interference and data accuracy are affected by the planting and topography of the peatland.

By performing DInSAR analysis with different frequencies by satellites and comparing the results, the amount and type of changes in peatland can be detected according to the respective frequency characteristics. The frequency determines where, what, and how much of the change can be detected in the peatland and the validation of the effectiveness of DInSAR analysis in peatland management. SAR data taken at different times allows the detection of the movement of peat soil surface and occurrence event detection reveals the influence of artificial land alteration and events as fire on the peat soil.

Step 1: Selection of SAR Data

This section focuses on the effectiveness of DInSAR analysis as soil decomposition index by organizing the detected peatland changes according to their frequency characteristics.

The L-band ALOS-2 satellite has been launched by JAXA as a successor to ALOS. ALOS-2 has higher resolution, wider observable area, and better data transfer capacity than ALOS. It will greatly contribute to the efficient management of land and conservation of the environment. TerraSAR-X is a X-band SAR providing consistent and high repetitive coverage thanks to time- and weather-independent acquisitions. It can detect subtle changes in the forest canopy due to high resolution and radiometric stability.

To select the suitable sensor for the research target, it is necessary to understand the characteristics of each sensor. That is, the shorter the wavelength of the microwave used for the interference SAR, the better the resolution of the ground change detection. However, in this case the analysis would be influenced by minute changes, such as vegetation on the ground surface, and is difficult to obtain interference. On the other hand, when the wavelength is longer, the resolution of the surface change detection gets worse but a wide range interference can be obtained.

SARs with different frequencies.

		TerraSAR-X	Sentinel-1	PALSAR-2
Frequency (ν)		9.65GHz (X-Band)	5.405GHz (C-Band)	1,257.5MHz (L-Band)
wavelength (λ)		3.1cm	5.6cm	22.9cm
Polarized wave	Single polarization	HH VV HV VH	VV HH	HH HV VH VV
	Dual polarized wave	HH+VV HH+HV VV+VH	HH+HV VV+VH	HH+HV VV+VH
Maximum resolution		0.25 m	5 m	3 m
Observation period		11days	12days	14days
Operation period		2007~	2014~	2014~

Step2: Burn Scar Estimation by PALSAR-2

This section describes the method of DInSAR analysis by using the actual application of PALSAR-2 sensor.

1) Data Mode Selection

To choose the mode of the data, their specifications, such as frequency, band width, spatial resolution, incidence angle, swath width, and polarization and noise levels (See Table), must be clarified according to the targeted research interest.

PALSAR-2 sensor observation mode and specification

Mode	Spot light	Fine-beam					Wide-beam		
		3m (SM1)	6m (SM2)	10m (SM3)	ScanSAR (WD1)		Scan SAR (WD2)		
Freq. (MHz)	1,257.5		1,236.5/1,257.5/1,278.5						
Band width (MHz)	84		42		28		14	28	14
Spatial resolution (m)	3*1 Rg*Az	3	6		10		100 (3 looks)		40
Incidence angle (deg.)	8-70			20-40	8-70	23.7	8-70		
Swath width (km)	25	50	50	40	70	30	350 (5 scans)		490 (7 scans)
Polarization(*1)	SP	SP DP	SP DP CP	FP	SP DP CP	FP	Sp DP		SP DP
Noise level (dB)	-24	-24	-28	-25	-26	-23	-26	-23	-26

*SP: HH or VV.

DP: HH+HV or VV+VH.

FP: HH+HV+VH+VV.

CP: Compact polarization (Circular or 45 degree linear polarization).

Step3: Master-Slave Data Pair Images

After clarifying the research interest in terms of multi-temporal analysis, interval of data, data pair acquisition for the multi-temporal analysis, and targeted site, the master and slave data pairs of the DinSAR analysis must be ensured.

As described above, a necessary condition for securing a high interference degree in DinSAR analysis is the selection of an interference pair having a short interorbital distance. In addition, it is important to consider the specifications of the sensors and the time intervals of the interference pairs. However, to objectively evaluate the coherence from the observation parameters, the critical baseline length B_c , which described by the following and often applied equation, must be considered.

$$B_c = \frac{\lambda \rho \cdot \tan \theta}{2R_{rg}} \quad (1)$$

Where λ is the wavelength of the microwave, ρ is the range distance in the line of sight direction, θ is the incident angle, R_{rg} is the range resolution, and the critical baseline lengths of WD1 and SM3 (Table) are considered as 4,672 m and 9,974 m, respectively. The degree of interference of the DInSAR analysis decreases as the interorbital distance increases with a gradient of approximately 1/critical baseline length. As shown in Table 1, the WD1 and SM3 images by PALSAR-2 have the same wavelength, range length, and incident angle, but WD1 has lower spatial resolution than SM3. Since the critical baseline length of WD1 is shorter, even if all the other observation conditions are the same, its degree of interference inevitably tends to decrease. In the case of SM3, a pair whose interorbital distance is as close to zero as possible and whose time interval is within one year would be preferentially selected. The figure shows the dependence of the coherence value of the entire image on the time interval. The coherence value rapidly decreases until the time interval reaches about 100 days, and then it gently decreases. Finally, it converges to the smallest value (0.3-0.35) around 200 days.

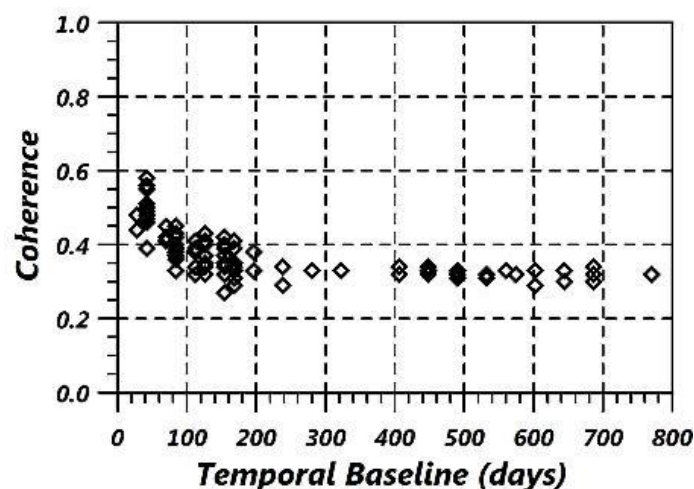


Figure Dependence of coherence value on the time interval of the interference pair.

Step4: Coherence Generation

The interference image is an image obtained by calculating the phase difference between the master image and the slave image and visualizing the change in the distance between the sensor and the ground surface in terms of radian angle. Since the interference image depends on the relative distance change, it indicates how much the ground surface approaches or gets away from the sensor.

In the differential interference analysis, the phase information of the component from which the microwave scatters backward is used. Therefore, the measurement accuracy of the analysis depends on the phase stability of this component. A previous research [11] reports that the phase stability decreases as the interorbital distance of the interference pair increases, and hence it is necessary to position the pairs so that their interorbital distance is as close to zero as possible.

In addition, since the state changes of the water vapor layer and the ionosphere between the sensor and the ground are factors lowering the measurement accuracy of the DInSAR analysis, a process for correcting their influence is necessary.

Since the process of differential interference analysis passes through an image averaging processing called multi-look processing, it is necessary to determine which are the optimal settings that likely cause interference in both the range direction and the azimuth direction.

Rodriguez et al. (1992) describes the relationship between coherence and interference phase by the following equation.

$$\phi = \sqrt{\frac{1}{2N}} \times \sqrt{\frac{1 - \gamma^2}{\gamma^2}}$$

Here, ϕ is the standard deviation of the phase difference obtained by differential interference analysis, N is the number of looks, and γ is the coherence value. In the analysis using the data of WD1, since the number of looks in the range and azimuth directions are fixed to 2 and 8, respectively, the standard deviation of the phase given by a coherence value of 0.3 is 0.56 radians, with a displacement amount of about 1 cm. Furthermore, it is good to visually confirm the actual differential interference analysis results in the analysis target range and adopt the combination that obtained sufficient interference.

Step5: Interpretation of Results

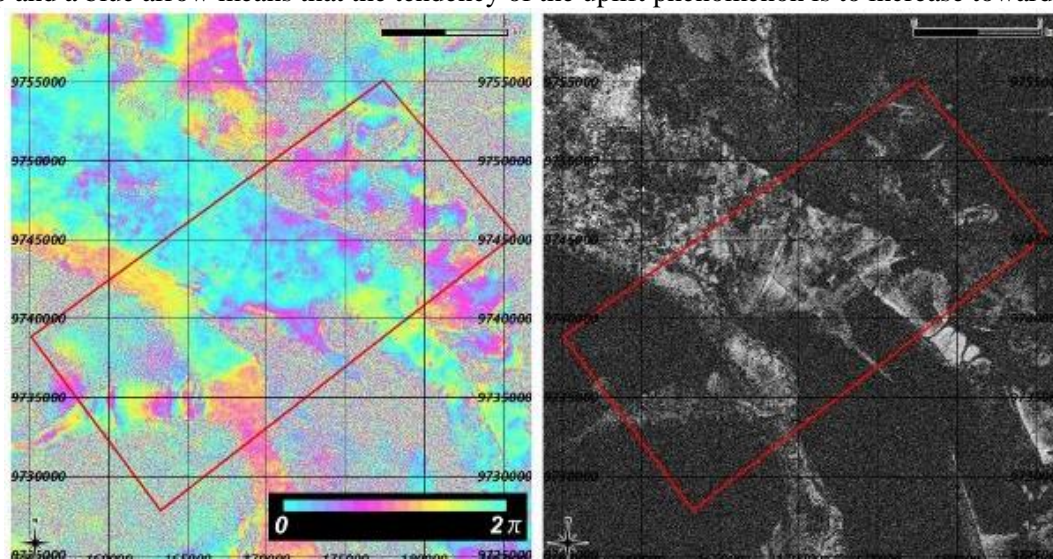
The key to interpret the results is that a change of the color tone from blue to red to yellow to green indicates that the ground surface is displaced away from the sensor, while a change from blue to green to yellow to red corresponds to a ground surface displaced toward the sensor.

Usually, it is necessary to eliminate the 2π uncertainty by applying the phase unwrapping process. However, in the target area of this work, the phase change in a short period of time is intense and, especially in water systems, many phase discontinuous lines are observed and the phase unwrapping process does not function properly. Therefore, we decided to not apply the phase unwrapping process in this work and to interpret the results with the phase indication as it is.

The coherence image is obtained by indexing the similarity between the master image and the slave image from 0 to 1. Higher coherence values result in a higher correlation (white in the image), and vice versa (black in the image). For example, if the water is submerged or dried due to the difference between the rain precipitation rates of the rainy and the dry season, the coherence decreases.

Coherence decreases even if the surface covering form changes due to forest fires or logging. The coherence value is a synonym of the degree of interference in the differential interference analysis and is often used for objectively evaluating the measurement accuracy of the ground surface displacement.

Red and blue arrows are shown in each interference images to assist the interpretation of major phase anomalies. A red arrow indicates that the subsidence phenomenon of the earth surface increases toward the tip and a blue arrow means that the tendency of the uplift phenomenon is to increase toward the tip.



In order to proceed with further detailed consideration, it is necessary to analyze fore and aft fires at short time intervals.



Several points should be considered to improve and apply the Water Table Models and Carbon Emission Models presented in this guidebook. To improve these models further, an Integrated Sensing System is necessary for the next program. It is distributed here to develop the concept of a model for an Integrated Sensing System.

5.1. Integrated Sensing System

Peatlands are dynamic ecosystems in relation to groundwater at both vertical and horizontal scales. Thus, each component of interest such as biomass, fire impact, ground subsidence, and landslide must be measured relative to ground movement. In addition to peatlands' significant movement and our index for peatland condition, sensing data lack suitable time-series intervals to monitor dynamic situations. Previously, sensed geospatial information was treated as static data. However, given the dynamics of peatland ecosystem, a new observation system that captures overall spatial dynamics in peatlands is necessary. In this section, we describe the specification of each sensor which can be applied to peatland ground surface measurement (5.1.1.) and illustrate the key concept of an Integrated Sensing System which can monitor the spatial dynamics of peatlands (5.1.2.).

5.1.1. Sensing Systems

In this section, we describe various sensing systems applied to conduct ground surface measurements in peatlands.

(1) Needs for Precise Measurement of Peatland Dynamics

The detection target in peatland ground surface can be summarized as follows (Fig. X).

- Biomass changes
- Fire impacts
- Ground subsidence
- Landslides

The various sensing methods such as the Synthetic Aperture Radar (SAR), Light Detection and Ranging (LiDAR), and camera have been applied to investigate the spatial dynamics of peatlands. To precisely measure field conditions, it is necessary to choose the most suitable sensor.

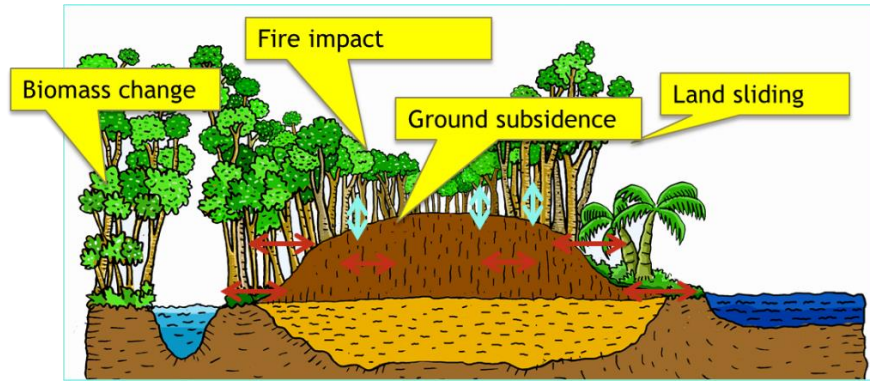


Figure 1:

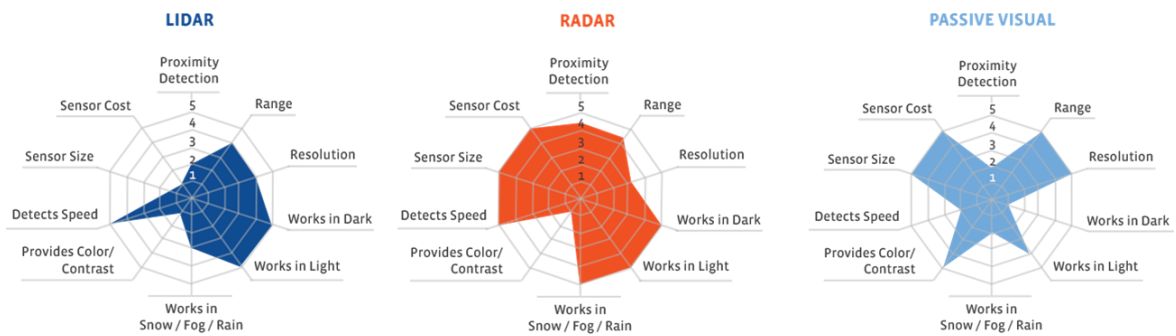


Figure 2: Derived from <https://www.unitedlex.com/news-and-insights/blog/2017/google-tesla-it%E2%80%99s-war-lidar-or-radar/>

Table X. Advantages and disadvantages of Light Detection and Ranging (LiDAR), RADAR, and camera sensors

	LiDAR	RADAR	Camera
Advantages	<ul style="list-style-type: none"> - Possible to detect objects with low reflectivity of radio waves - Distance and direction can be detected with high spatial resolution - Fast detection 	<ul style="list-style-type: none"> - Does not depend on light source and weather conditions - Accurately measures distance to a target object - Fast detection 	<ul style="list-style-type: none"> - Objects can be identified from features
Disadvantages	<ul style="list-style-type: none"> - Because infrared light is used, the detection performance deteriorates in bad weather conditions 	<ul style="list-style-type: none"> - Low spatial resolution - Difficult to detect objects with low reflectivity of radio waves 	<ul style="list-style-type: none"> - Inspection ability is reduced in bad weather conditions

(2) Hyperspectral sensor

Hyperspectral imaging collects and processes information from across the electromagnetic spectrum. The goal of hyperspectral imaging is to obtain the spectrum for each pixel in the image of a scene with the purpose of finding objects, identifying materials, or detecting processes. Hyperspectral images are suitable for analyzing specific crops by Normalized Vegetation Index (NVI) and in specific climates. The use of hyperspectral remote sensing is increasing for monitoring the development and health of crops.

(3) LiDAR

The LiDAR system can rapidly transmit laser pulses during the day and night. The result is therefore a reflection of both landscape and man-made features. The known speed of light as well as the measured time interval of the laser pulses from transmission to return allows the determination of distances. An aerial survey of a zoning area can be performed either by a fixed-wing airplane, helicopter, or in parts by a drone with LiDAR equipment including an Inertial Navigation System with a GPS. The result is an innovative tool for analyzing the ground and surface. Applications are possible for hydrology, measurements of peat domes, extraction of tree height, estimation of above-ground biomass, the design of infrastructure such as roads, water canals, plantations, etc.

The eye-safe laser in the system has a very narrow beam called a small-footprint LiDAR that can penetrate gaps in vegetation to reach the ground through trees and other elements. This penetration allows for an accurate determination of ground levels in vegetated areas. Due to the instrumentation in the LiDAR system that provides accurate position and altitude information for the laser points as well as an installed camera, very few ground control points are required, which means that accurate surveys are possible for inaccessible areas. These include quarries, wetlands, flood plains, etc. LiDAR data produce a Digital Surface model (DSM) with infrastructure, trees, canopy, and a Digital Terrain Model (DTM) of the topography of the landscape.

Tree height (h) can be obtained as follows:

$$h = \text{DSM} - \text{DTM}$$

The accuracy of the surface generated is ~ 15 cm in elevation (z), ideal for agricultural planning, peatland research, river catchments surveys, and flood mapping. Eroded areas can be accurately surveyed even through long grass layers.

The main objective was to map changes in the vertical structure of trees and vegetation with the multi-temporal LiDAR technology to identify both sources and sinks of carbon across peat dome-shaped gradients.

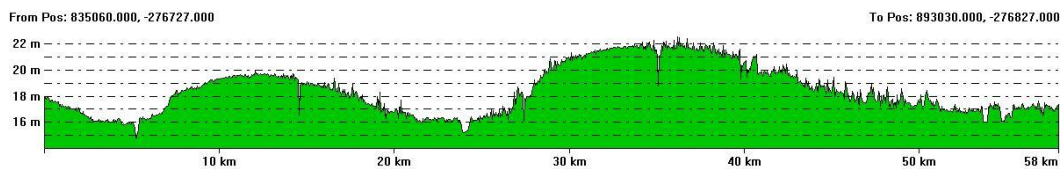


Figure 3: Peat profile with a Digital Terrain Model covering the rivers Sebangau (left), Kahayan (middle), and Kapuas (right)

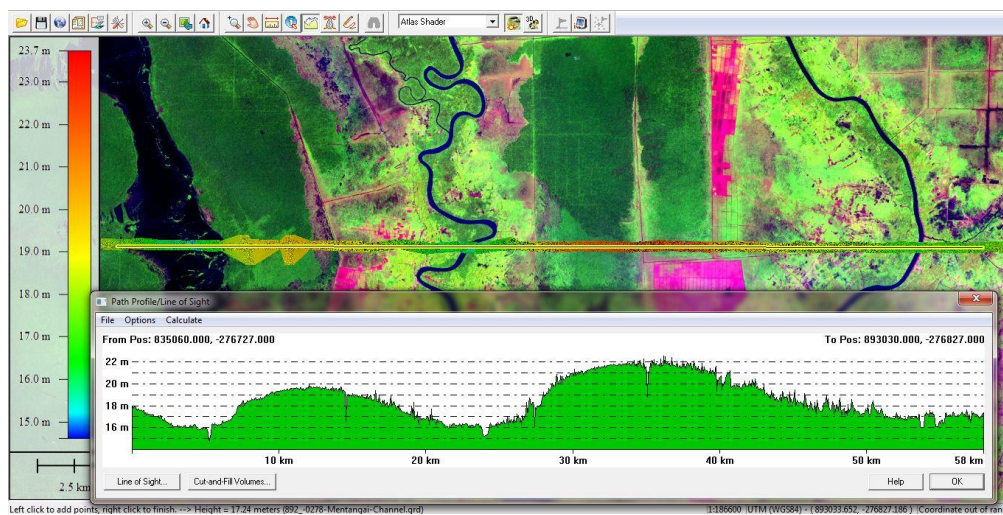


Figure 4: Light Detection and Ranging Digital Terrain Model and peat profile in the Pulang Pisau Province

(4) Radar

To conserve and manage peat soil properly, it is necessary to comprehensively and precisely understand the behavior of peat soil in each area. In principle, the decomposition rate of peat soil can be extracted as the amount of ground surface displacement by SAR differential interferometry analysis (DInSAR). SAR-satellites can cover a greater area and they are nearly independent of clouds. The L-Band ALOS-2 was launched by JAXA as a successor to ALOS. ALOS-2 has higher resolution, wider observable area, and better data transfer capacity than ALOS. ALOS-2 is expected to positively contribute to the efficient management of land and environment conservation. TerraSAR-X is a X-band SAR providing consistent and high repetitive coverage due to time- and weather-independent acquisitions. Subtle changes in the forest canopy are detected with TerraSAR-X due to its high resolution and radiometric stability.

(5) Ortho Photo

Photogrammetry is the process of authoring a digital surface model using multiple photos of the objects based on the principle of triangulation. A high-quality three-dimensional surface model of objects is modeled in a broad-scale application of photogrammetry to photos acquired

by drones or unmanned aerial vehicles (UAVs). By taking multiple photos in at least two locations, “lines of sight” (LOS) can be developed from each camera to point to objects. These LOS are mathematically intersected to produce three-dimensional coordinates of points of interest.



Figure 5: Example of the Ortho-Photo method in Palangkaraya-Pahandut Harbour on the Kahayan river

5.1.2. Key Concept of an Integrated Sensing System

In this section, we highlight two key concepts in an Integrated Sensing System considering the accuracy and reliability of sensing data.

(1) Sensor fusion technology

In the near future, large amounts of data will become available using drones, UAVs, helicopters, and satellites. To enhance the utility of such data, it is necessary to develop not only individual sensing technologies but also sensor fusion technologies using LiDAR, RADAR, camera, thermal and hyper-spectrum sensors. The combination of such data acquired by different sensor types will be useful for monitoring the rewetting of peatlands and for analyzing peatland deformation.

(2) Ground Control Network

To enable precise field measurements, careful design of a Ground Control Network is necessary. The Ground Control Network determines locations and deformations with improved precision everywhere and anytime on earth to satisfy societal and science requirements (United Nations Global Geospatial Information Management resolution).

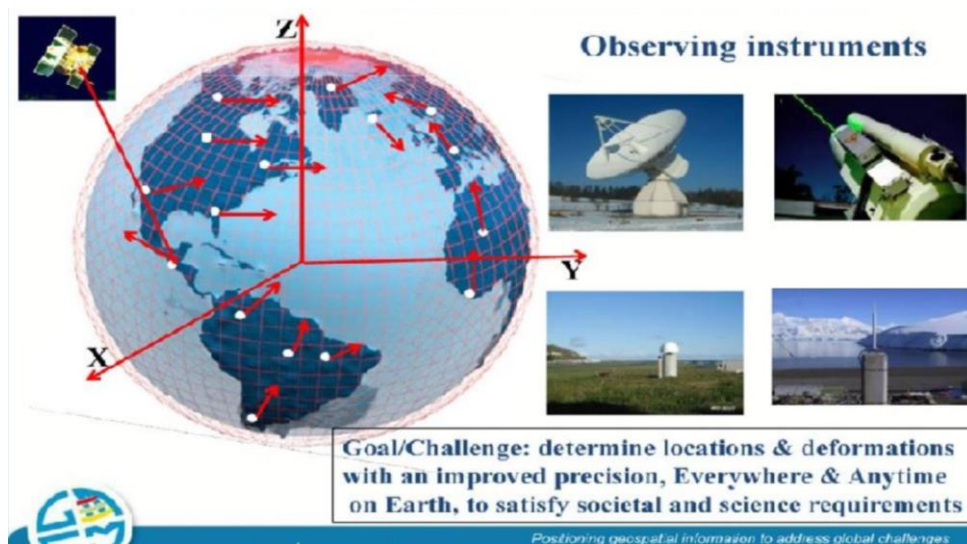


Figure 6:

Implementation of the Geodetic Control Network would contribute to increased application of geospatial data. It will also help observe the spatial dynamics of peatlands. For example, real-time location data would be applied to DInSAR analysis and used to verify the results of the analysis. The points to implement the Geodetic Control Station should be occupied by humans, located in stable ground, and should not be affected by construction activities. The site for setting the Geodetic Control station needs to be selected at a stable point, avoiding swampy or loose-soil areas.

5.2. Mapping Platform

To enable responsible management, it is important to monitor the spatial dynamics of peatlands. Such dynamic information on peatlands should be managed and operated on the integrated mapping platform to contribute to the decision-making process of policy makers. To ensure the high usability of the peatland mapping platform, ensuring the reliability of data will be the crucial for the system operators.

To create a reliable system, data to be uploaded to the system need to pass a screening test to check the accuracy of the contents and attributes of geospatial information. All data should therefore be automatically screened by the system. The mapped secondary data should include accuracy-validation information which is to be used for screening. To ensure the reliability of the material contents, it would be effective to ensure data are public. In addition, timely updating of the system is also important to improve operability. Timely updating would be achieved by the data server which manages data obtained from each SESAME system in Indonesia using a network connection. Improvement of network connection between the server and each SESAME system installed in the field would contribute to real-time updating of metadata by reducing the number of data gaps. Considering the high reliability of the system, the operational cost would be the crucial factor for operationalization. Thus, data processing, collection, evaluation, screening, and updating should be automated in the future.

REFERENCES

- DNPI. (2014). Updating Indonesia's Greenhouse Gas Abatement Cost Curve. Dewan National Perbahaan Iklim. Jakarta, Indonesia.
- Hirano, T., Segah, H., Kusin, K., Limin, S., Takahashi, H., and Osaki, M. (2012): Effects of disturbances on the carbon balance of tropical peat swamp forests. *Global Change Biology*, 18, 3410-3422.
- ICCC. (2012): Peatland Definition: From Uncertainty to Certainty. Policy Memo, Indonesia Climate Change Center, Jakarta, Indonesia, 27 p.
- Putra E.I., Hayasaka H., Takahashi H., and Usup A. (2008): Recent peat fire activity in the Mega Rice Project Area, Central Kalimantan, Indonesia. *Journal of Disaster Research*, 3(5), 334-341.
- Putra E.I. and Hayasaka H. (2009): Carbon emission from severe peat fires in Mega Rice Project area, Indonesia. *Proceedings of Japan Association for Fire Science and Engineering (JAFSE) Annual Symposium 2009*, pp.226-227, Tokyo.
- Shigenaga, Y., Saito, H., Takahashi, H., Teguh, R., Kencana, W., Jaya, A., and Setiadi, B. (2016): Field data transmission system by universal mobile telecommunication network. In: Osaki, M. and Tsuji, N. (eds.), *Tropical Peatland Ecosystems*, Springer, 479-489.
- Wahyunto, Ritung, S., and Subagjo, H. (2004) Peta Sebaran Lahan Gambut, Luas dan Kandungan Karbon di Kalimantan (Map of Peatland Distribution Area and Carbon Content in Kalimantan) 2000-2002. Wetlands International-Indonesia Programme (WI-IP) & Wildlife Habitat Canada (WHC), Bogor, Indonesia.
- Wösten JHM, van den Berg J, van Eijk P, Gevers GJM, Giesen WBJT, Hooijer A, Idris A, Leenman PH, Rais DS, Siderius C, Silvius MJ, Suryadiputra N, Wibisono IT. (2006): Interrelationships between hydrology and ecology in fire degraded tropical peat swamp forests. *International Journal of Water Resources Development* 22(1), 157–174.